Roxanne Ligi
Observatoire de la Côte d'Azur

Gaia
PLUS
INTERFEROMETRIC OBSERVATIONS

Sagan Exoplanet Summer Workshop
Exoplanet Science in the Gaia Era

July 26, 2022

EXOPLANETS: where do we stand?

~ 5000 exoplanets detected so far
Wide diversity of methods
Raise many questions!

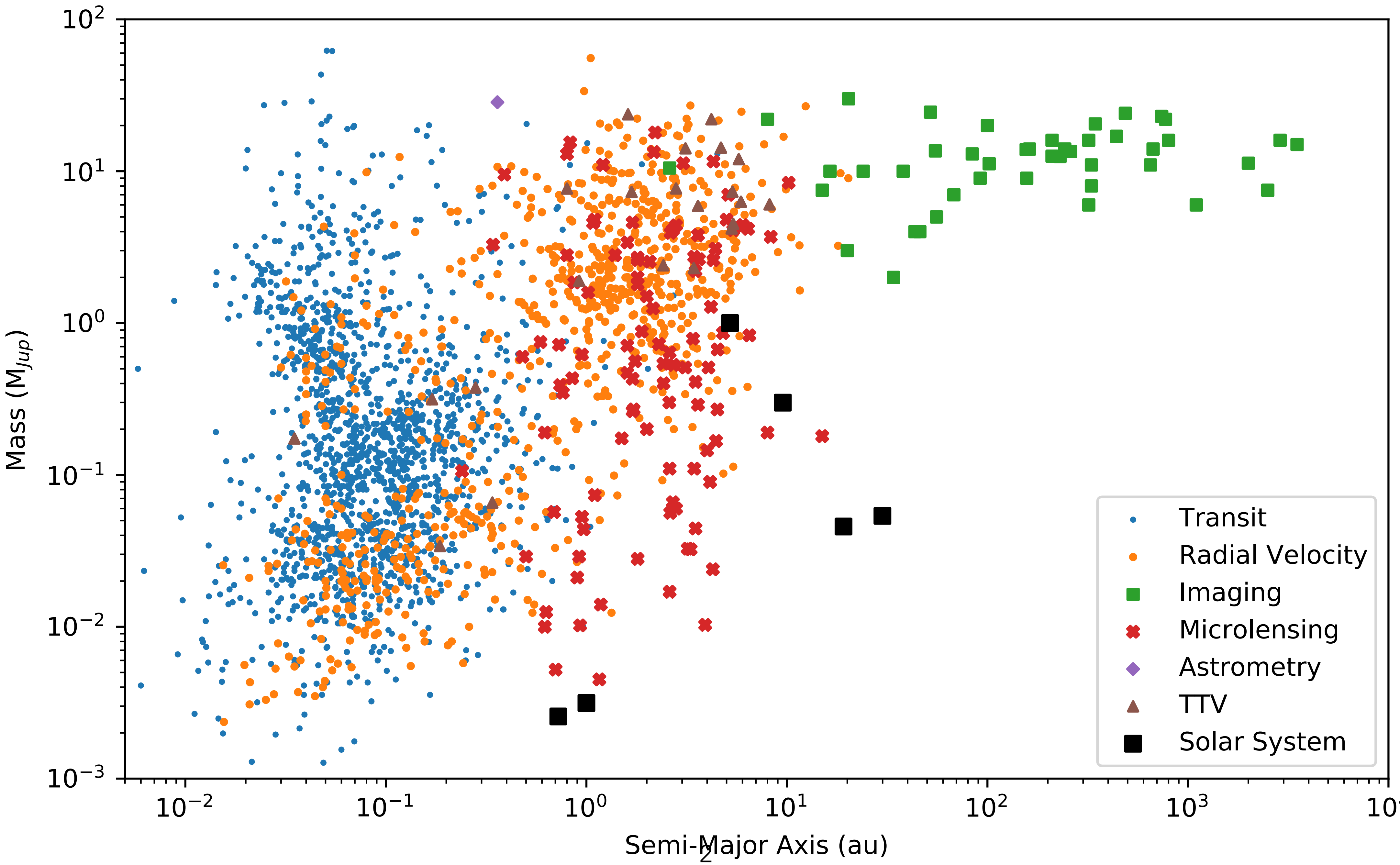

EXOPLANETS: where do we stand?

~ 5000 exoplanets detected so far

Wide diversity of methods

Raise many questions!

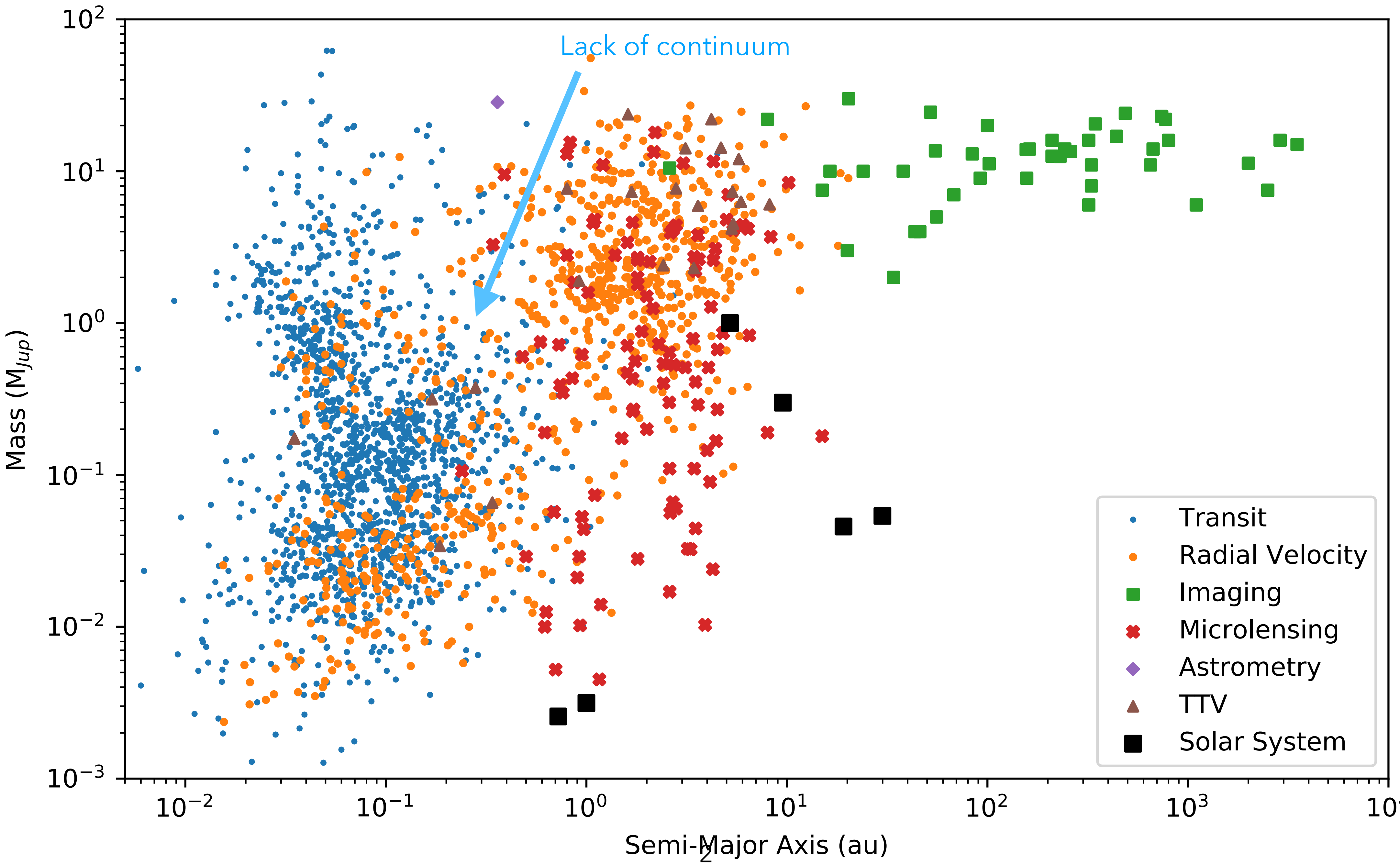

EXOPLANETS: where do we stand?

~ 5000 exoplanets detected so far

Wide diversity of methods

Raise many questions!

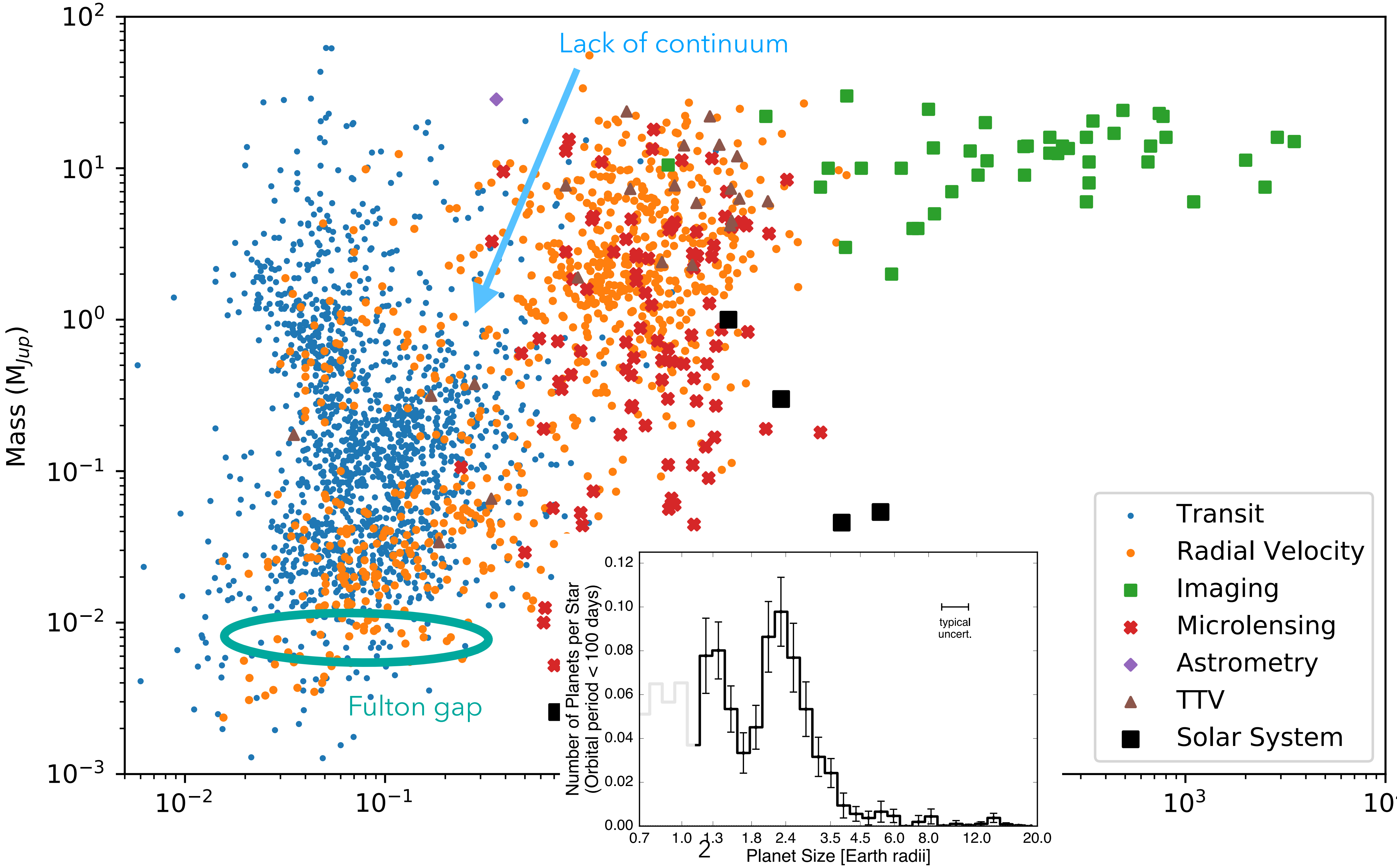

2

EXOPLANETS: where do we stand?

~ 5000 exoplanets detected so far
Wide diversity of methods
Raise many questions!

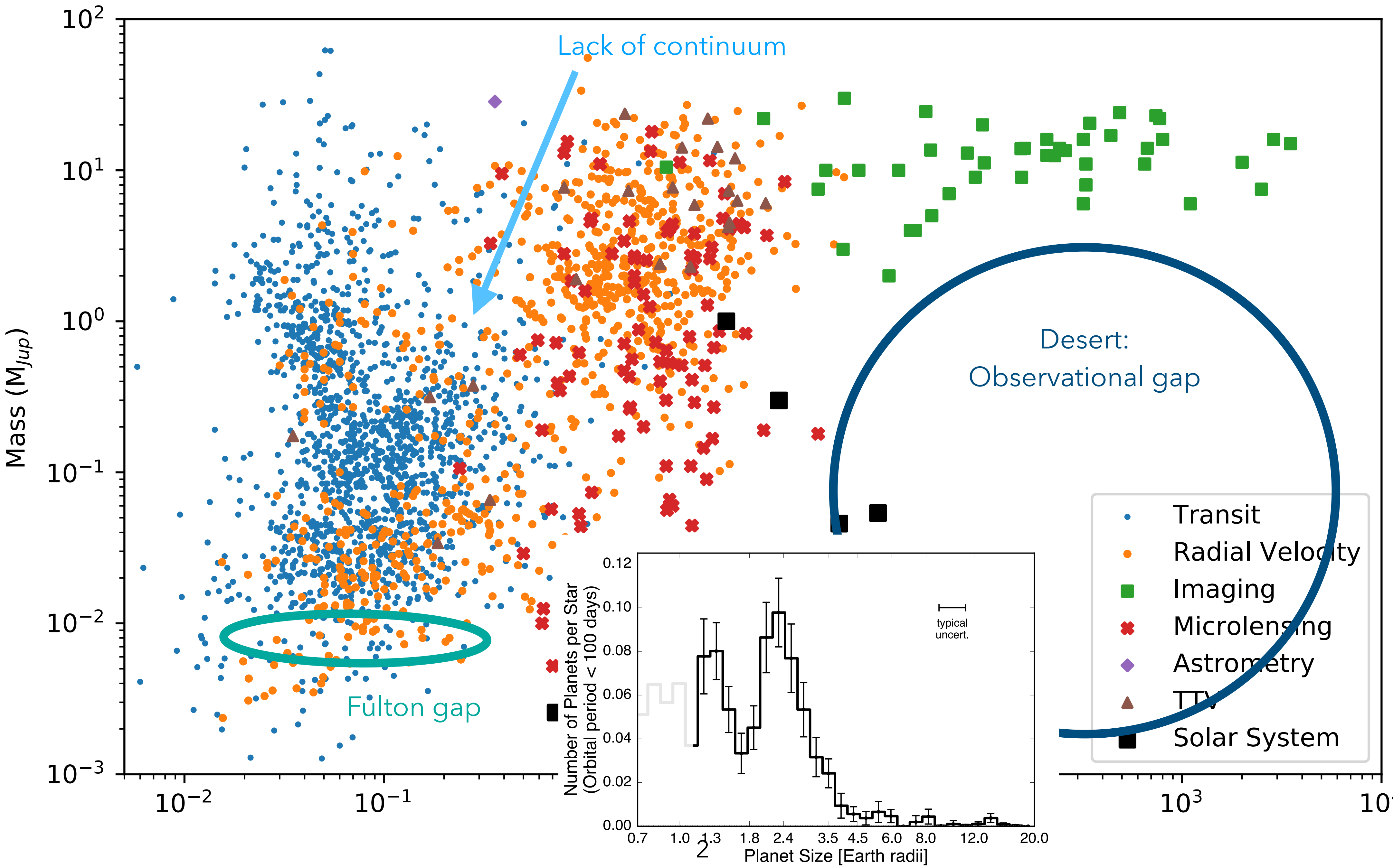

Several problematics

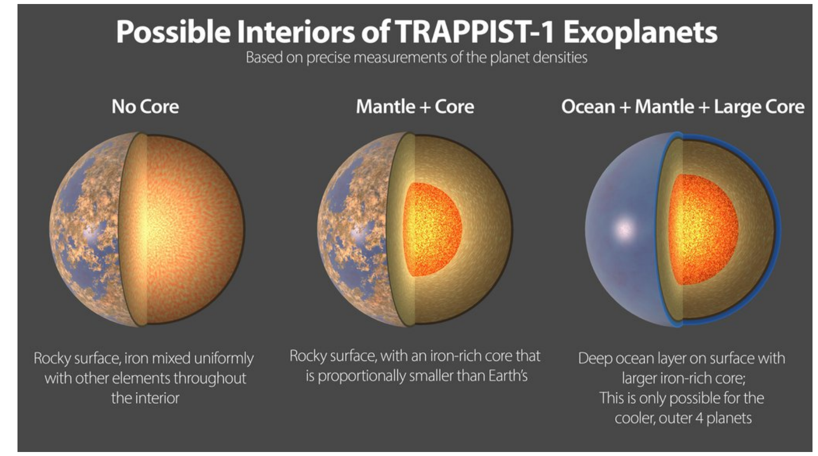

- Nature of the planets?
  ➔ Composition, size…

- Formation?
  ➔ Place of birth, migration…

- « Habitability »?
  ➔ Distance to the star (temperature), tectonic…

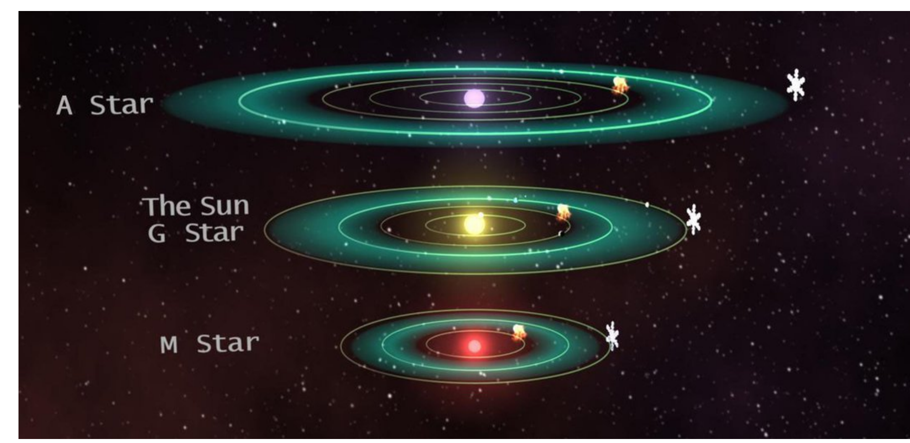

- Is our solar system unique?
  ➔ Need to probe many systems!

Indirect detection methods

Transit method

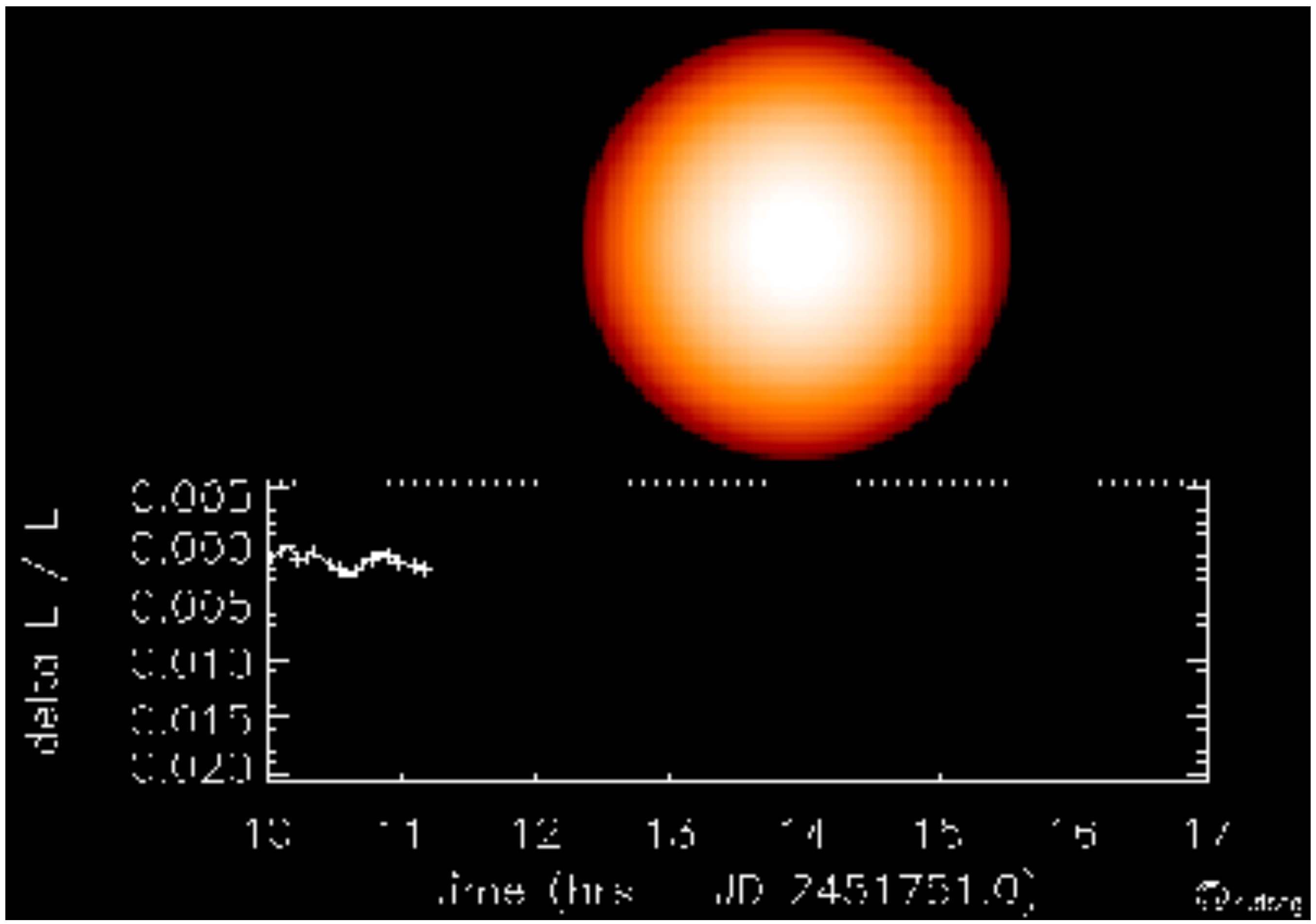

$$\frac{\Delta F}{F} = \left(\frac{R_P}{R_\star}\right)^2$$

→ Knowing R_p depends on $R_\star$

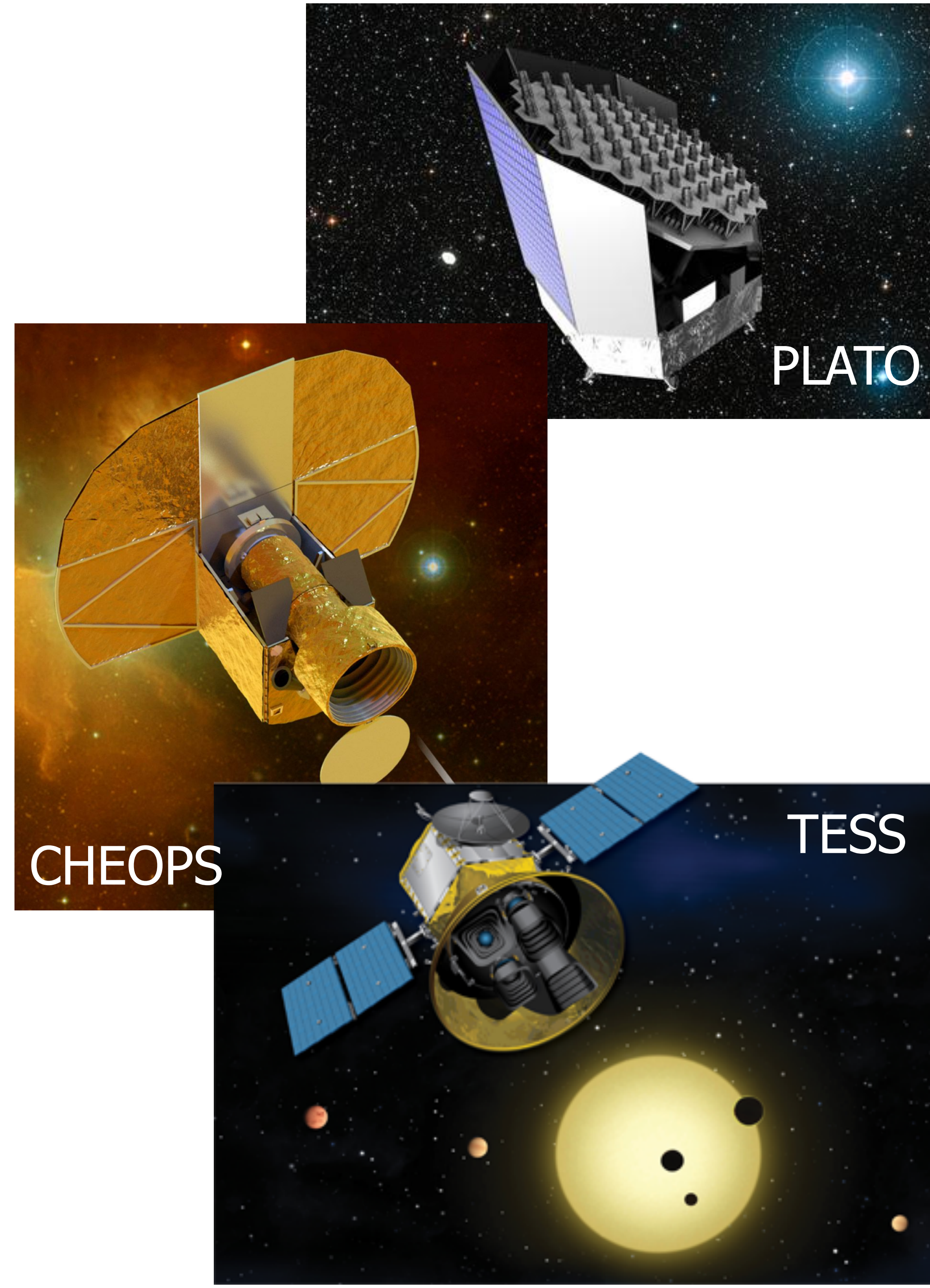

Indirect detection methods

Transit method

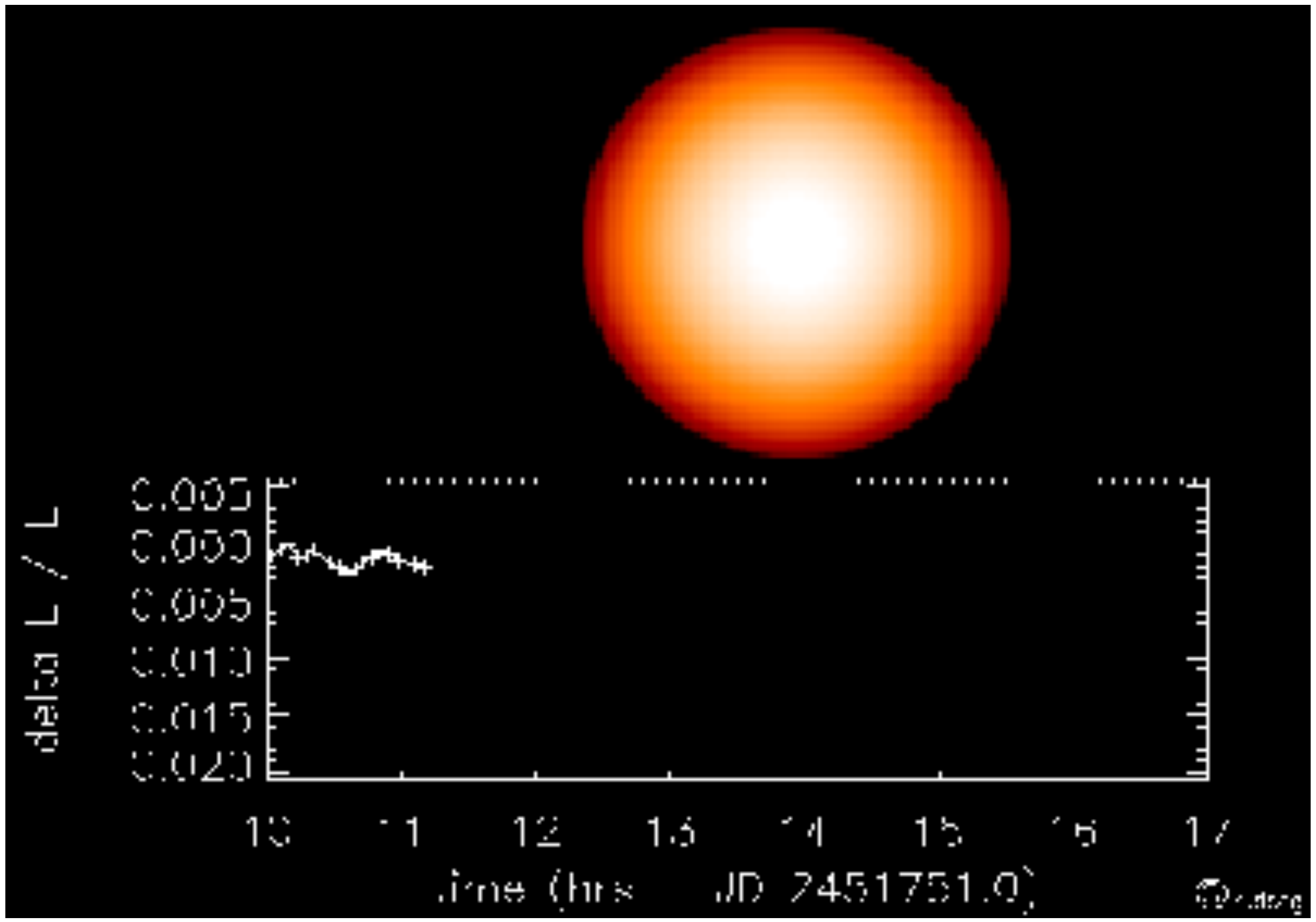

$$\frac{\Delta F}{F} = \left(\frac{R_P}{R_\star}\right)^2$$

→ Knowing **R_p** depends on **$R_\star$**

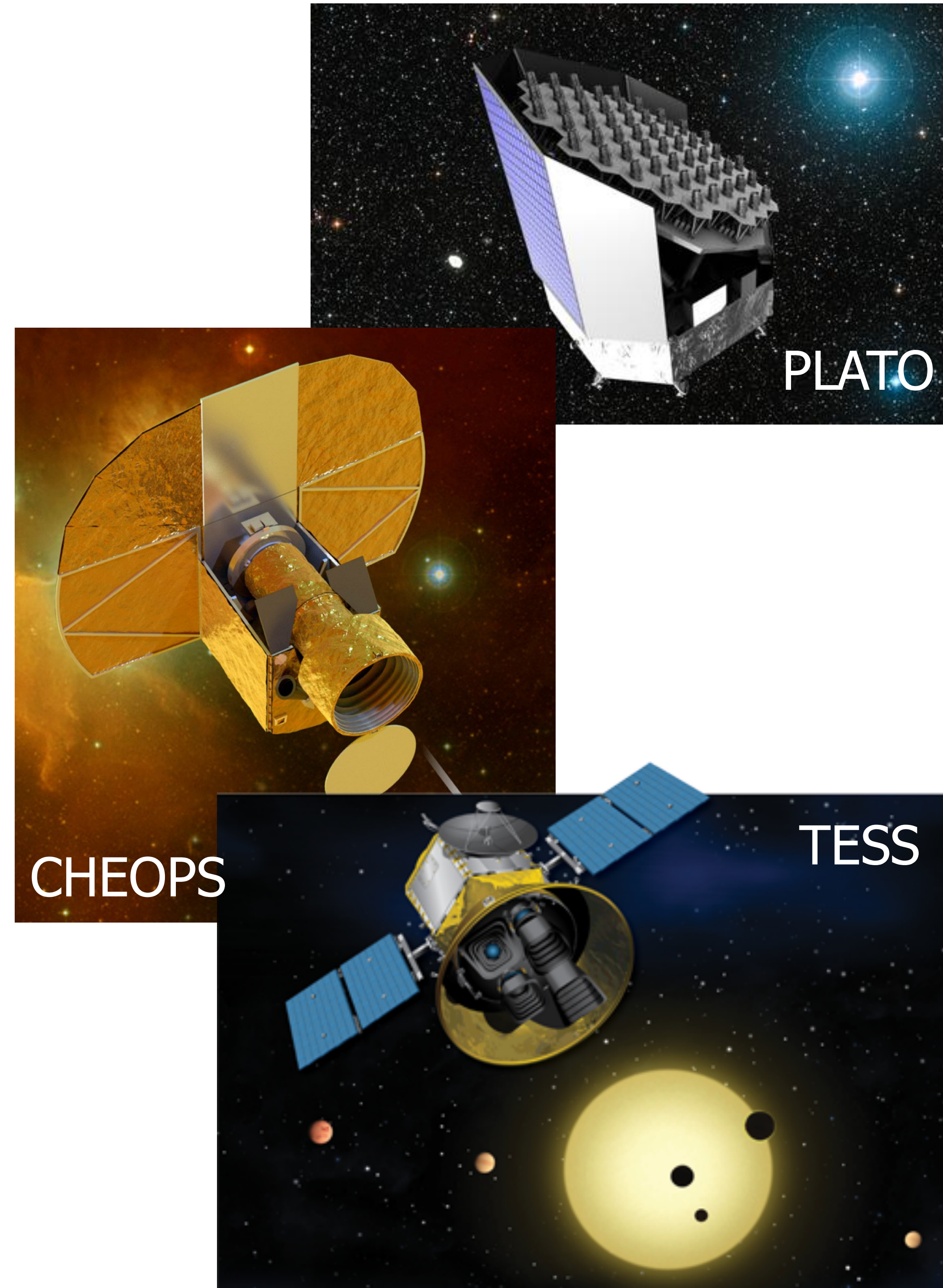

Indirect detection methods

Radial velocity method

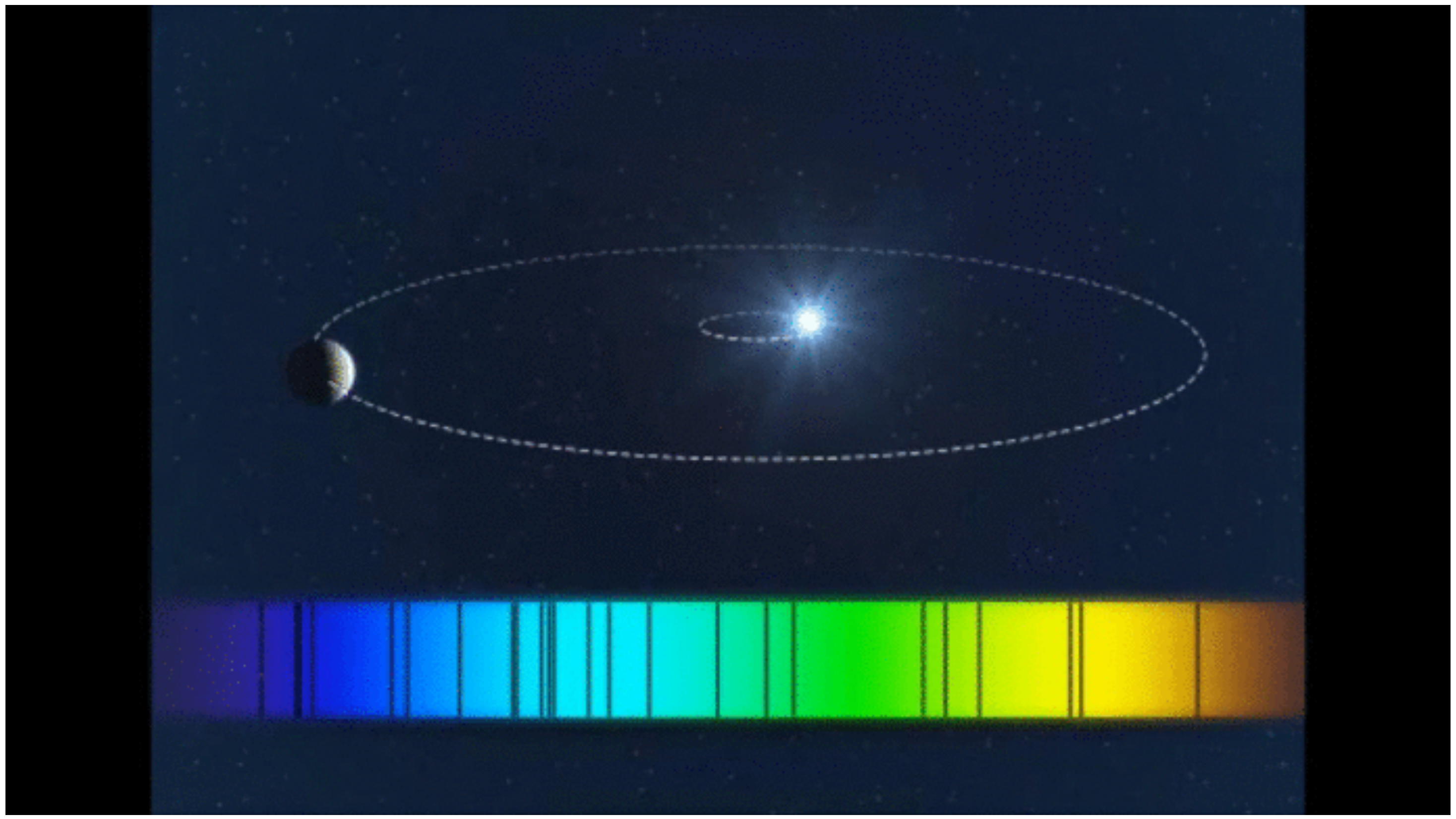

HARPS/La Silla

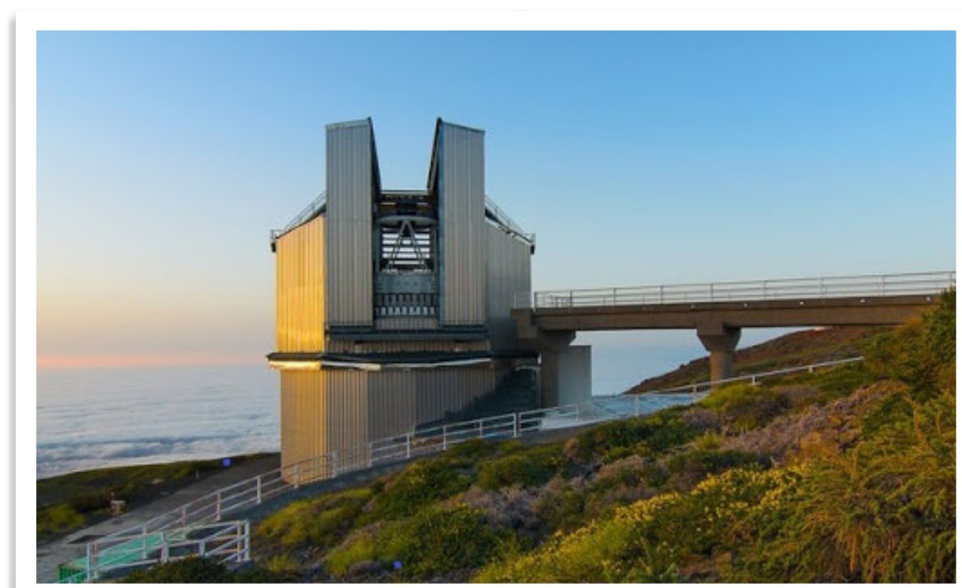

HARPS-N/TNG

$$\frac{(m_p \sin i)^3}{(M_\star + m_p)^2} = \frac{P}{2\pi G} K^3 (1 - e)^{3/2}$$

→ Knowing **M_p** depends on **$M_\star$**

Indirect detection methods

Radial velocity method

HARPS/La Silla

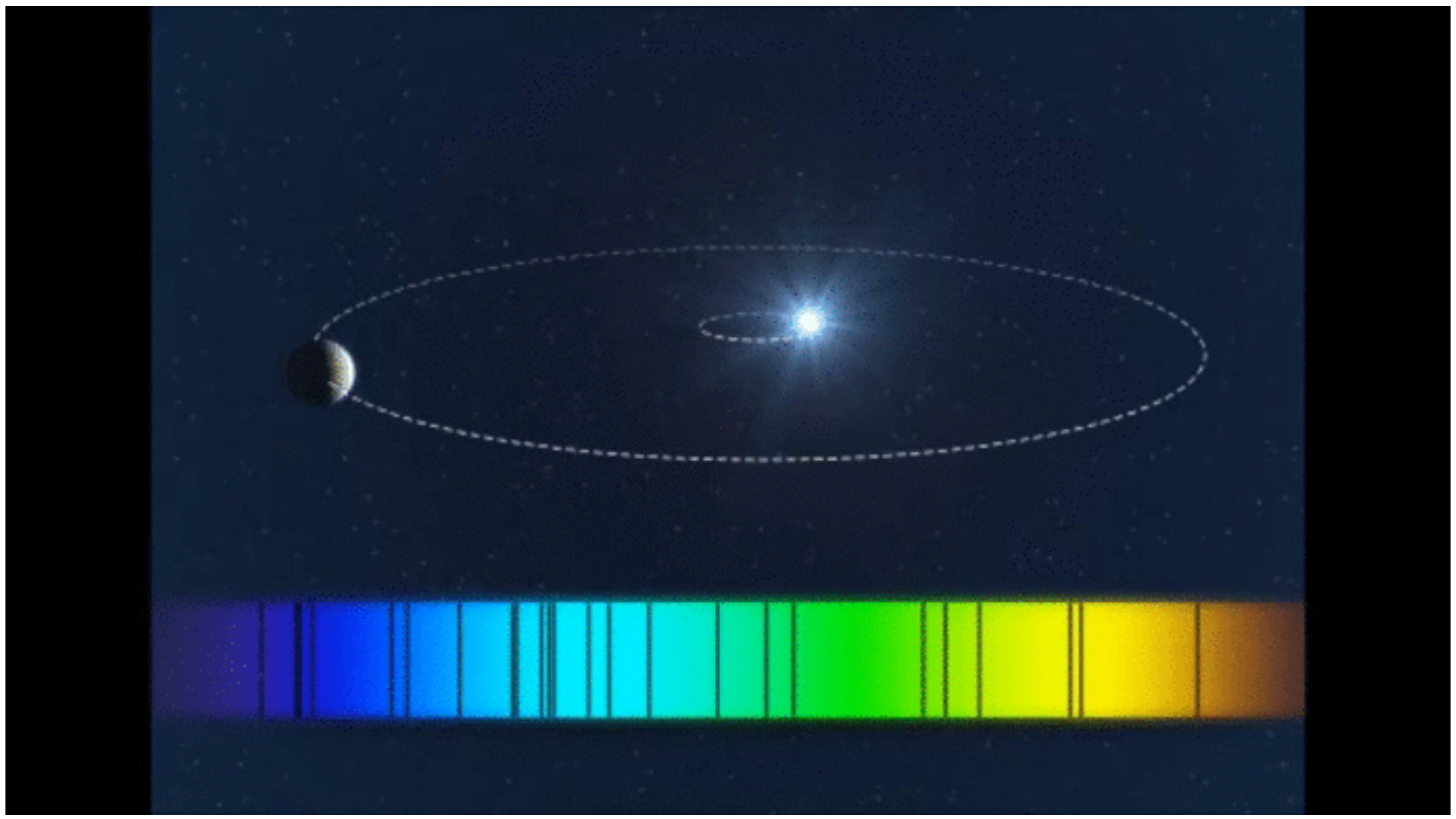

$$\frac{(m_p \sin i)^3}{(M_\star + m_p)^2} = \frac{P}{2\pi G} K^3 (1-e)^{3/2}$$

→ Knowing **M_p** depends on **$M_\star$**

HARPS-N/TNG

Direct detection method

Direct imaging

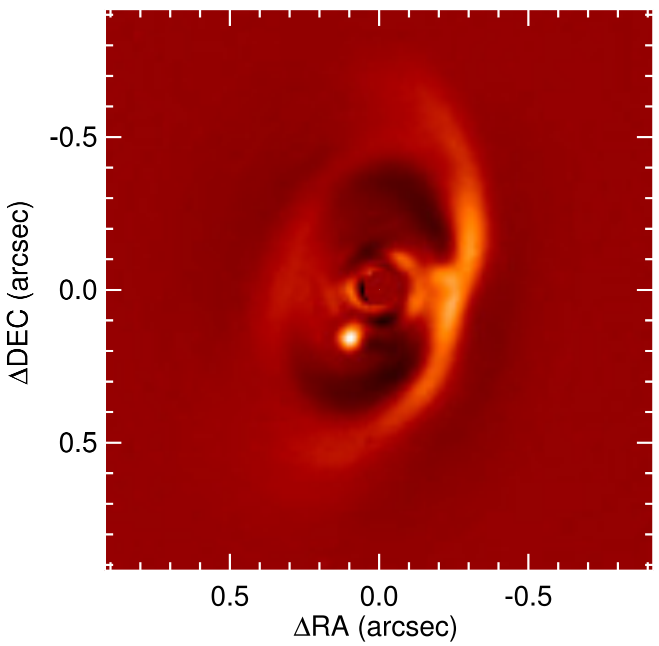

PDS70, SPHERE
Muller+ 2018

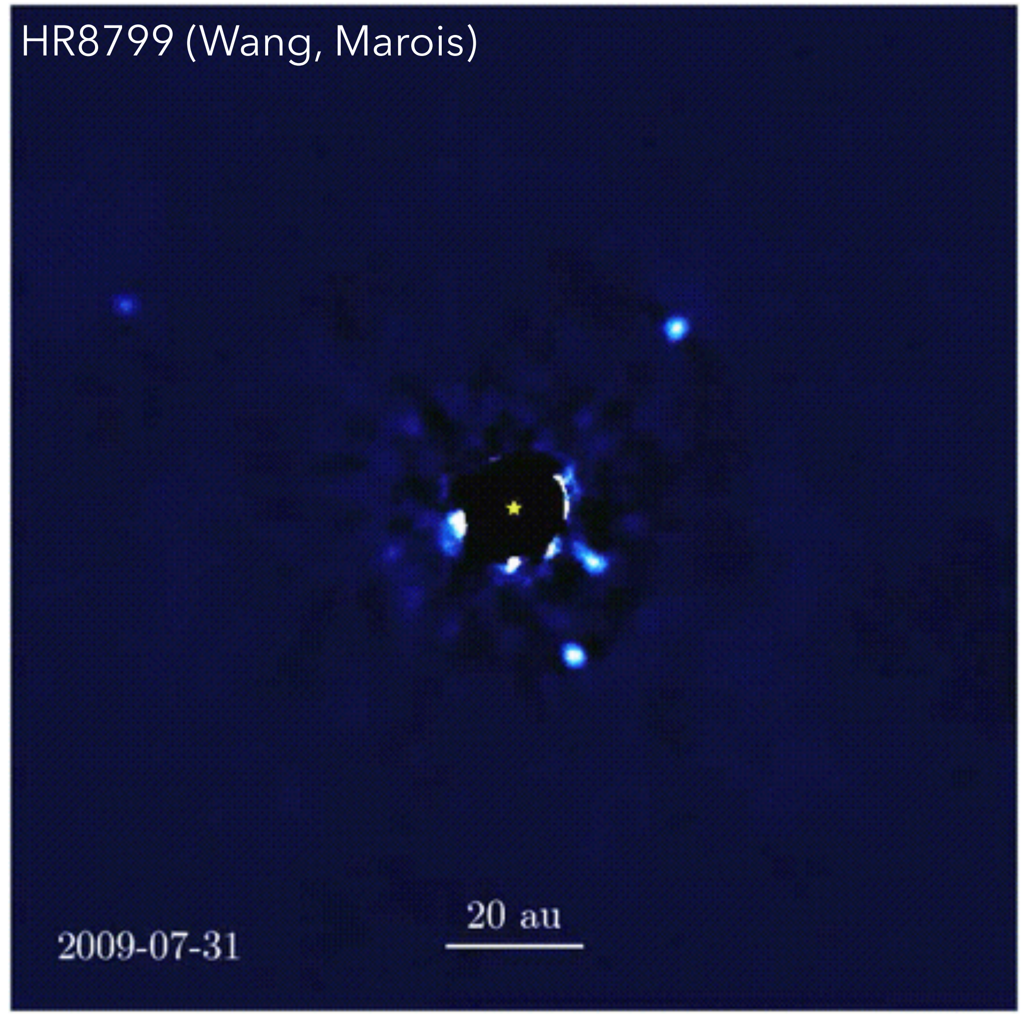

→ Need the stellar **age**

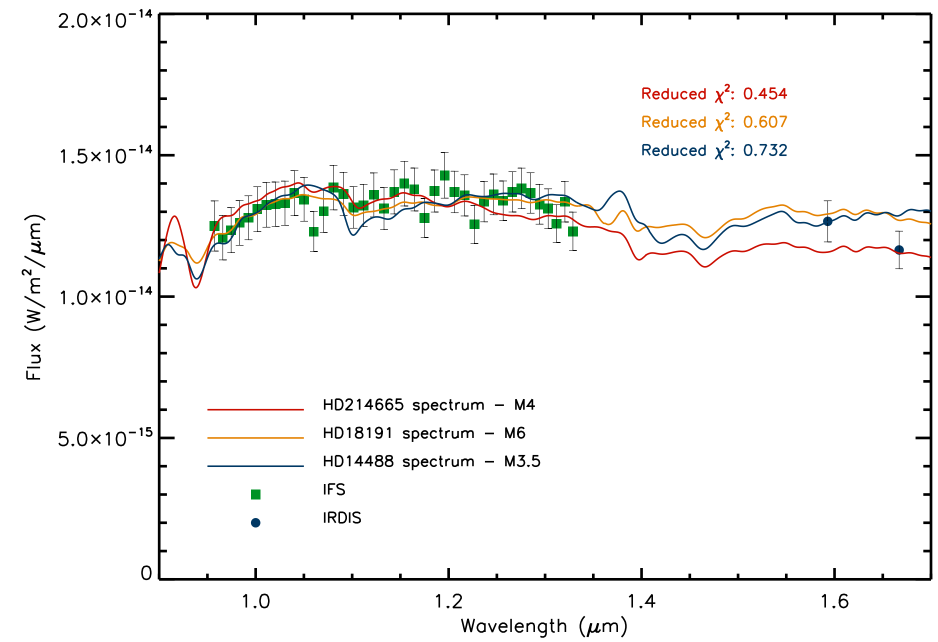

Ligi+ 2018b

H2 (1.593μm)

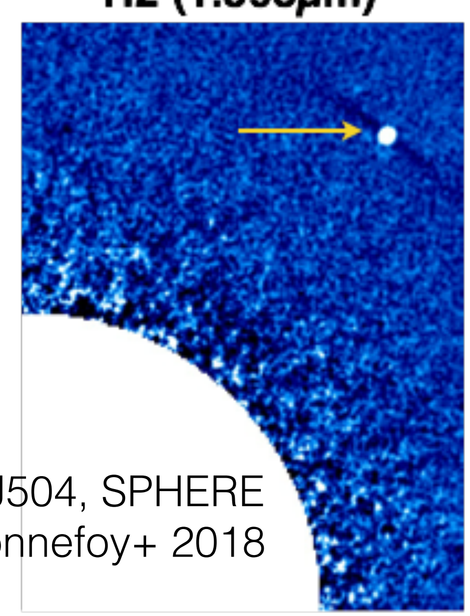

GJ504, SPHERE
Bonnefoy+ 2018

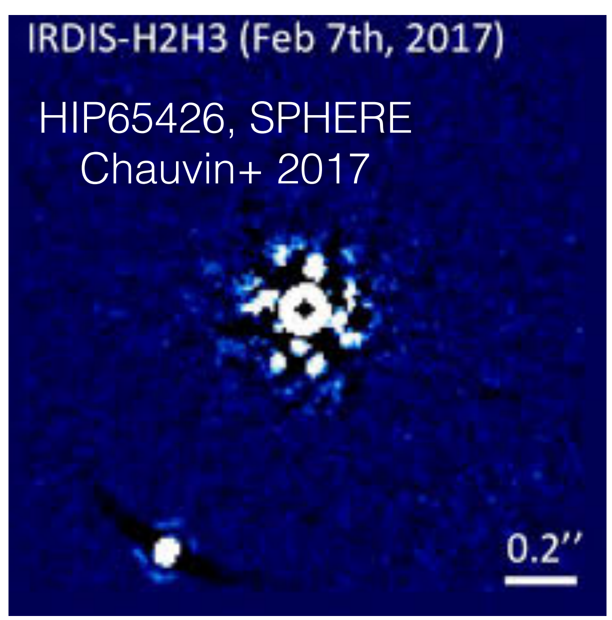

HIP65426, SPHERE
Chauvin+ 2017

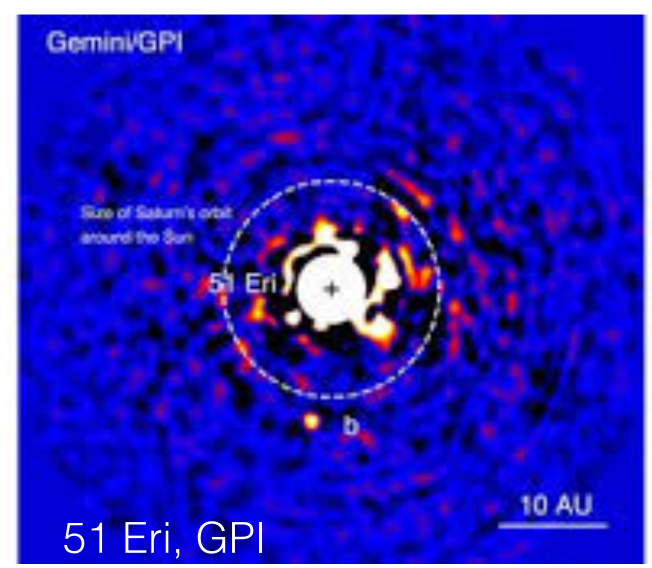

51 Eri, GPI
Macintosh+2015

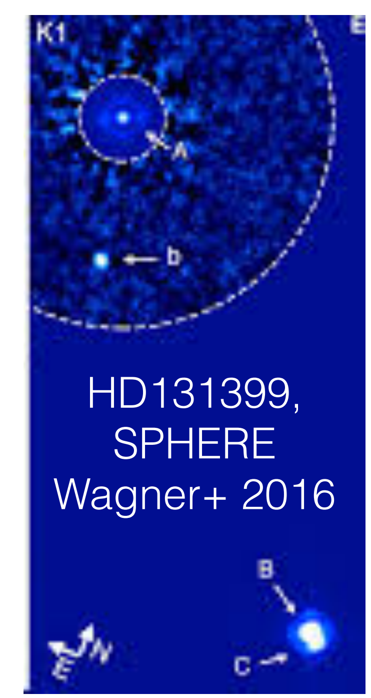

HD131399,
SPHERE
Wagner+ 2016

Direct detection method

Direct imaging

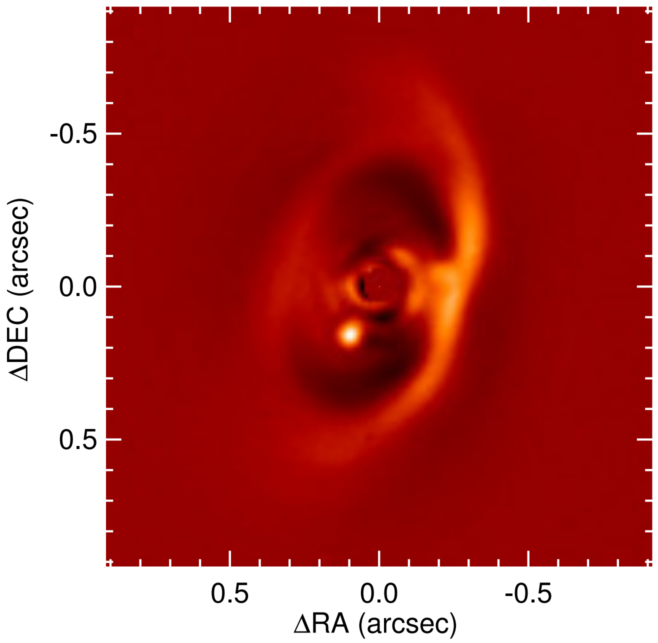

PDS70, SPHERE
Muller+ 2018

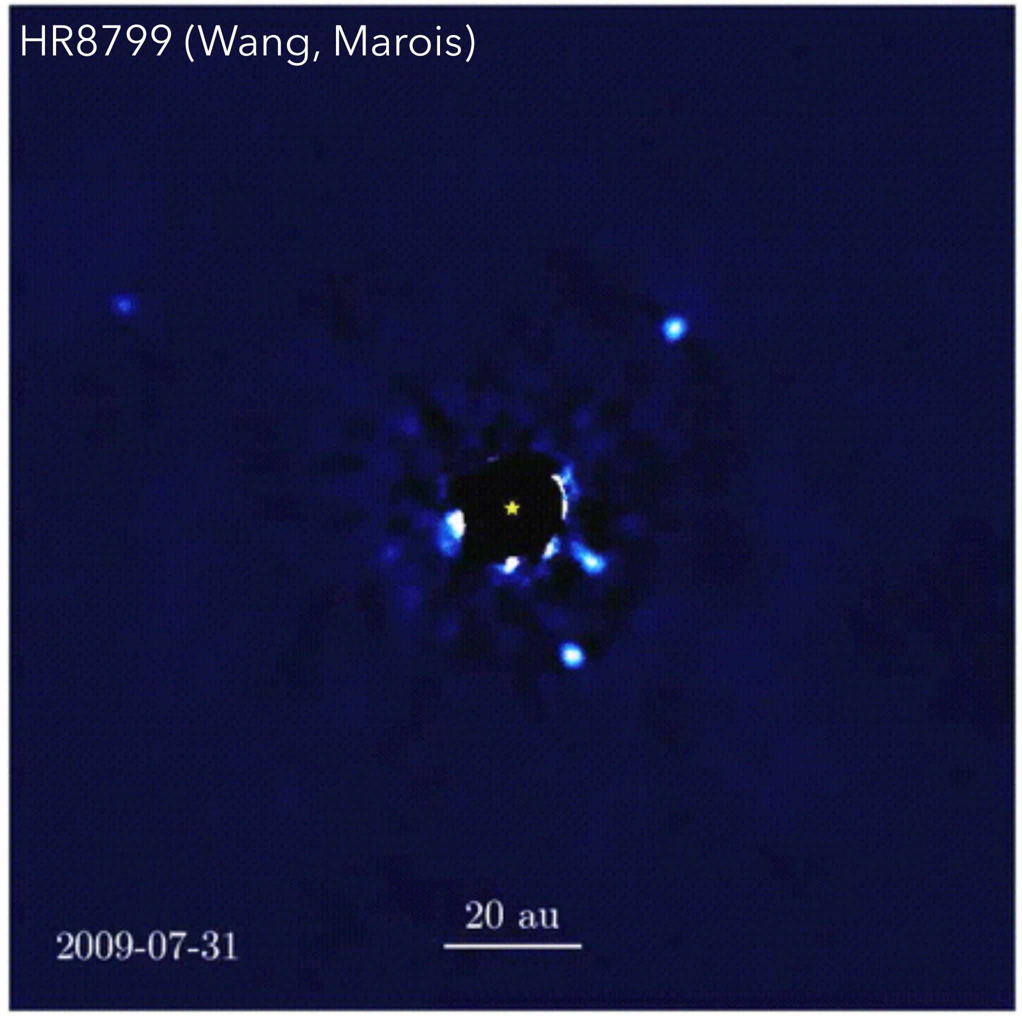

→ Need the stellar **age**

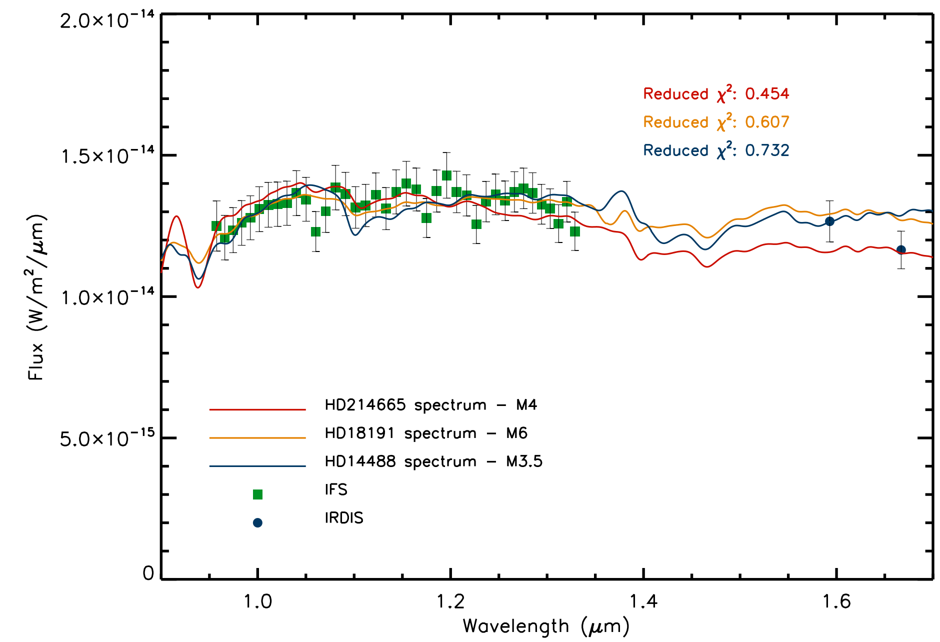

Ligi+ 2018b

H2 (1.593μm)

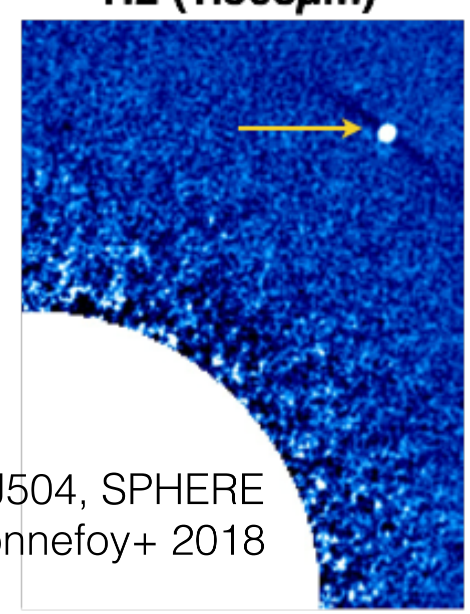

GJ504, SPHERE
Bonnefoy+ 2018

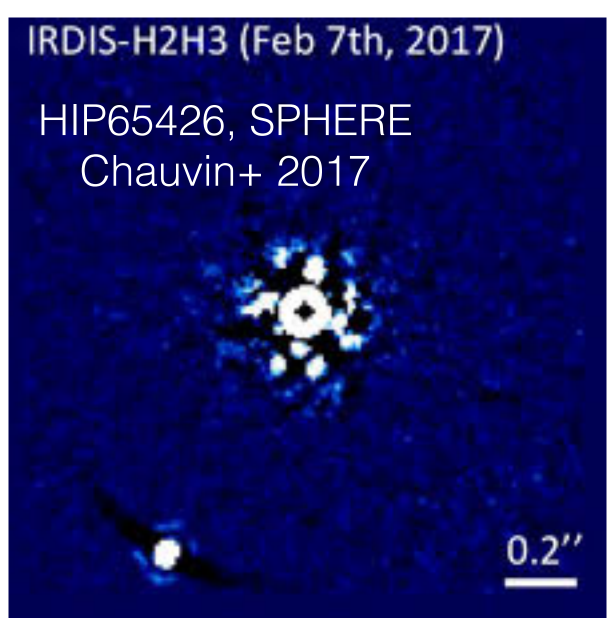

HIP65426, SPHERE
Chauvin+ 2017

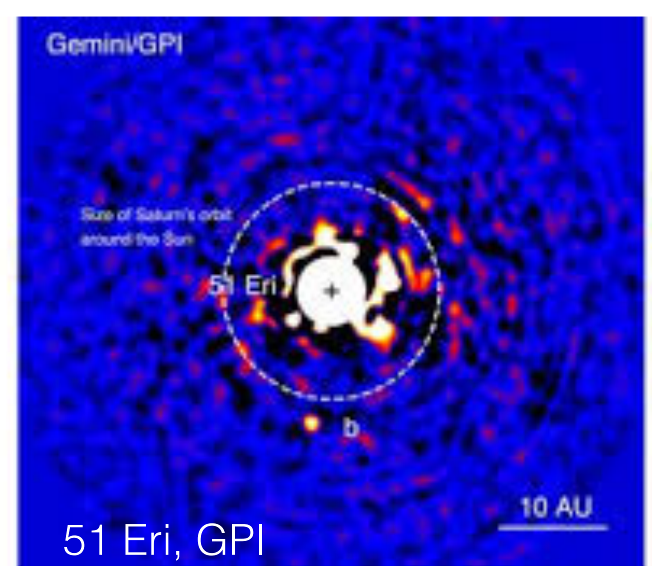

51 Eri, GPI
Macintosh+2015

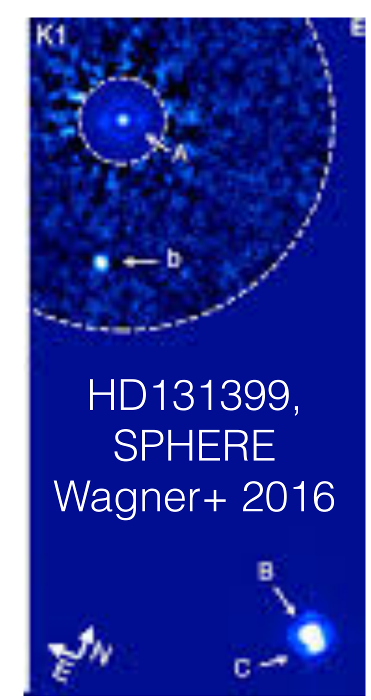

HD131399,
SPHERE
Wagner+ 2016

Internal composition of exoplanets

The internal composition of exoplanets is inferred from planetary interior models:

- Need parameters as inputs (stellar and planetary)
- Hint toward formation and habitability
- Suffer from degeneracy

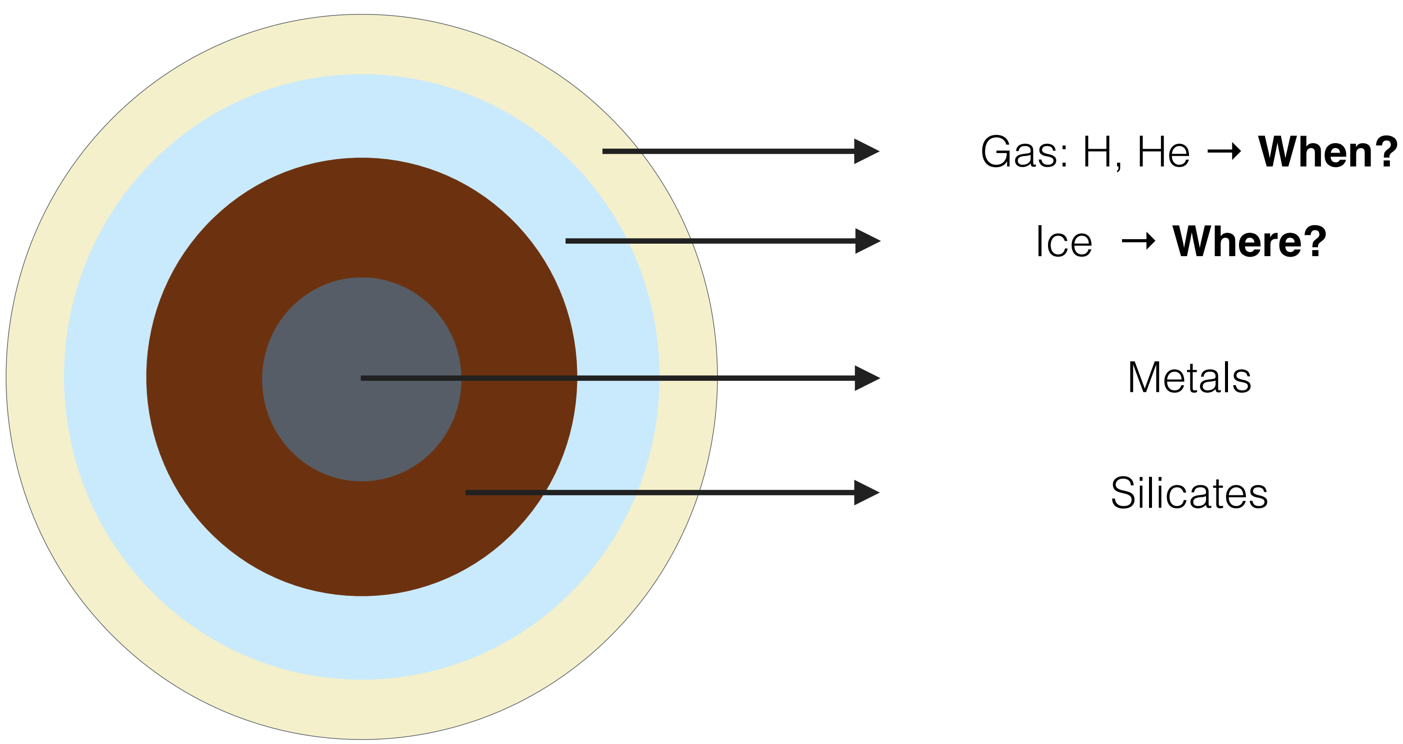

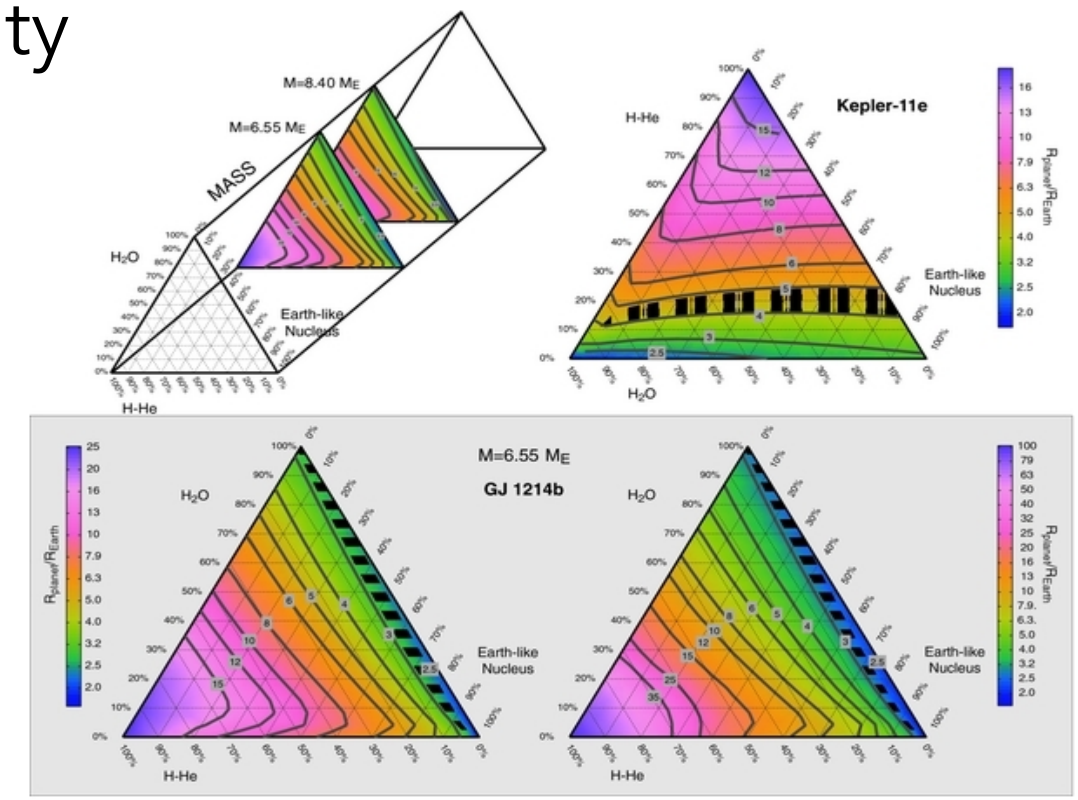

Valencia+ 2013
(Bulk Composition of GJ 1214b and Other Sub-Neptune Exoplanets)

Need ~2-3% precision on R_p to derive an internal structure

Habitable zone

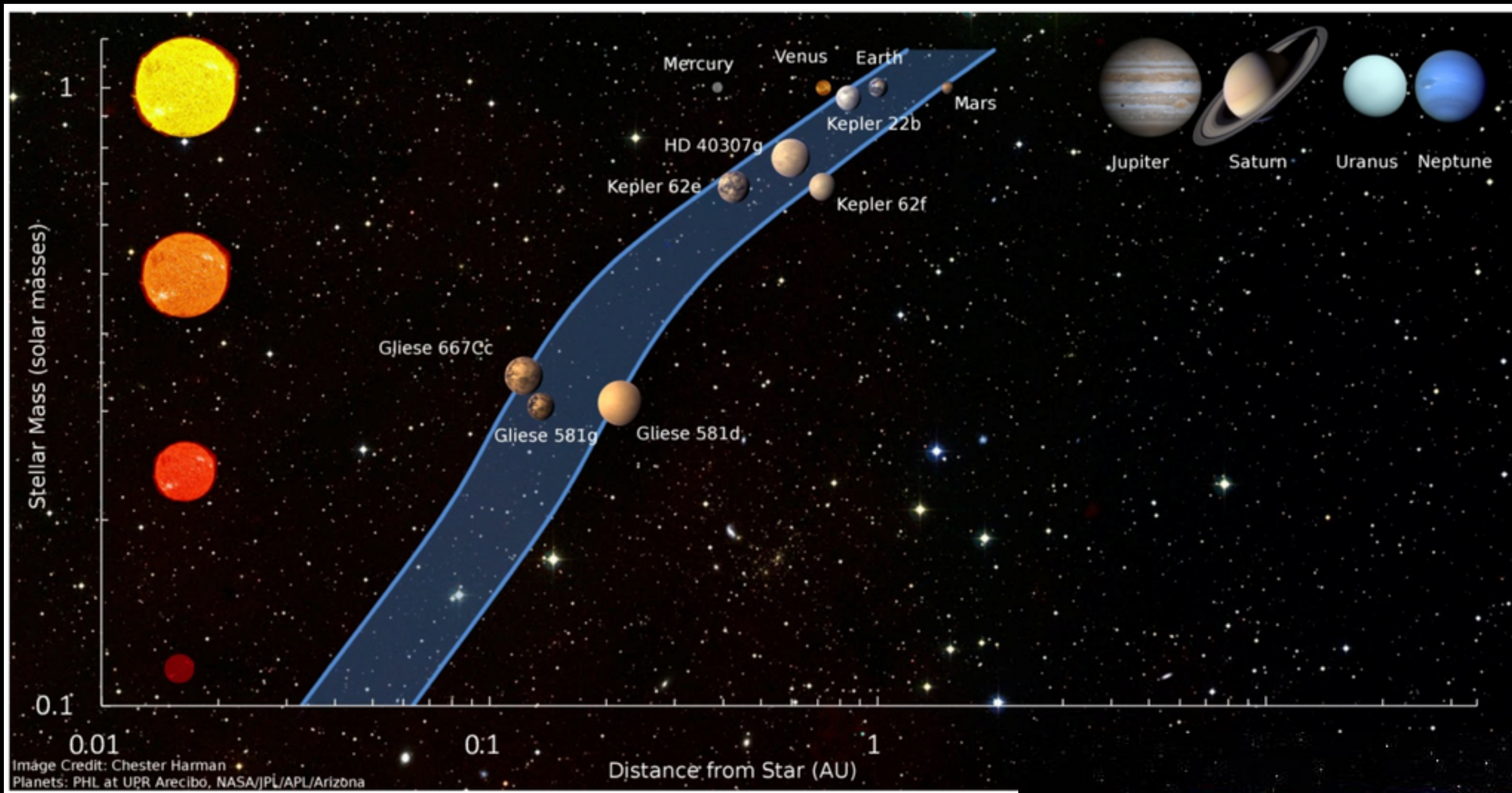

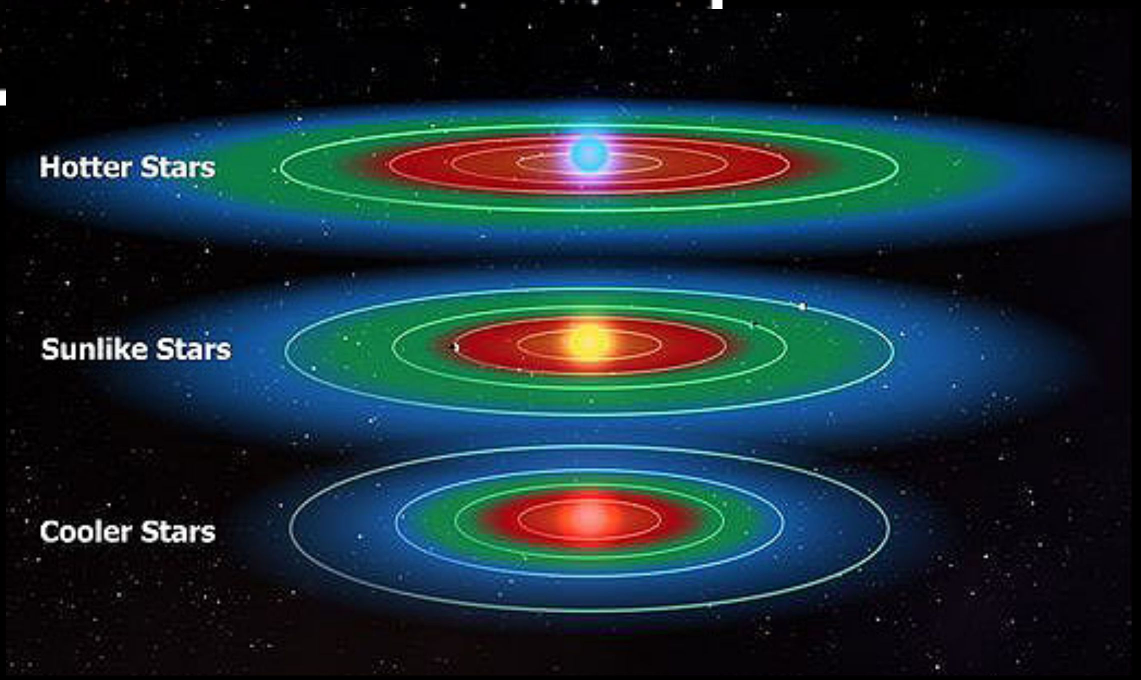

Find planets with suitable atmosphere and liquid water in the habitable zone

→ T_{eff}, $L_{\star}$

Links between exoplanets occurence and stars

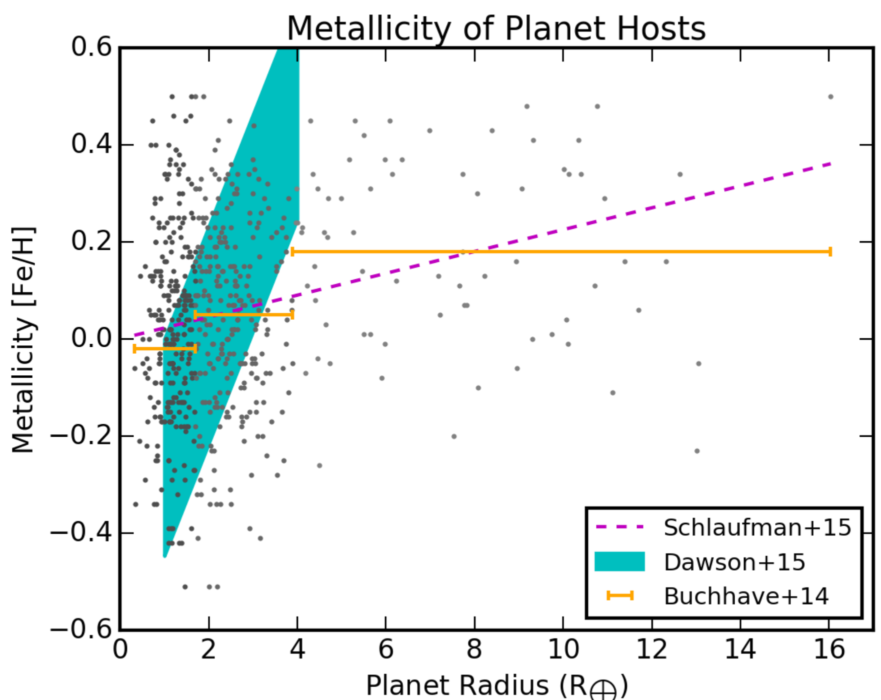

Mulders+ 2018

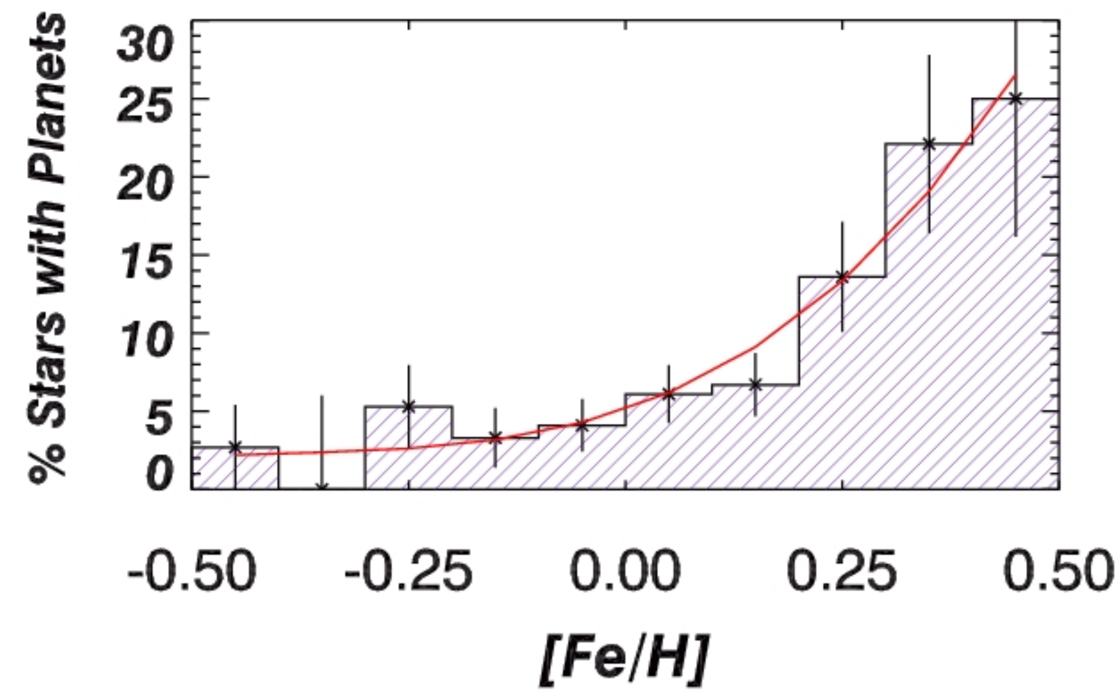

Fischer & Valenti 2005

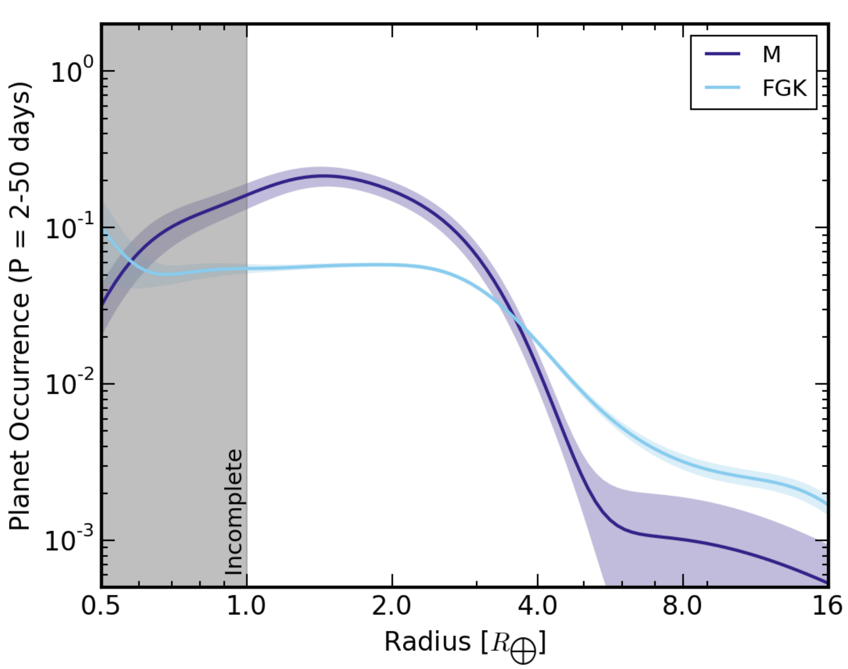

Mulders+ 2018

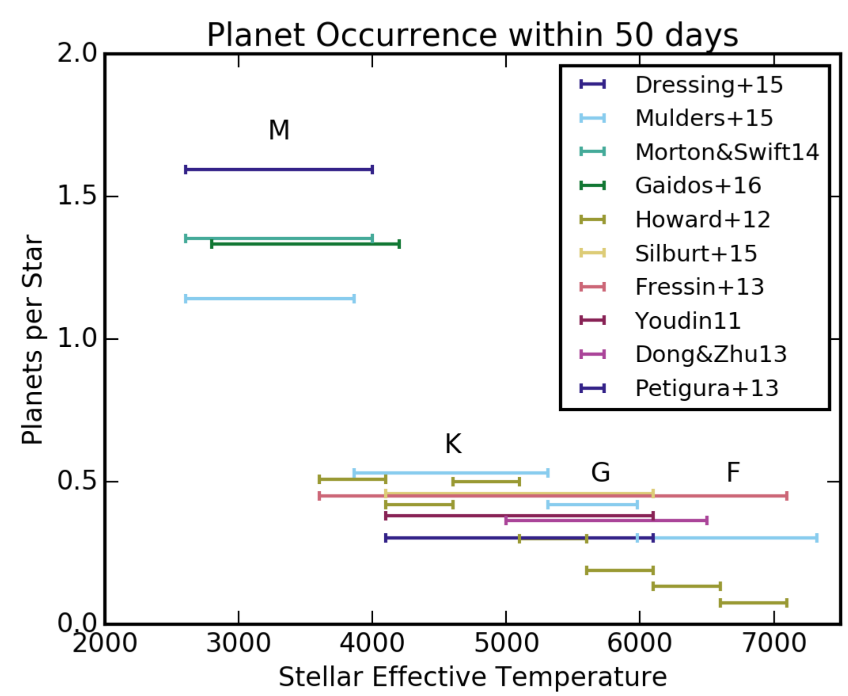

Mulders+ 2015c

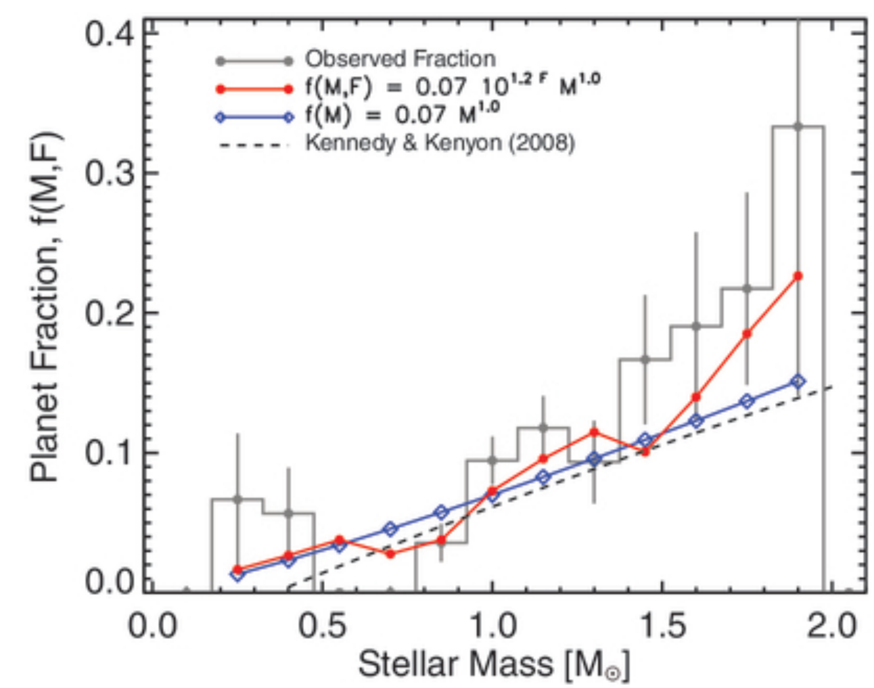

Johnson+ 2010

Stellar parameters dependence

Stellar parameters drive our knowledge of exoplanets.

- Direct and indirect methods do not provide the same observables.
- Need of stellar parameters to derive exoplanets properties.
- The « basic » planetary parameters depend on the stellar mass, radius, density…
- Often, need of a model to derive additional parameters, that are important to characterize the system (like the stellar age).
- Open questions on the link between stellar parameters and exoplanets population.

Interferometry can help in this context by providing stellar parameters.

$$T_{\rm env} = \alpha T_{\rm eff} \sqrt{\frac{R_\star}{2a}}$$

$$\frac{(m_p \sin i)^3}{(M_\star + m_p)^2} = \frac{P}{2\pi G} K^3 (1-e)^{3/2}$$

$$\frac{\Delta F}{F} = \left(\frac{R_P}{R_\star}\right)^2$$

See Dan and Orlagh's talks!

INTERFEROMETRY

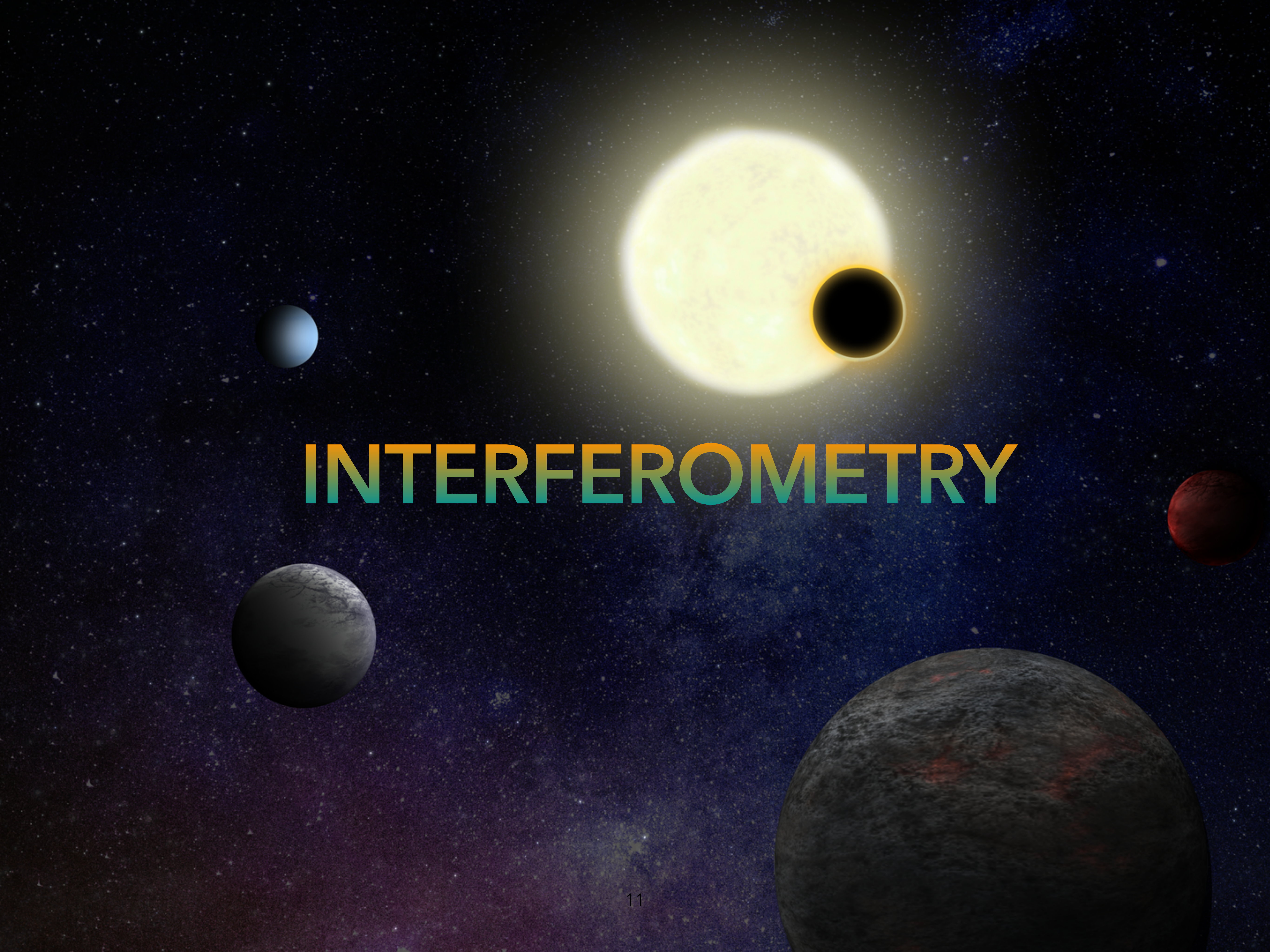

Interferometers worldwide

CHARA

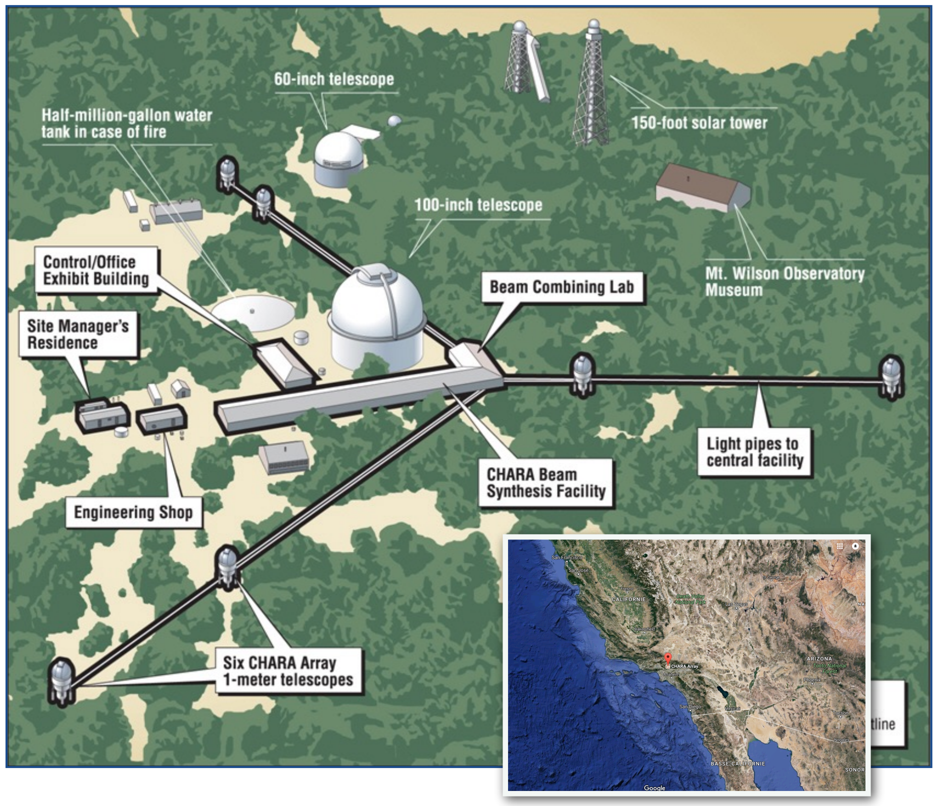

SUSI

NPOI

VLTI

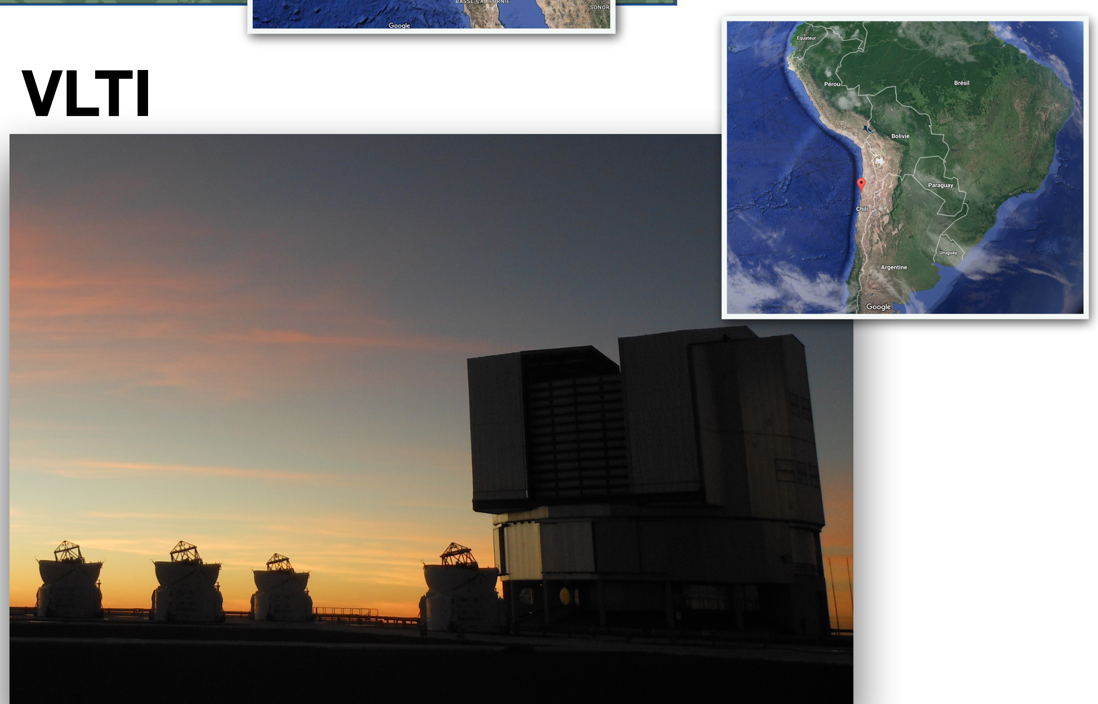

Principles of interferometry

Classical telescope

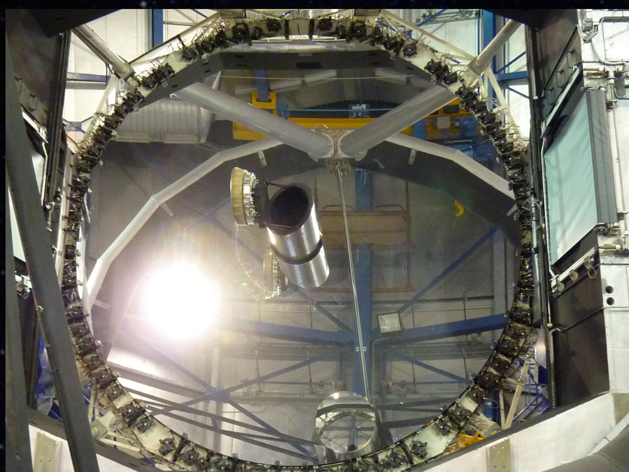

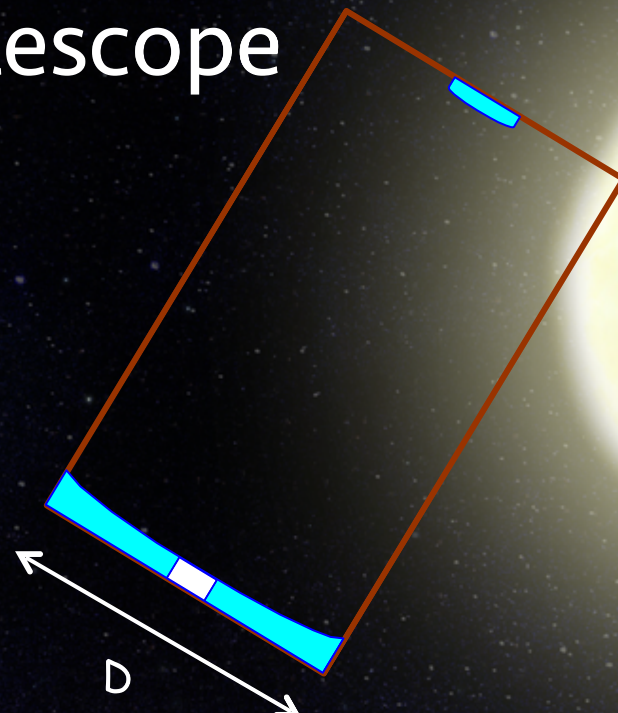

Angular resolution
$\approx \lambda/D$

➜ larger sensitivity
➜ fainter objects

Interferometer

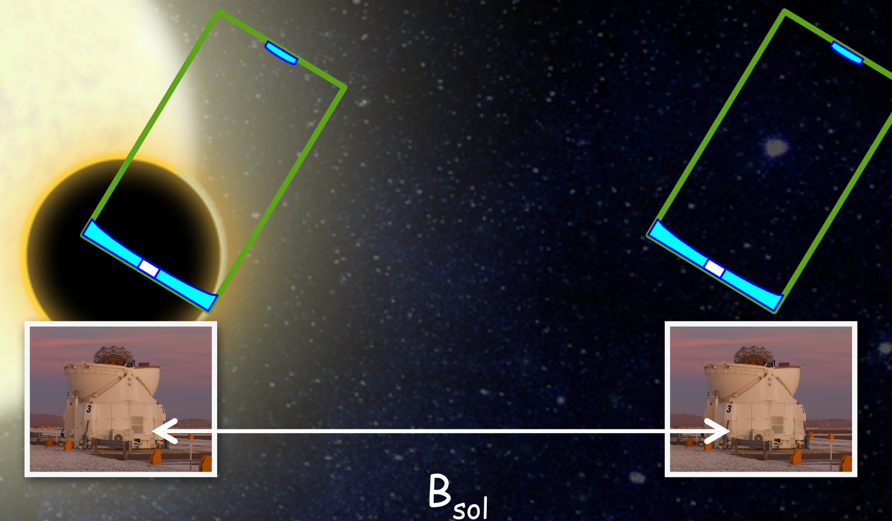

Angular resolution
$\approx \lambda/B$

➜ larger resolution
➜ smaller objects

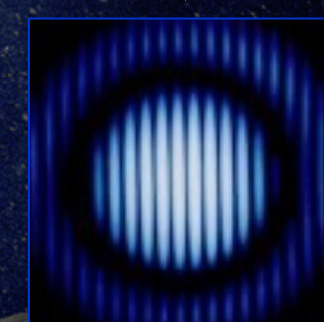

Inter-fringes λ/B

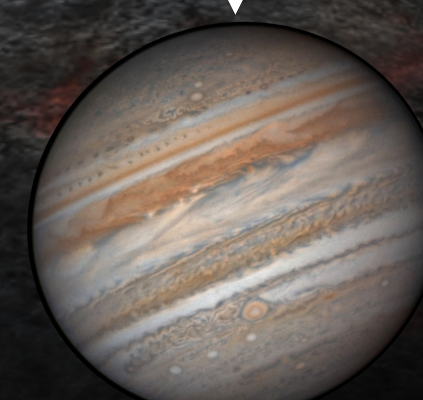

Principles of interferometry

I =  $\otimes$ 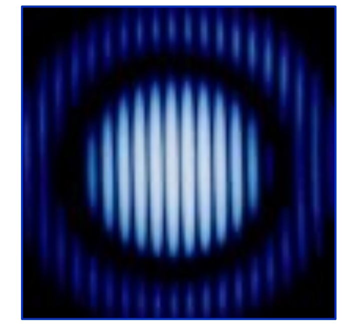

Contrast of fringes
= Complex visibility (V)
= FT of the surface brightness distribution of the star

(van Cittert-Zernike theorem)

I = **O** $\otimes$ **PSF**

TF(**I**) = TF(**O**) x TF(**PSF)**

TF(**I**) = V(**B**) = $|\gamma(0)|$

Phase Φ

Modulus |V|

In the case of a uniform disk:

$$V_\lambda{}^2\left(\frac{B}{\lambda}\right) = 4\left|\frac{J_1(z)}{z}\right|^2 \qquad \text{with} \qquad z = \pi\theta_{UD}\,{}^{B}/_{\lambda}$$

angular diameter of the star

Principles of interferometry

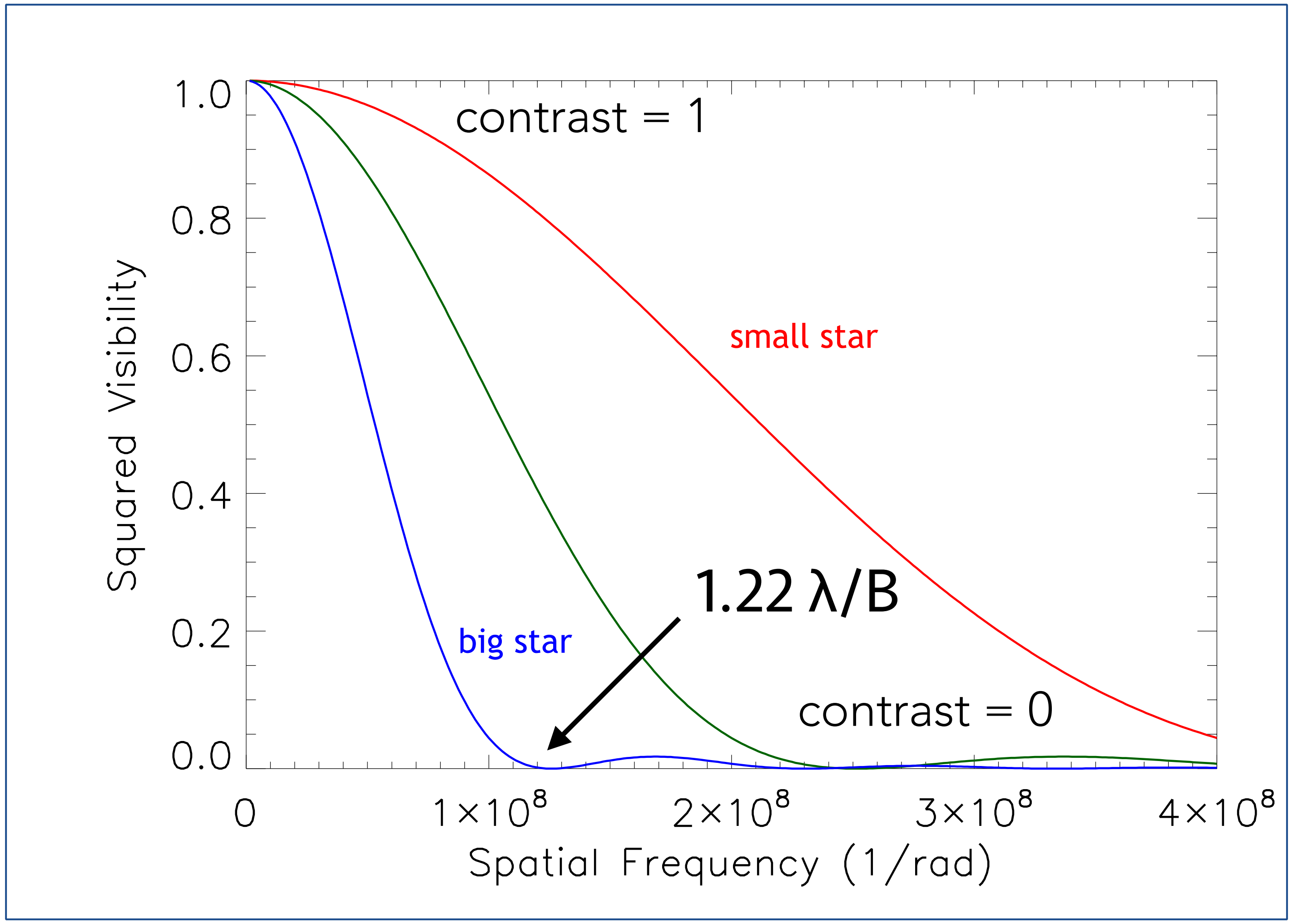

Point source → contrast = 1 (Young).

Extended source
→ several fringe patterns which don't overlap exactly
→ contrast < 1, depends on telescope separation (baseline).

Principles of interferometry

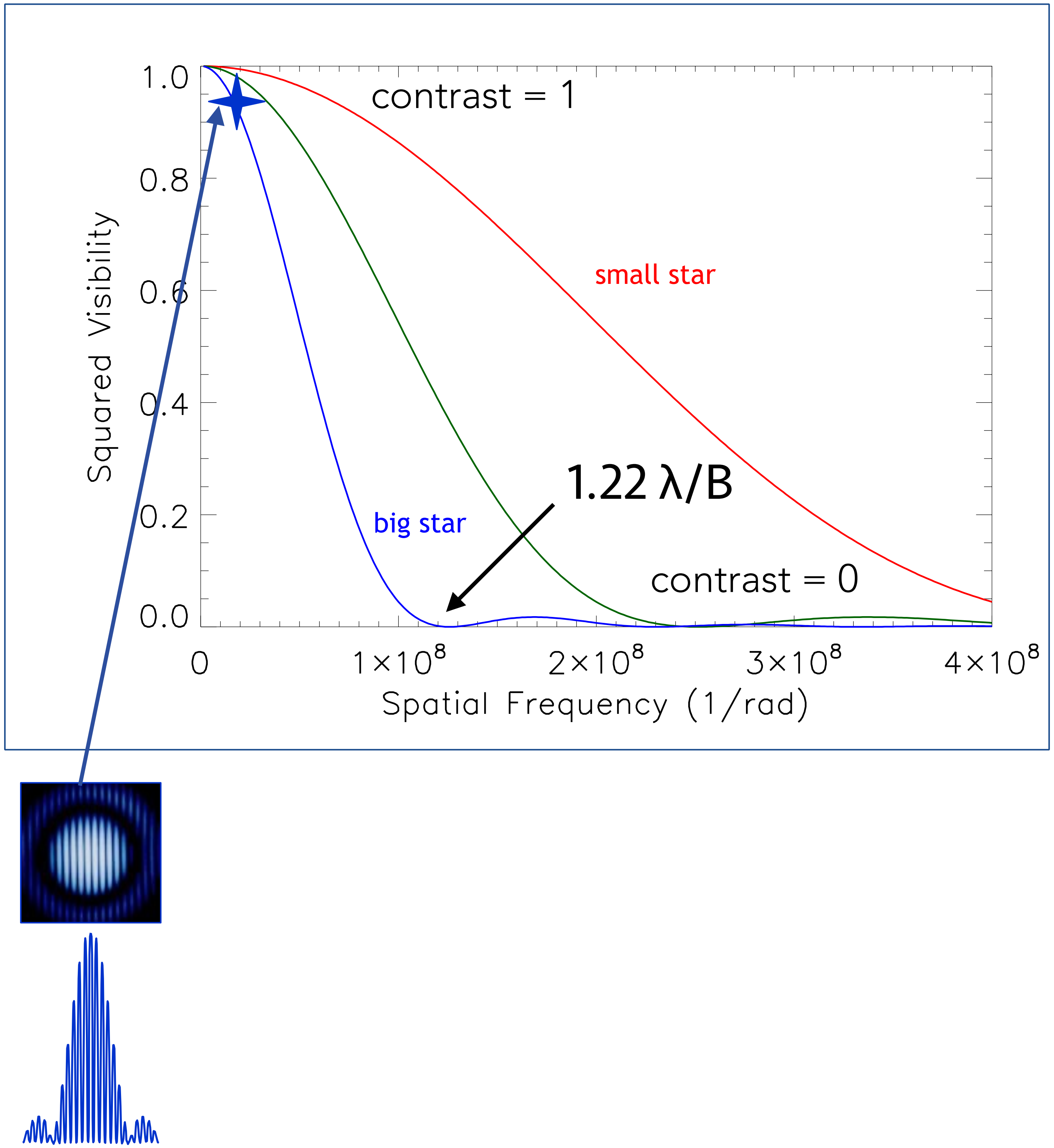

Point source → contrast = 1 (Young).

Extended source
→ several fringe patterns which don't overlap exactly
→ contrast < 1, depends on telescope separation (baseline).

Principles of interferometry

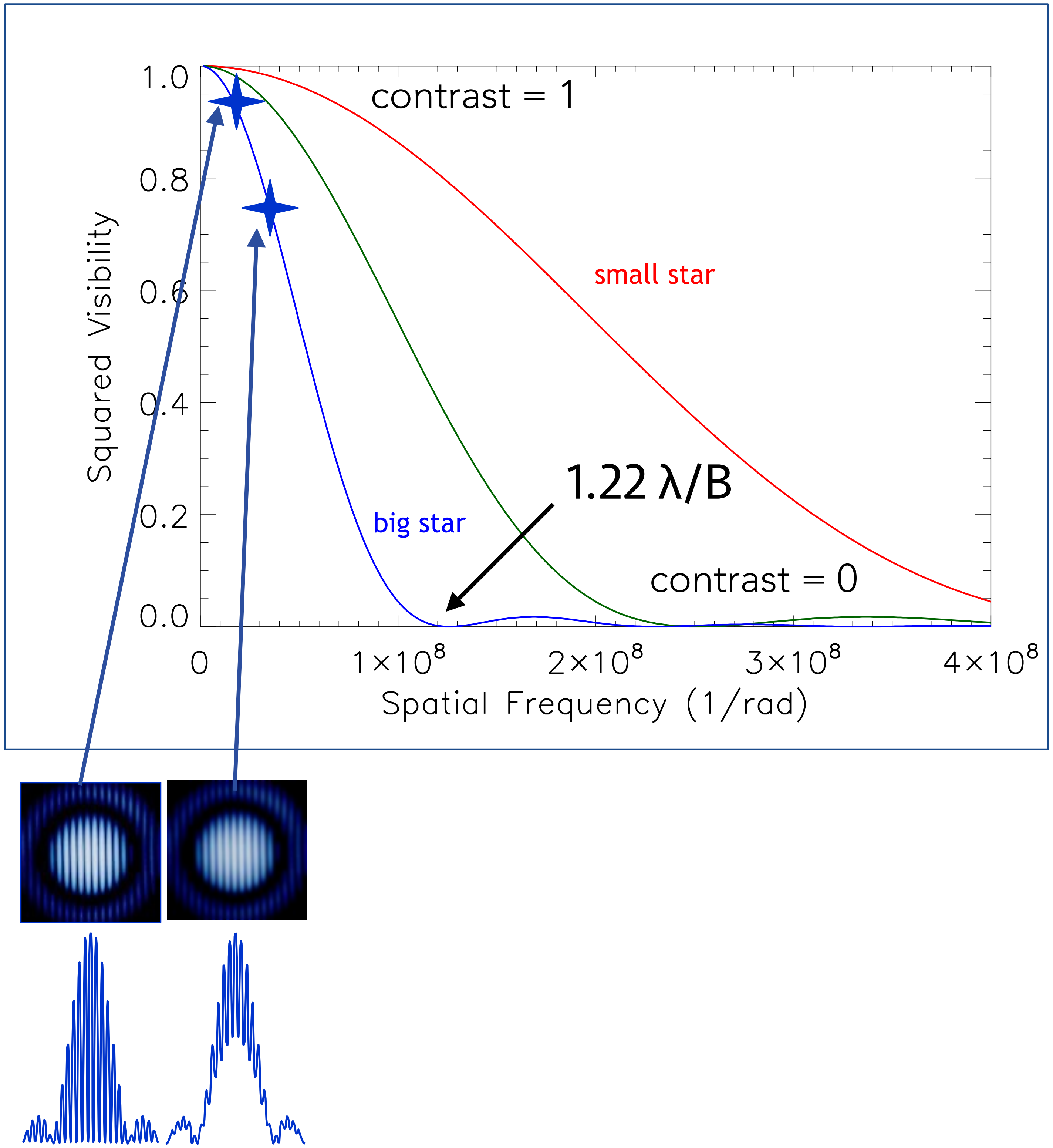

Point source → contrast = 1 (Young).

Extended source
→ several fringe patterns which don't overlap exactly
→ contrast < 1, depends on telescope separation (baseline).

Principles of interferometry

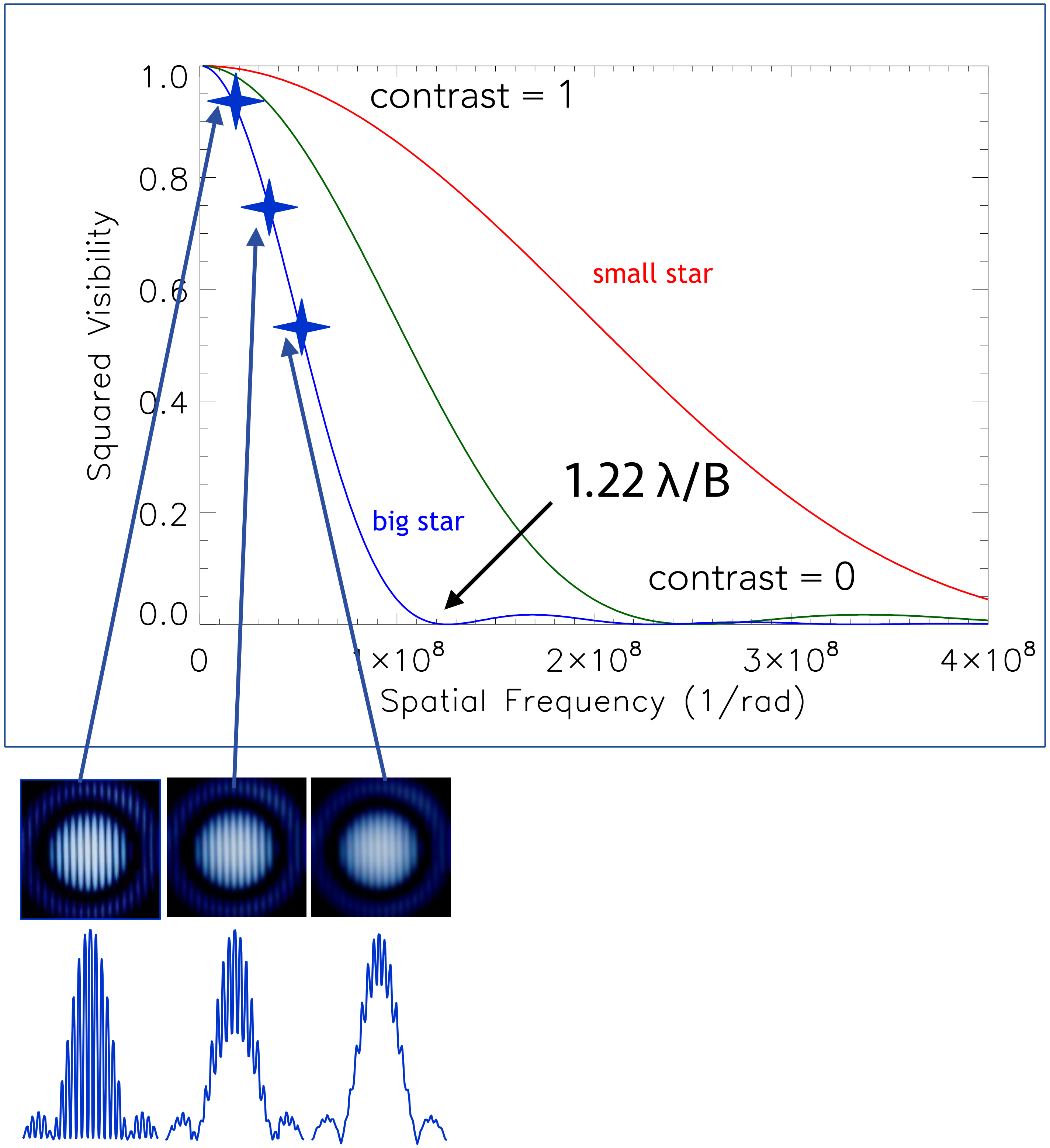

Point source → contrast = 1 (Young).

Extended source
→ several fringe patterns which don't overlap exactly
→ contrast < 1, depends on telescope separation (baseline).

Principles of interferometry

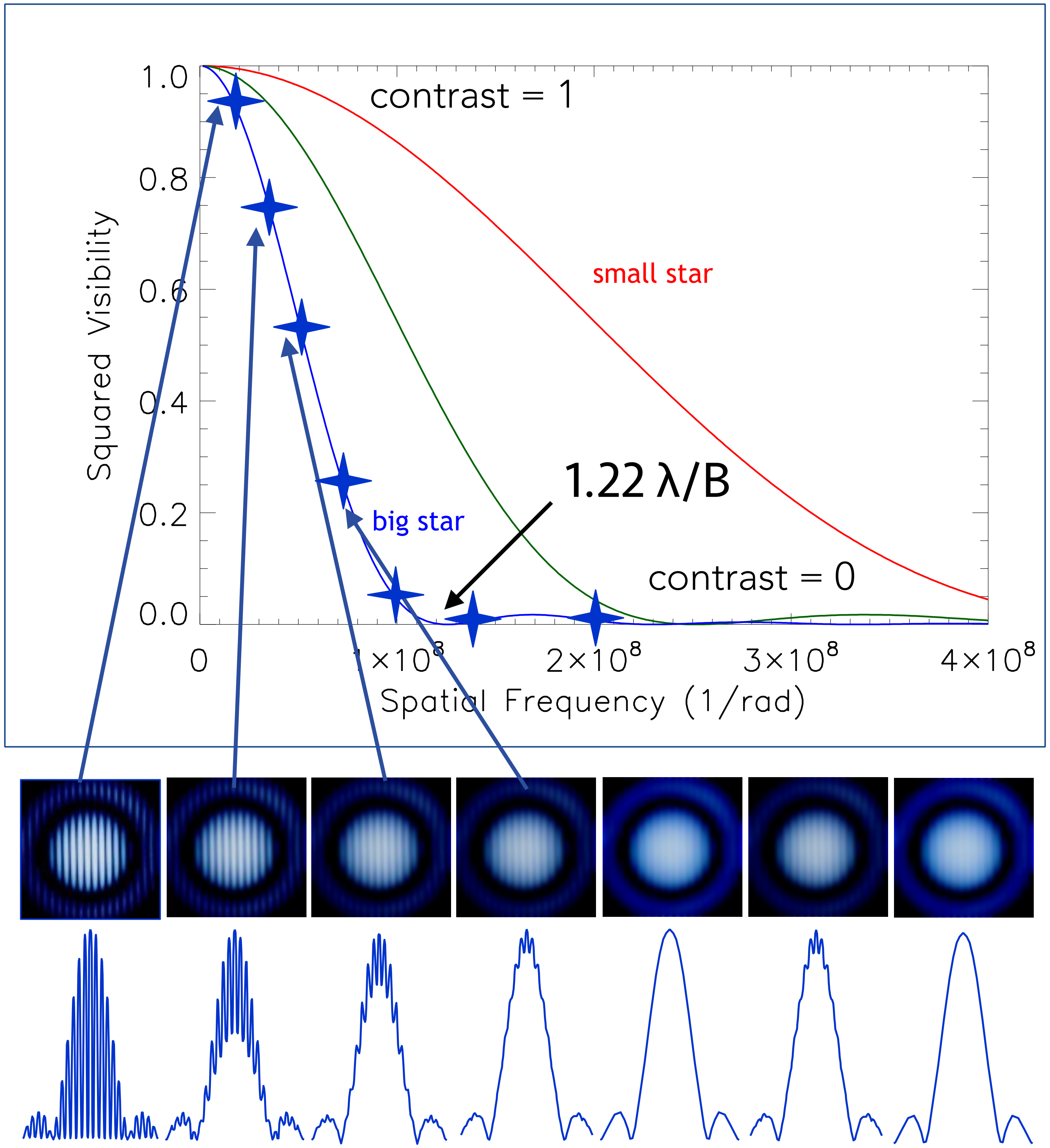

Point source → contrast = 1 (Young).

Extended source
→ several fringe patterns which don't overlap exactly
→ contrast < 1, depends on telescope separation (baseline).

Principles of interferometry

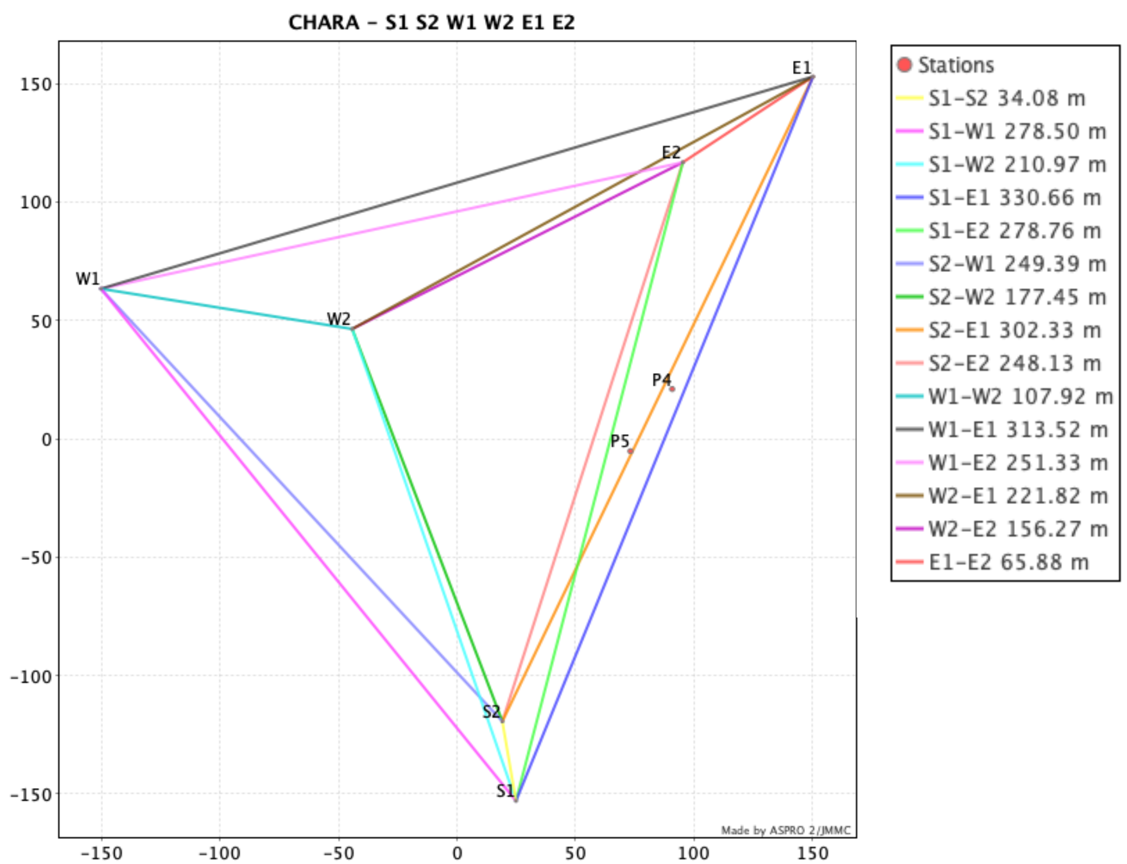

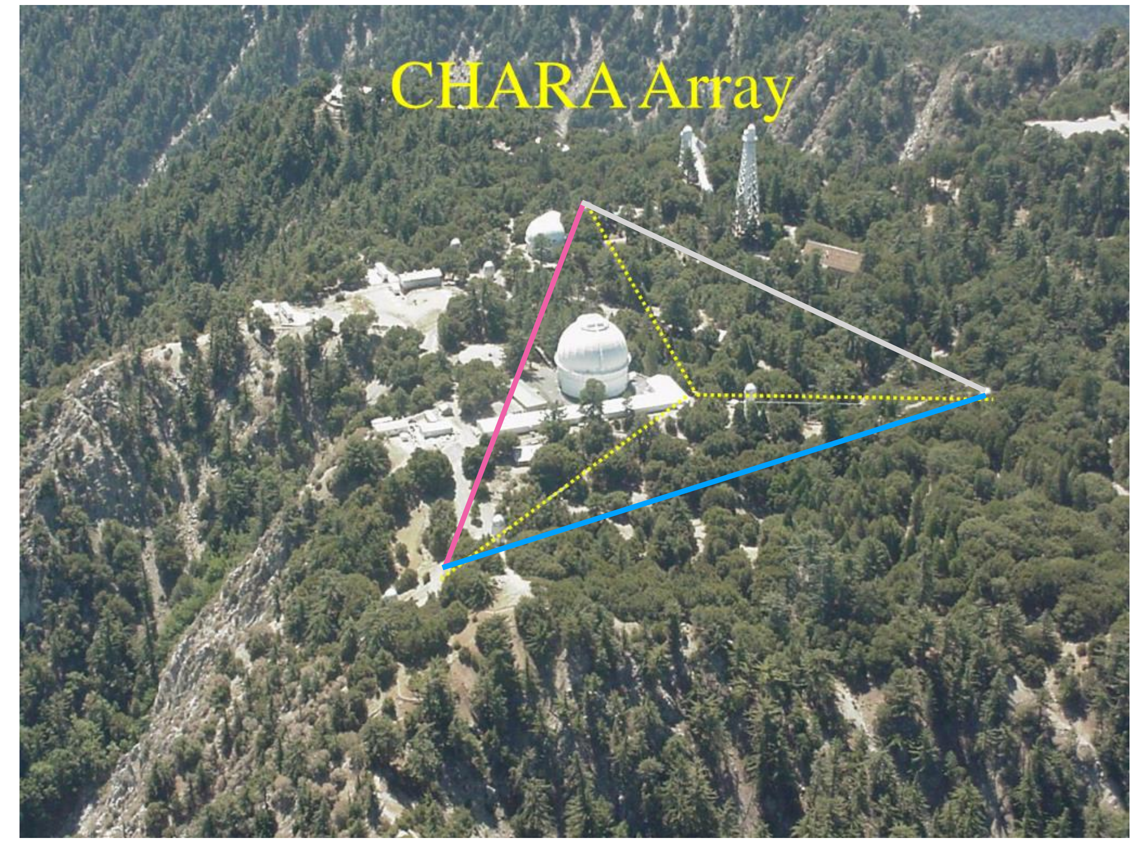

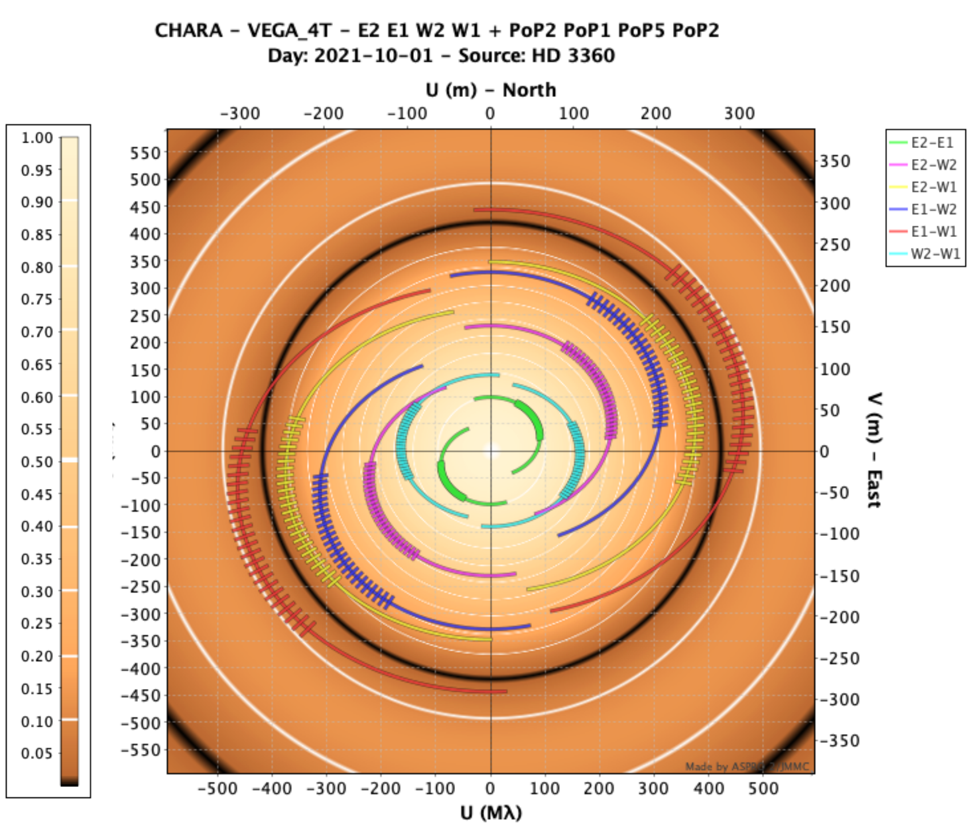

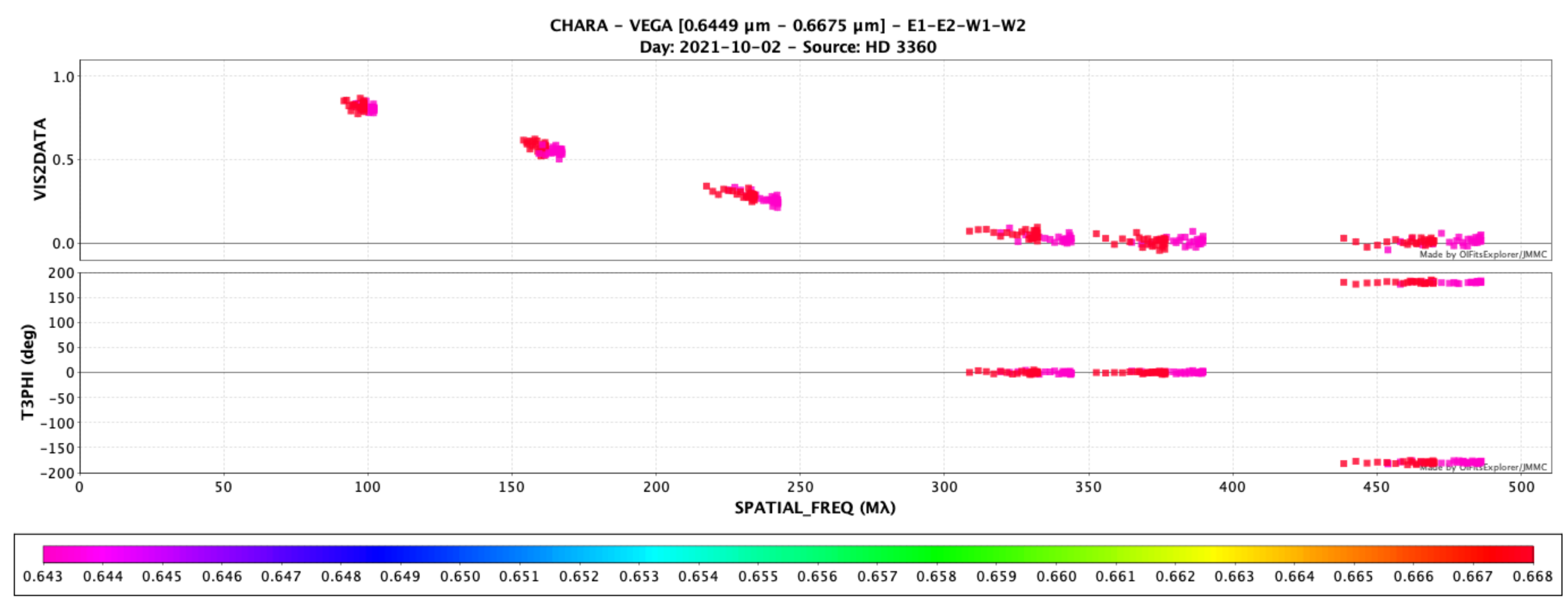

Aspro2 (JMMC)

The problem of limb-darkening

Claret & Bloemen 2011

the linear law

$$\frac{I(\mu)}{I(1)} = 1 - u(1-\mu),$$

the quadratic law

$$\frac{I(\mu)}{I(1)} = 1 - a(1-\mu) - b(1-\mu)^2,$$

the square root law

$$\frac{I(\mu)}{I(1)} = 1 - c(1-\mu) - d(1-\sqrt{\mu}),$$

the logarithmic law

$$\frac{I(\mu)}{I(1)} = 1 - e(1-\mu) - f\mu\ln(\mu),$$

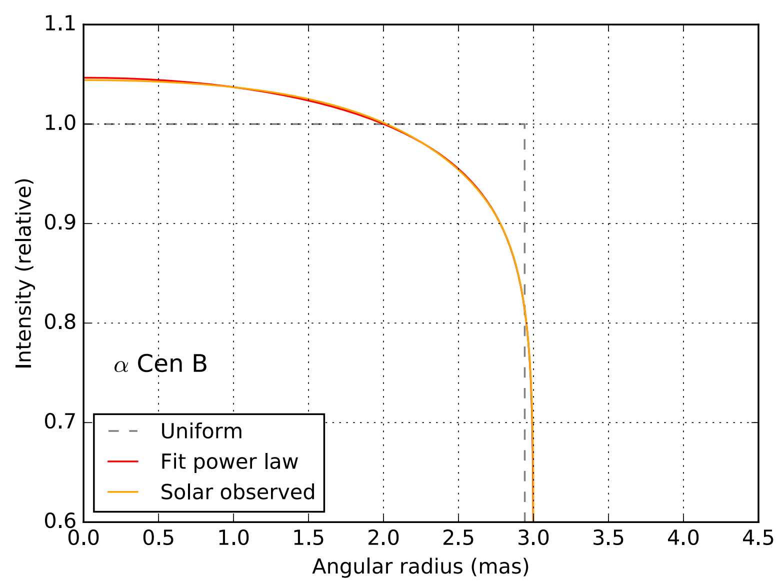

Fig. 9. Comparison of the best-fit power law intensity profiles of α Cen A and B (red curves) with the observed solar profile in the H band (orange curves) measured by Pierce et al. (1977). The horizontal scale is the same for both diagrams to show the difference in size of the two stars.

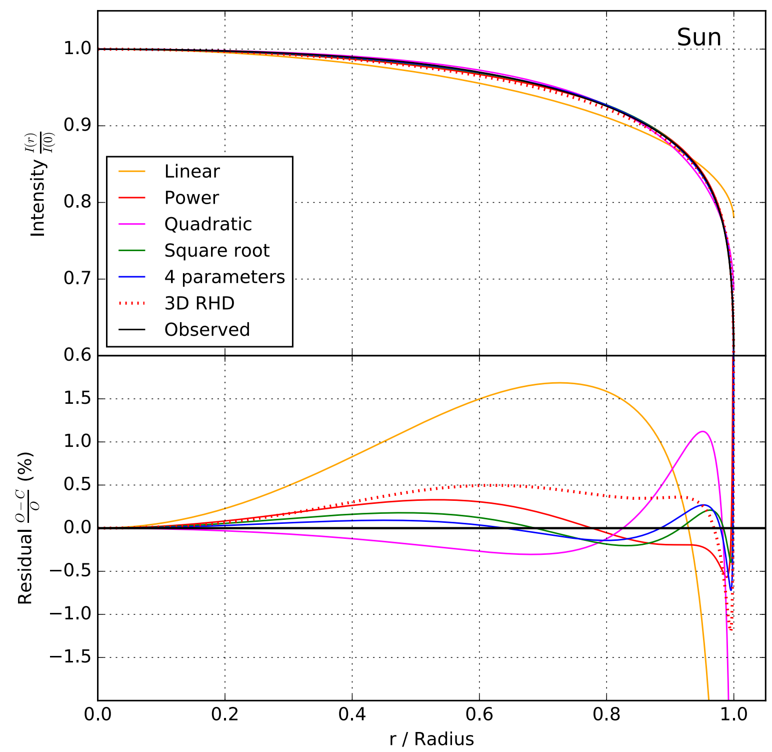

Fig. 2. Comparison of different parametric limb darkening models of the Sun with the observed limb darkening profile measured by Pierce et al. (1977) in the H band. The residuals in percentage of the observed intensity profile are shown in the *lower panel*.

Kervella+ 2017

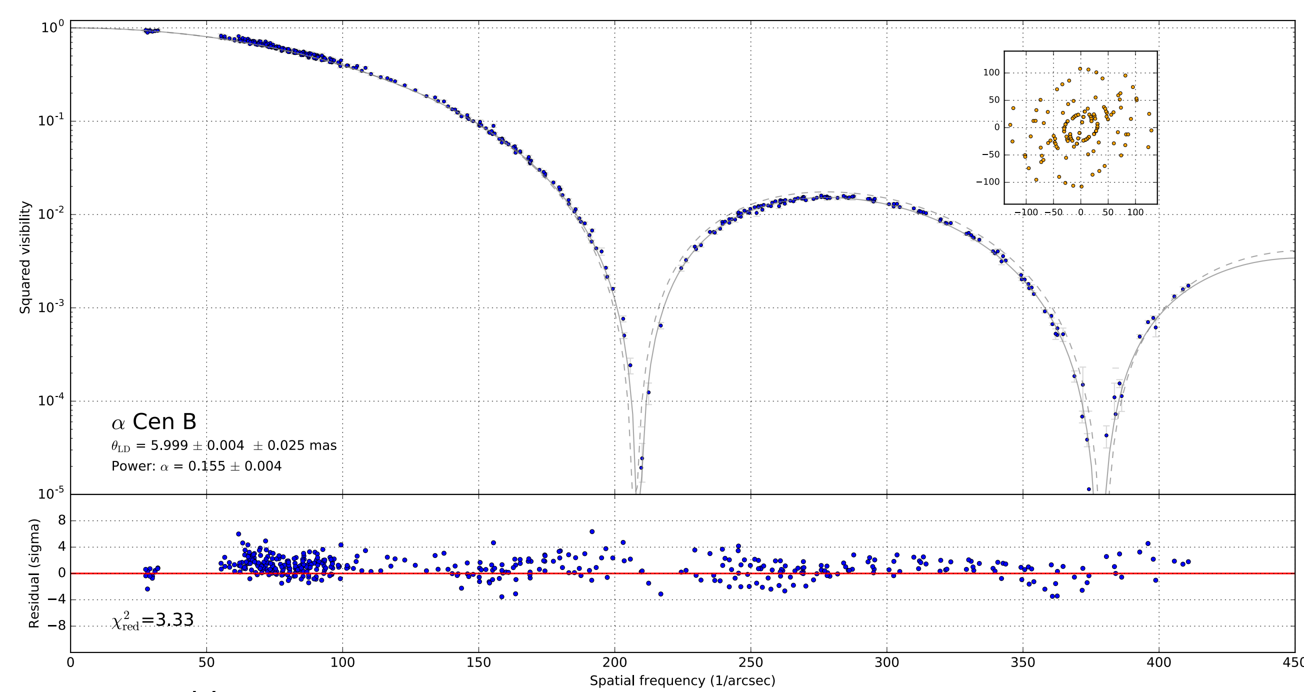

- Difficult to measure the LD
- Discrepancies between transit/interferometry and different laws
- Impact on final radius

Gaia and INTERFEROMETRY
The magic combo

Stellar radius

Inteferometers measure the *angular diameter of stars. Coupled with the distance, we get the stellar radius!*

Interferometric angular diameter

Gaia distance

$$R_{\star[R_\odot]} = \frac{\theta_{\mathrm{LD[mas]}} \times d_{[\mathrm{pc}]}}{9.305}\,.$$

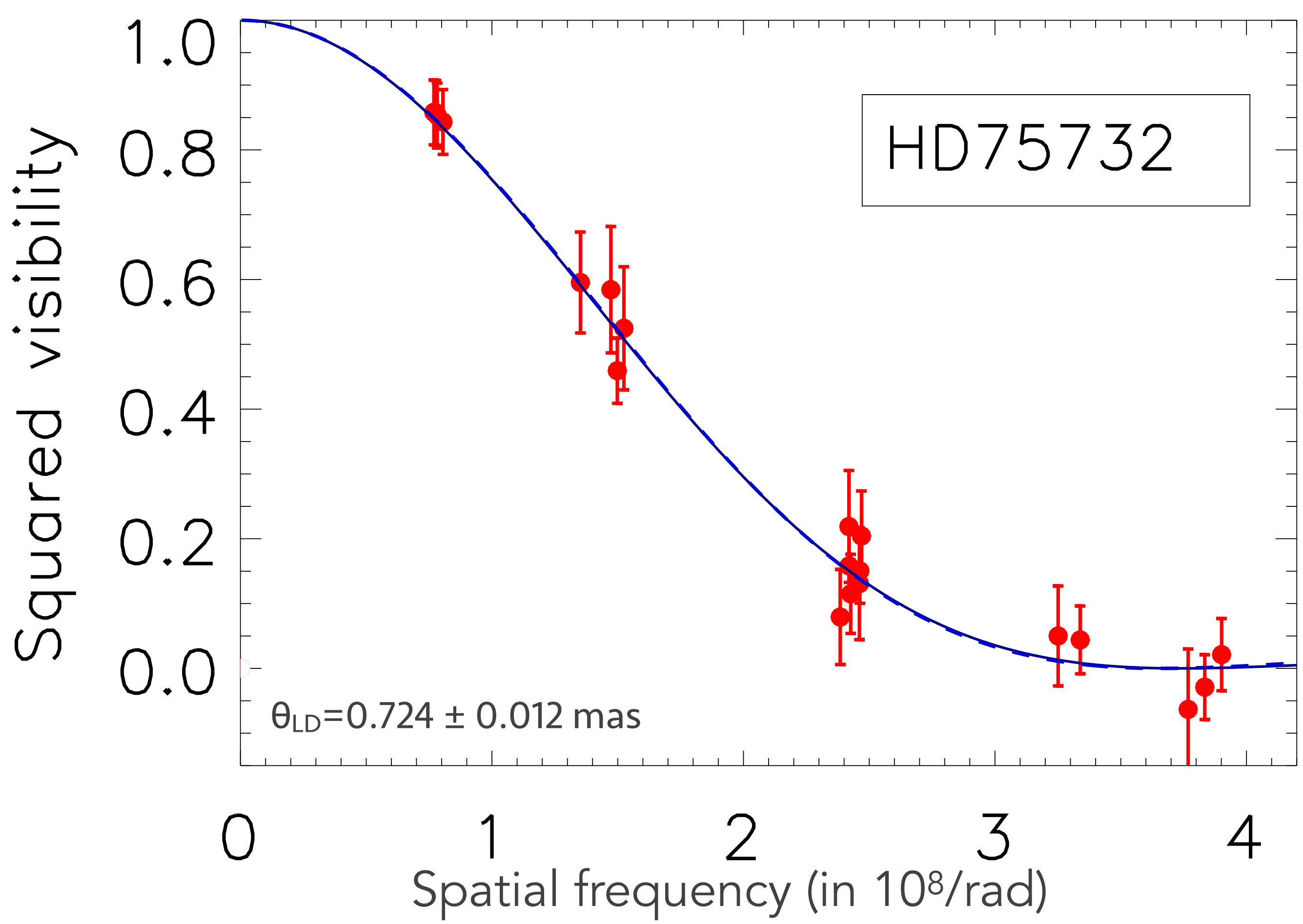

Ligi+ 2016

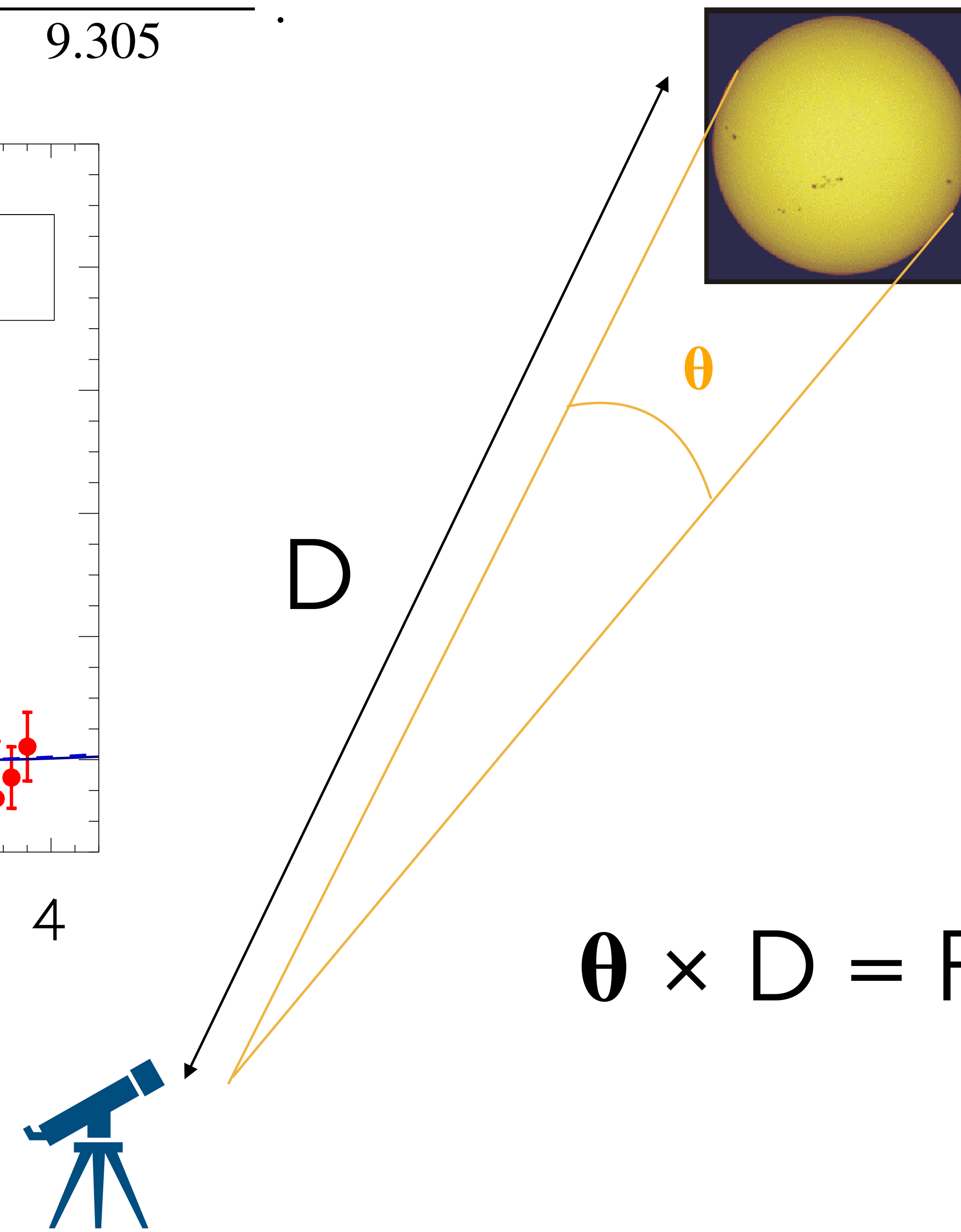

$$\theta \times D = R_\star$$

Stellar effective temperature

The *angular diameter* *is also used to derive* *the effective temperature of stars.*

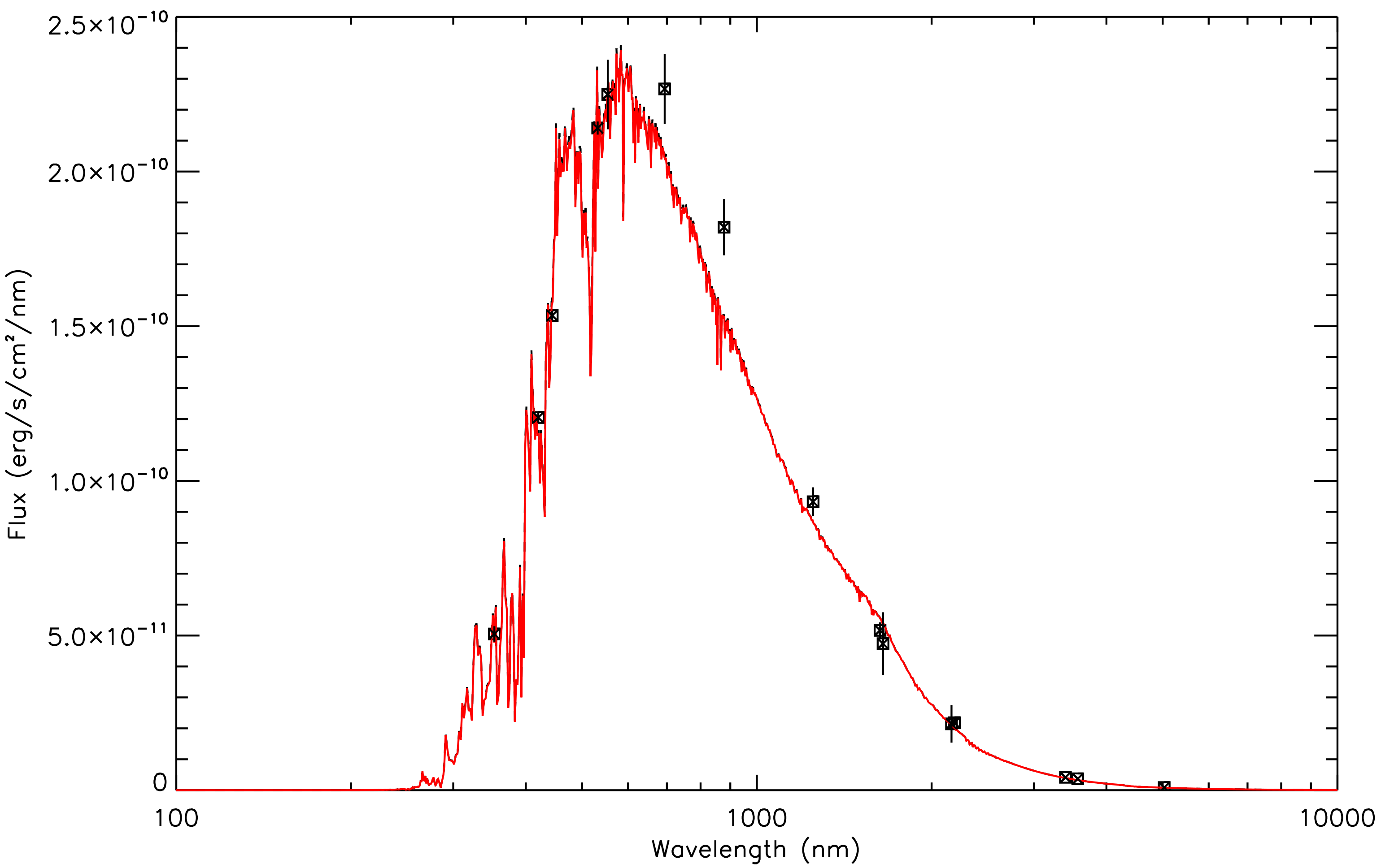

SED

$$T_{\mathrm{eff},\star} = \left(\frac{4 \times F_{\mathrm{bol}}}{\sigma_{\mathrm{SB}} \theta_{\mathrm{LD}}^2} \right)^{0.25}$$

Interferometric angular diameter

Catalogues:

Gaia

2MASS

...

→ see Photometric Viewer (CDS)

e.g.

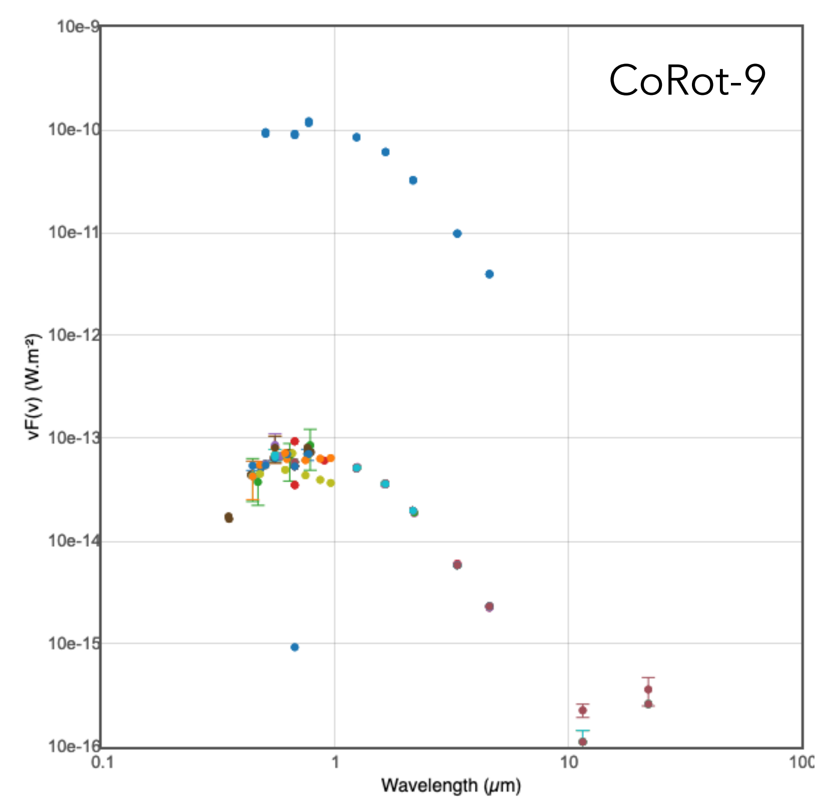

Stellar density and mass

Planetary transit

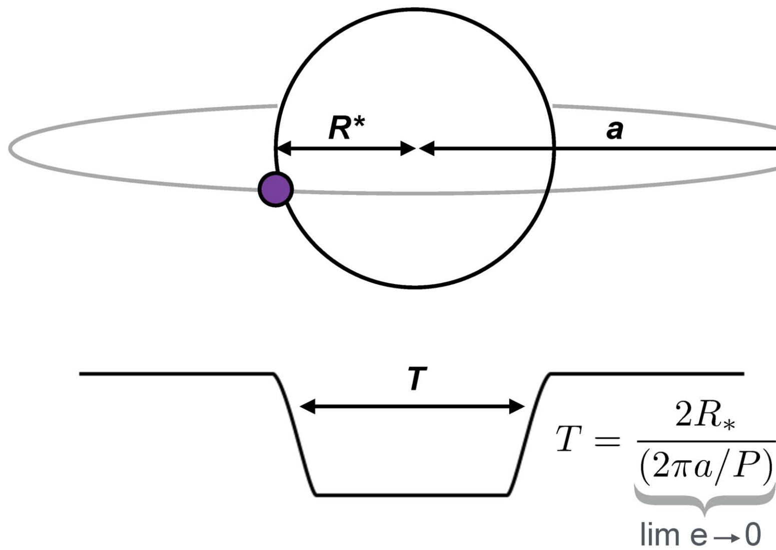

3rd Kepler law

$$\frac{P^2}{4\pi^2} = \frac{a^3}{G(M_* + M_p)} \simeq \frac{a^3}{GM_*}$$

Measure of stellar density $\rho_\bigstar$: $P/T^3 = (\pi^2 G/3)\,\rho_\bigstar$

(Maxted et al. 2015, Seager & Mallén-Ornelas 2003)

$$\rho_* \equiv \frac{M_*}{R_*^3} = \left(\frac{4\pi^2}{P^2 G}\right)\left\{\frac{\left(1+\sqrt{\Delta F}\right)^2 - b^2\left[1-\sin^2(t_T\pi/P)\right]}{\sin^2(t_T\pi/P)}\right\}^{3/2}$$ with $$\Delta F \equiv \frac{F_{\text{no transit}} - F_{\text{transit}}}{F_{\text{no transit}}} = \left(\frac{R_p}{R_*}\right)^2$$

Stellar density and mass

Planetary transit

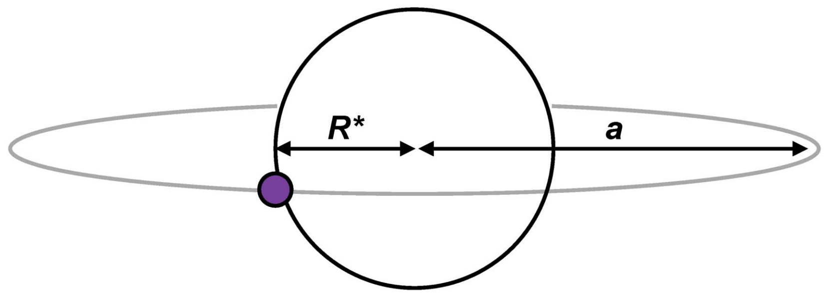

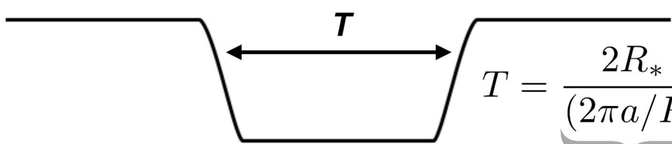

$$T = \underbrace{\frac{2R_*}{(2\pi a/P)}}_{\lim e \to 0}$$

3rd Kepler law

$$\frac{P^2}{4\pi^2} = \frac{a^3}{G(M_* + M_p)} \simeq \frac{a^3}{GM_*}$$

Measure of stellar density $\rho_\star$: $P/T^3 = (\pi^2 G/3)\,\rho_\star$

(Maxted et al. 2015, Seager & Mallén-Ornelas 2003)

$$\rho_* \equiv \frac{M_*}{R_*^3} = \left(\frac{4\pi^2}{P^2 G}\right)\left\{\frac{\left(1+\sqrt{\Delta F}\right)^2 - b^2\left[1-\sin^2(t_T\pi/P)\right]}{\sin^2(t_T\pi/P)}\right\}^{3/2}$$

with

$$\Delta F \equiv \frac{F_{\text{no transit}} - F_{\text{transit}}}{F_{\text{no transit}}} = \left(\frac{R_p}{R_*}\right)^2$$

Measure of stellar mass $M_\star = (4\pi/3) R_\star^3 \rho_\star$

Interferometry

Stellar density and mass

From the PDF of $R_\star$ and $\rho_\star$, analytic joint PDF of $M_\star$ - $R_\star$.

$$\mathcal{L}_{MR\star}(M,R) = \frac{3}{4\pi R^3} \times f_{R_\star}(R) \times f_{\rho_\star}\left(\frac{3M}{4\pi R^3}\right)$$

55 Cnc: $\rho_\bigstar = 1.079 \pm 0.005\ \rho_\odot$

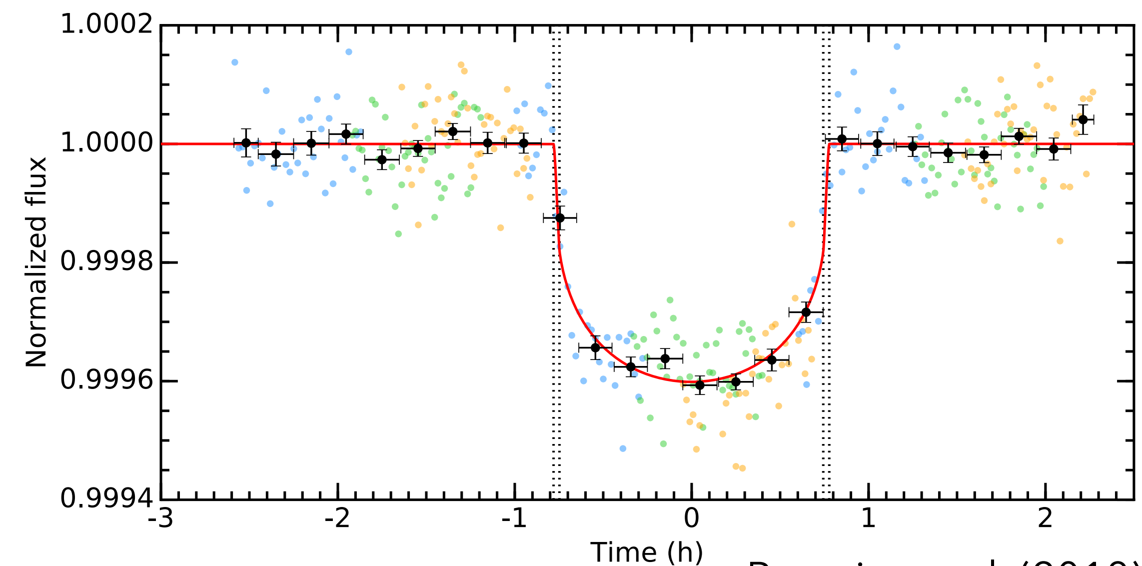

Bourrier et al. (2018)

→ Strong correlation: 0.85!
(Crida+ 2018a)

→ Different $M_\bigstar$ than von Braun+ 2011 based on isochrones.

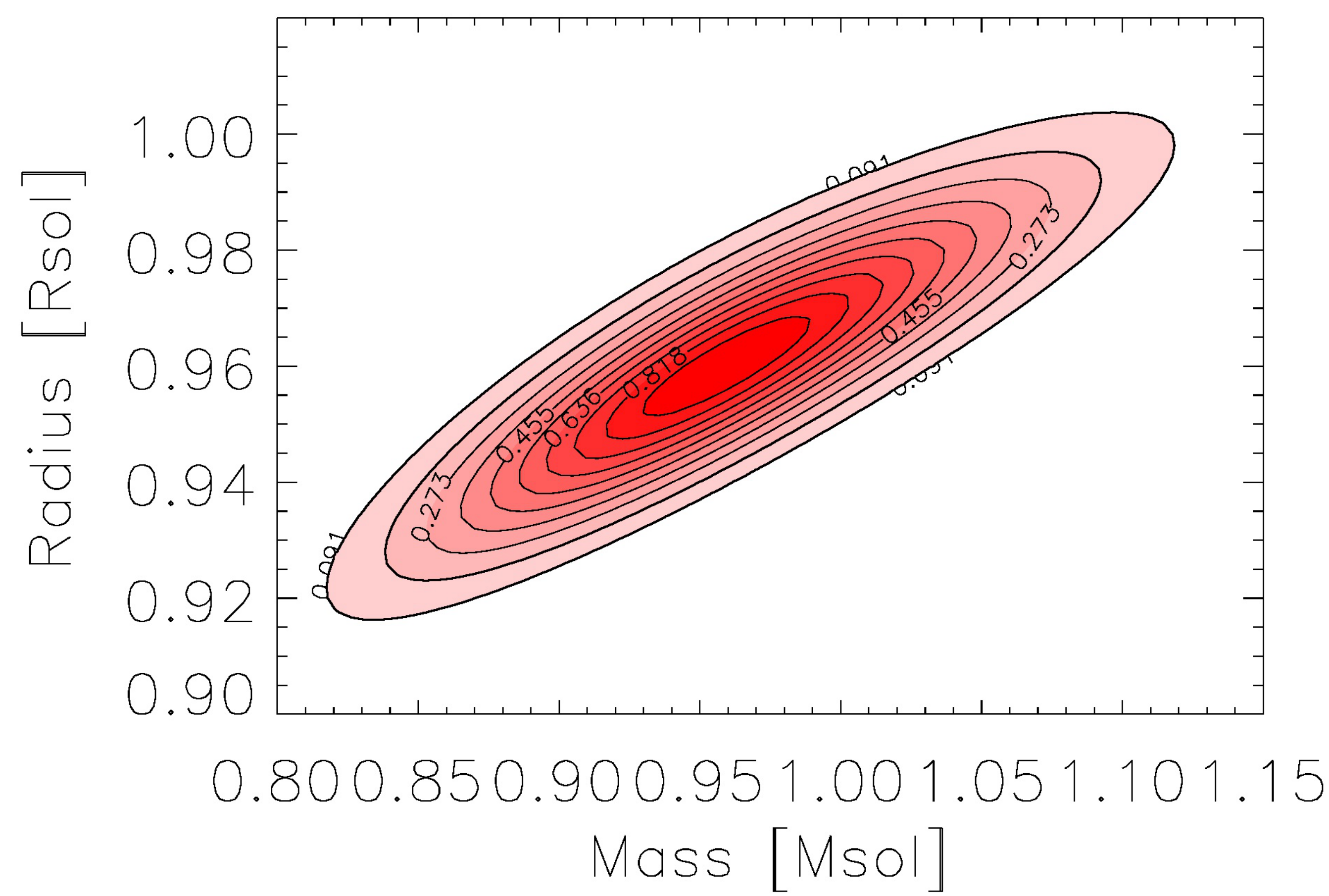

Stellar density and mass

From the PDF of $R_\bigstar$ and $\rho_\bigstar$, analytic joint PDF of $M_\bigstar$ - $R_\bigstar$.

$$\mathcal{L}_{MR\star}(M,R) = \frac{3}{4\pi R^3} \times f_{R_\star}(R) \times f_{\rho_\star}\left(\frac{3M}{4\pi R^3}\right)$$

55 Cnc: $\rho_\bigstar = 1.079 \pm 0.005\ \rho_\odot$

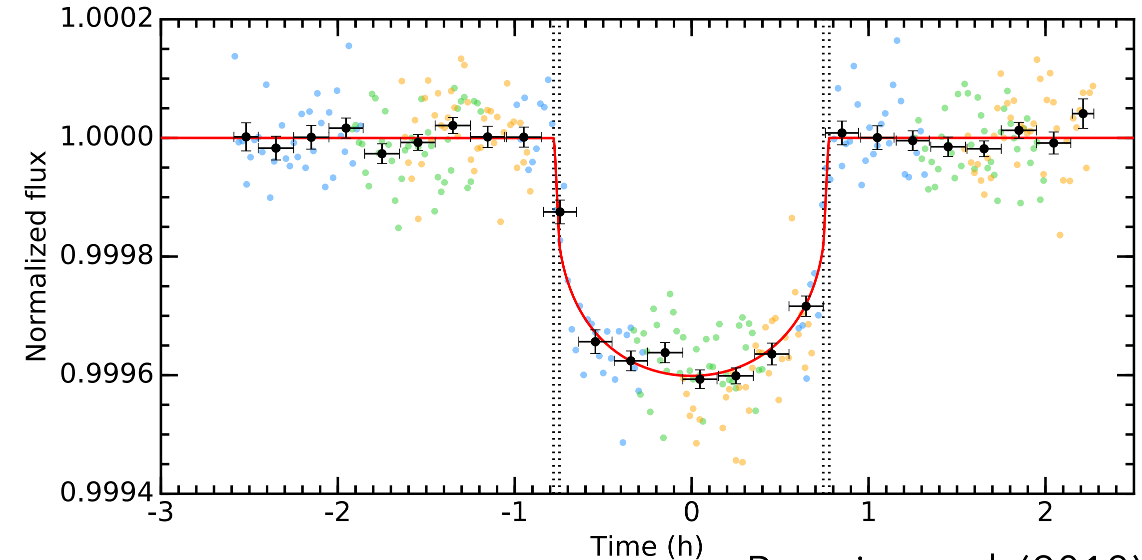

Bourrier et al. (2018)

→ Strong correlation: 0.85!
(Crida+ 2018a)
→ Different $M_\bigstar$ than von Braun+ 2011 based on isochrones.

Taking the values of $R_\bigstar$ and $M_\bigstar$ from Ligi+ 2016, one gets the large, wrong blue ellipse.

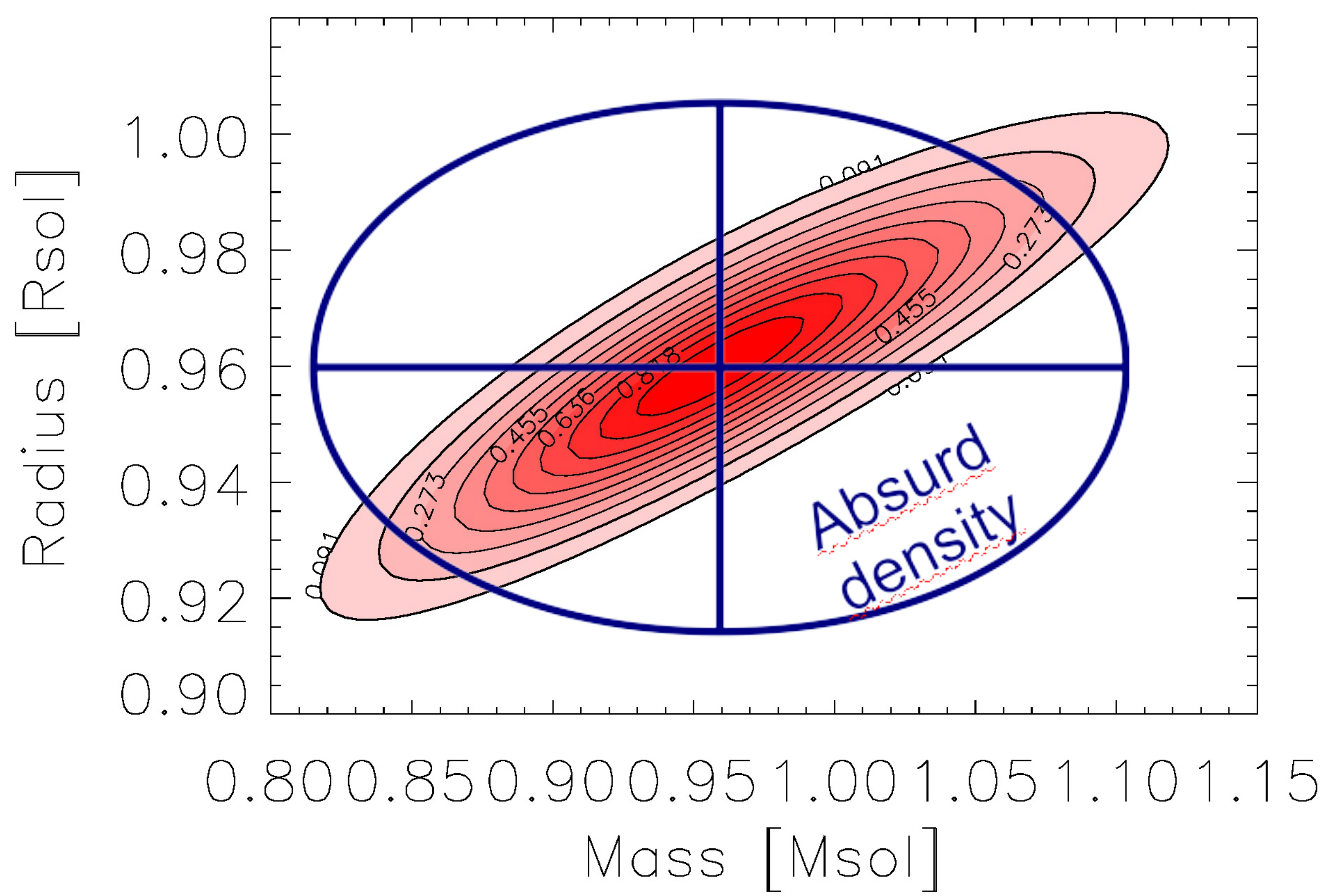

Stellar density and mass

Probability Distribution Function of M_p and R_p

$$f_p(M_p, R_p) \propto \iint \exp\left(-\frac{1}{2}\left(\frac{K(M_p, M_\star) - K}{\sigma_K}\right)^2\right) \quad \leftarrow \quad \text{RV measurements}$$
$$\times \exp\left(-\frac{1}{2}\left(\frac{\Delta F(M_p, M_\star) - \Delta F}{\sigma_{\Delta F}}\right)^2\right) \quad \leftarrow \quad \text{transit measurements}$$
$$\times \mathcal{L}_{MR\star}(M_\star, R_\star)\, \mathrm{d}M_\star\, \mathrm{d}R_\star \,.$$

Blue: our first estimate, with Hipparcos parallax + poor transit light-curve.
Correlation: 0.3.
→ $\rho_p = 1.06 \pm 0.13\ \rho_\oplus$

Black: our second estimate, with Gaia parallax + refined HST light-curve and radial velocity.
Correlation: 0.54.
→ $\rho_p = 1.164 \pm 0.062\ \rho_\oplus = 6421 \pm 342$ kg.m^{-3}

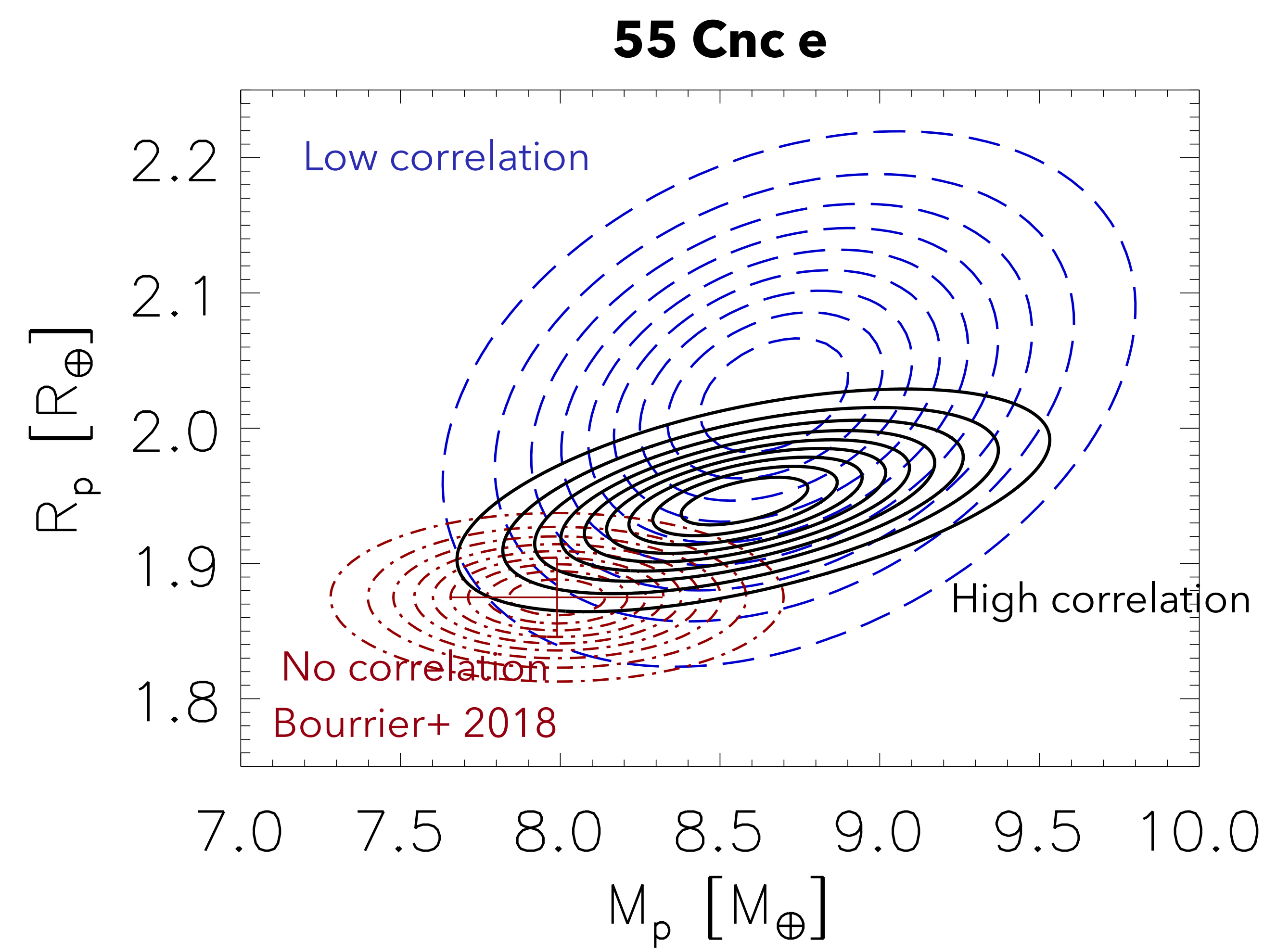

Crida+ 2018a,b

Stellar density and mass

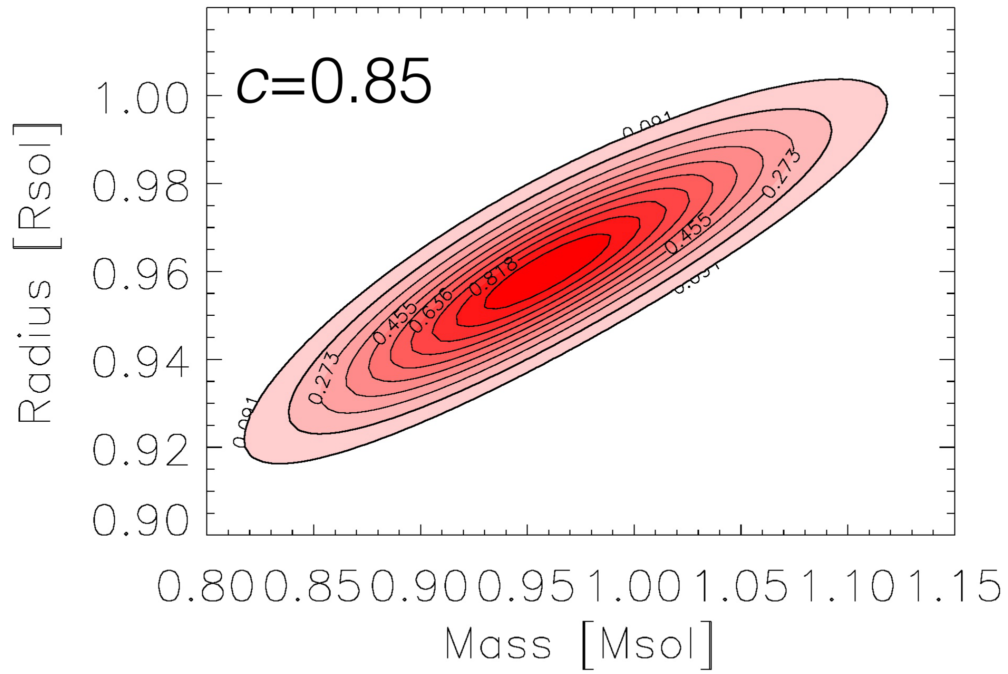

Stellar density and mass

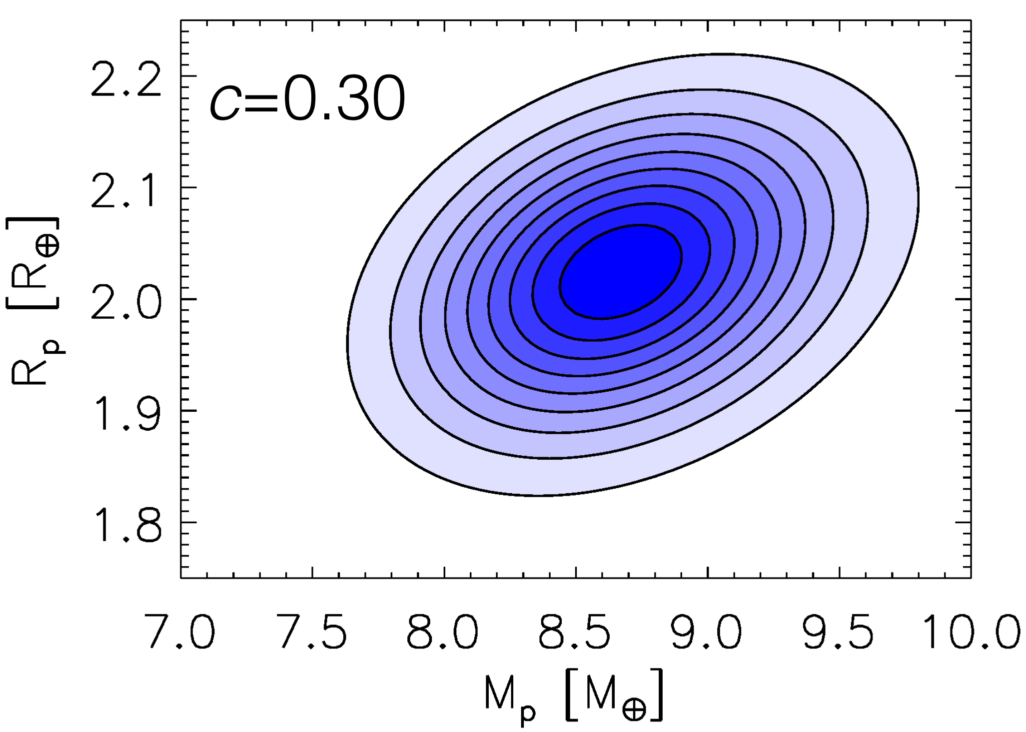

Uncertainties on TD and K degrade the correlation

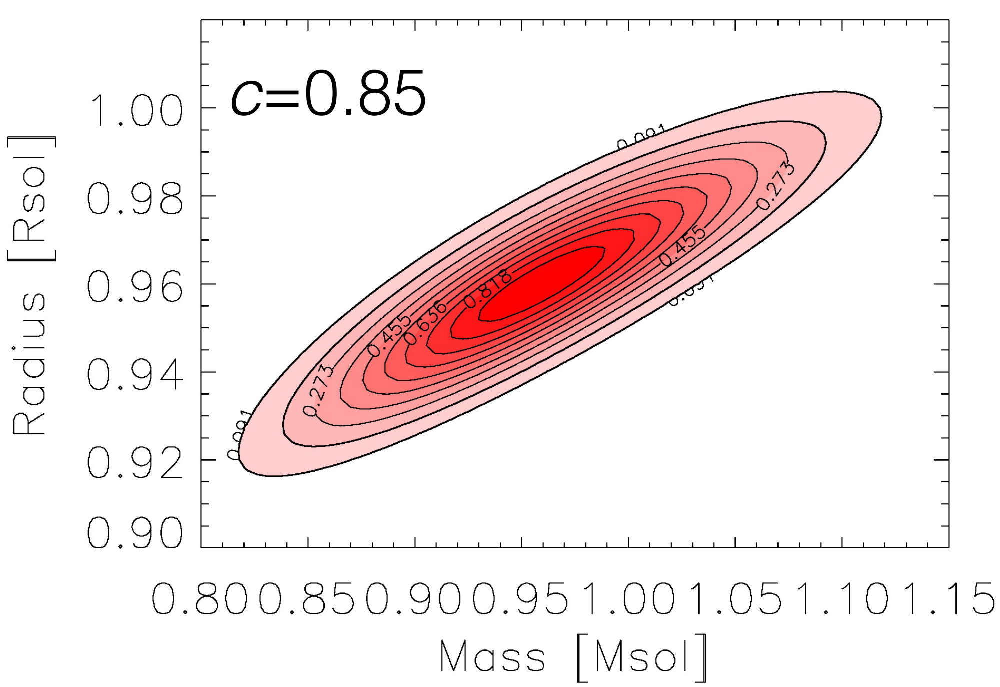

Stellar density and mass

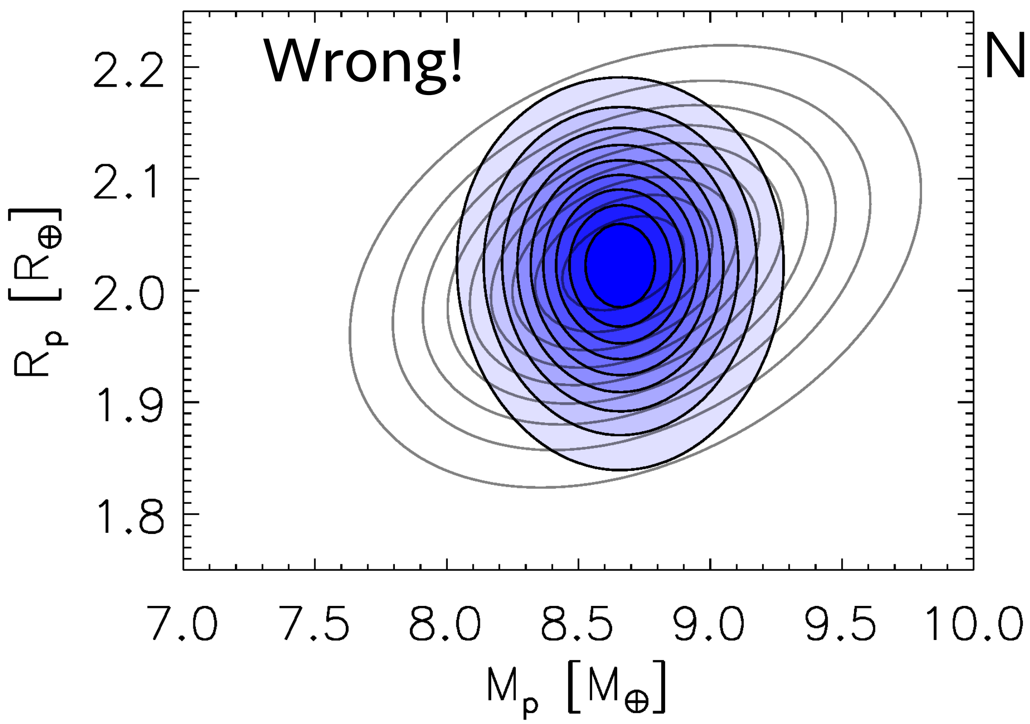

Neglecting stellar uncertainties

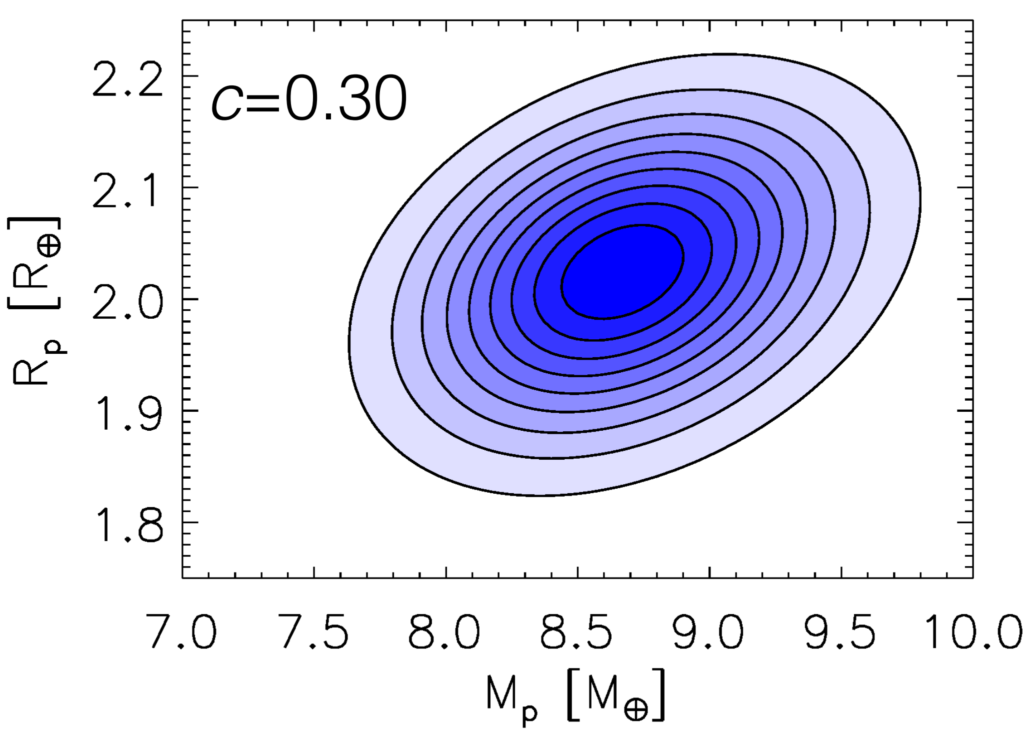

Uncertainties on TD and K degrade the correlation

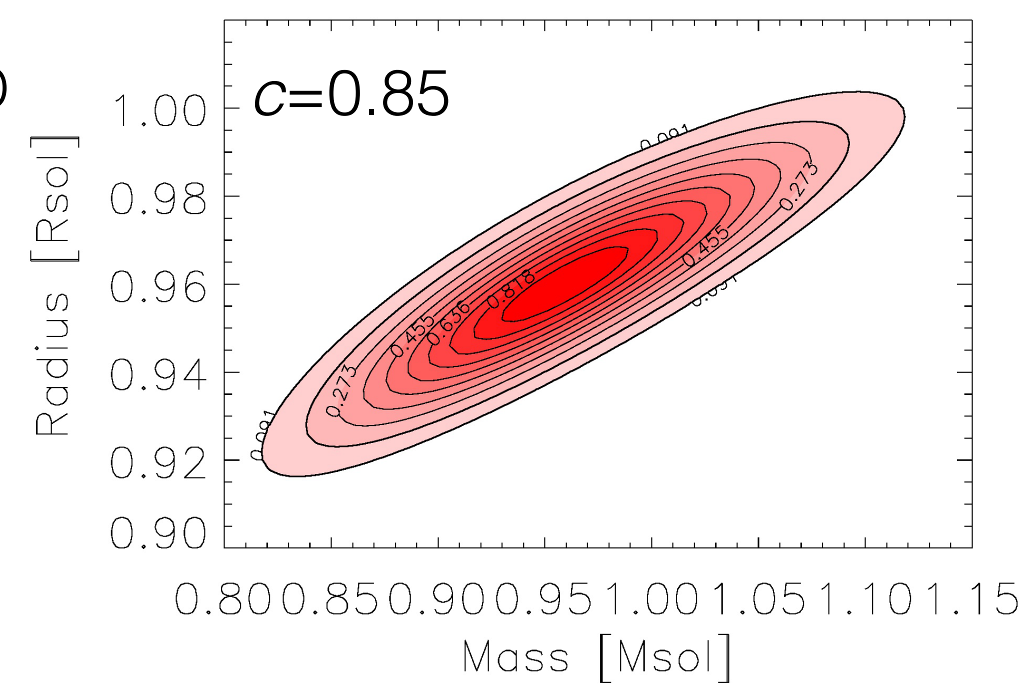

Stellar density and mass

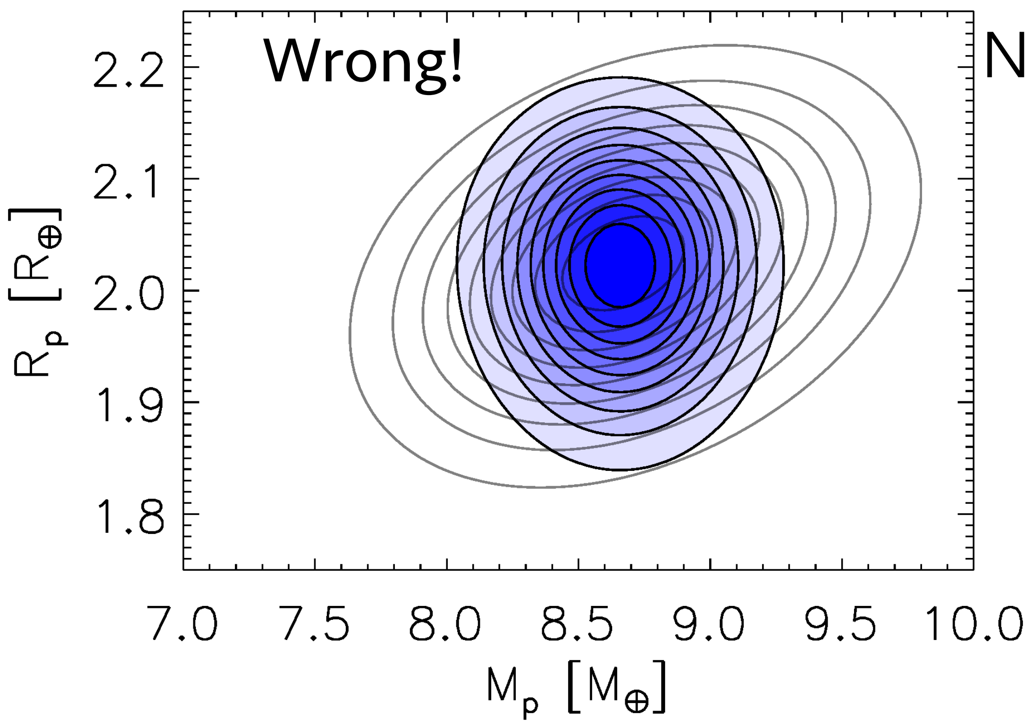

Neglecting stellar uncertainties

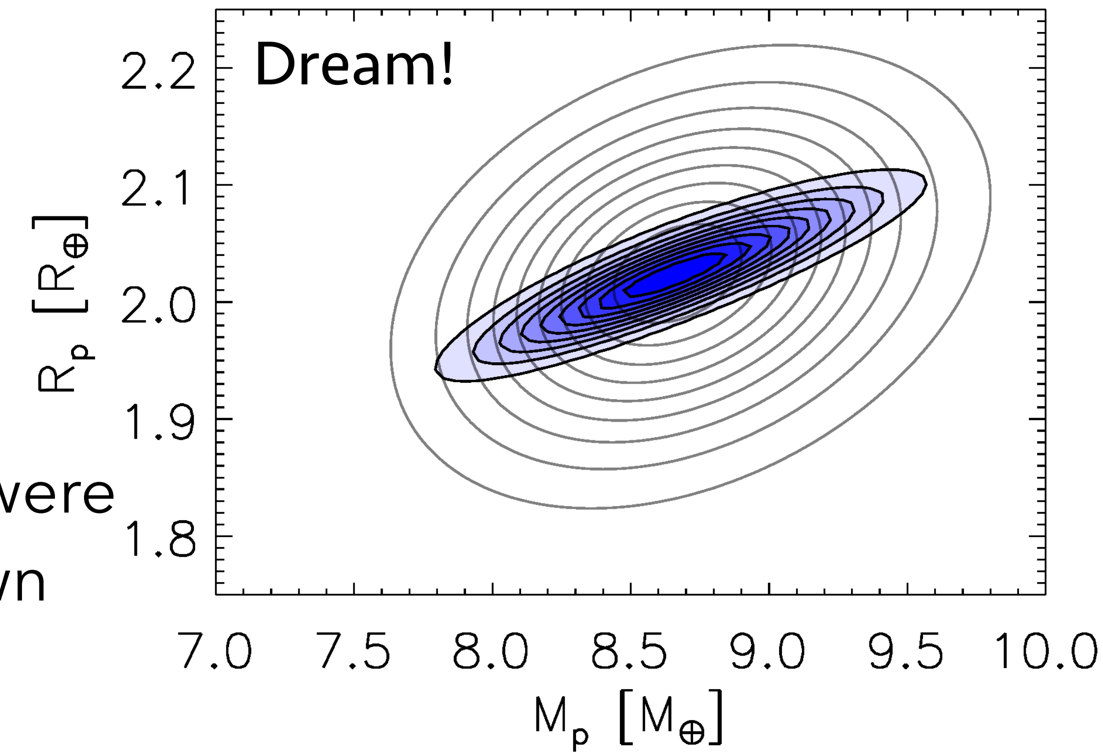

If TD and K were exactly known

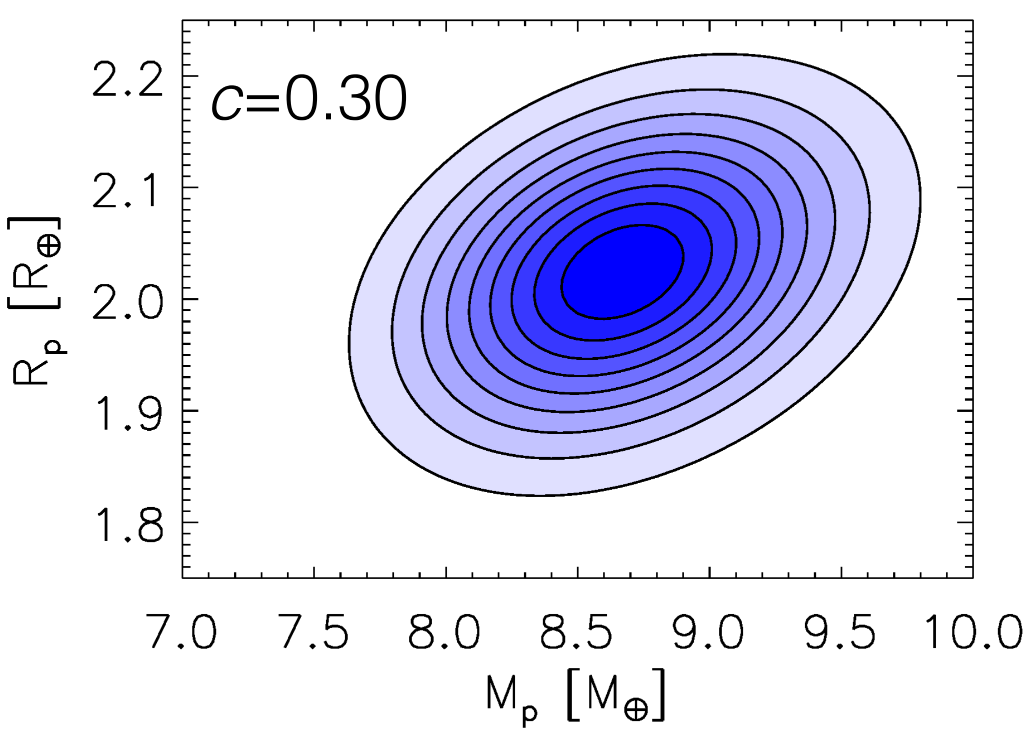

Uncertainties on TD and K degrade the correlation

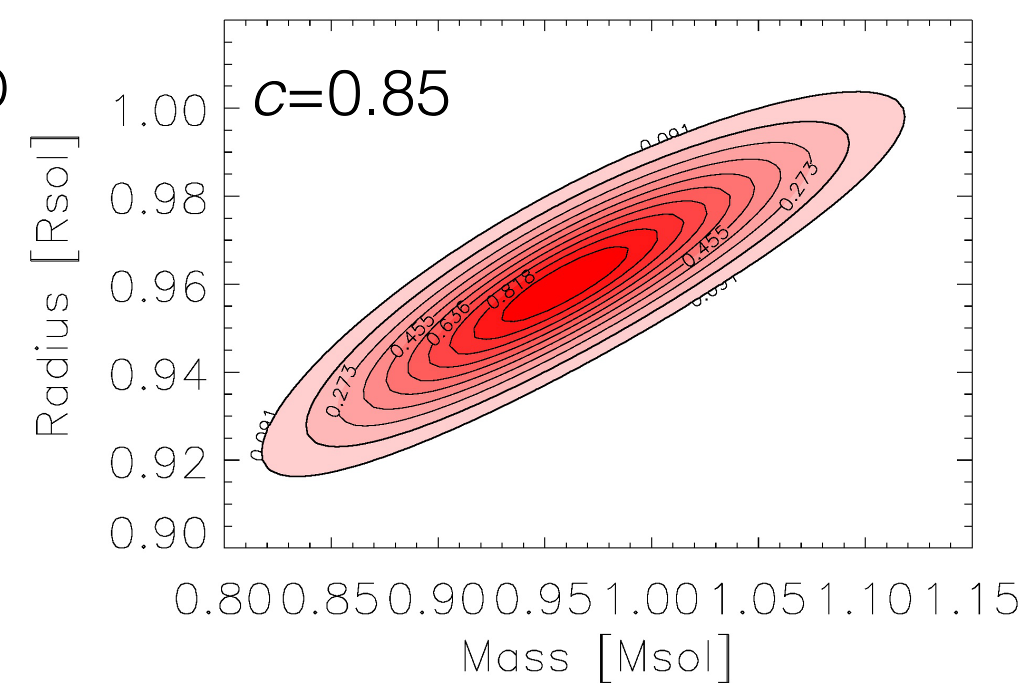

Stellar abundances and exoplanet interiors

Input :

Original data mp

Correl. mp-Rp (0.30)

Hypothetical corr. (0.85)

Abundances

Results :

A → composition of the mantle

C → gas layer

H → could rule out pure solid composition

Model from Dorn+ 2017

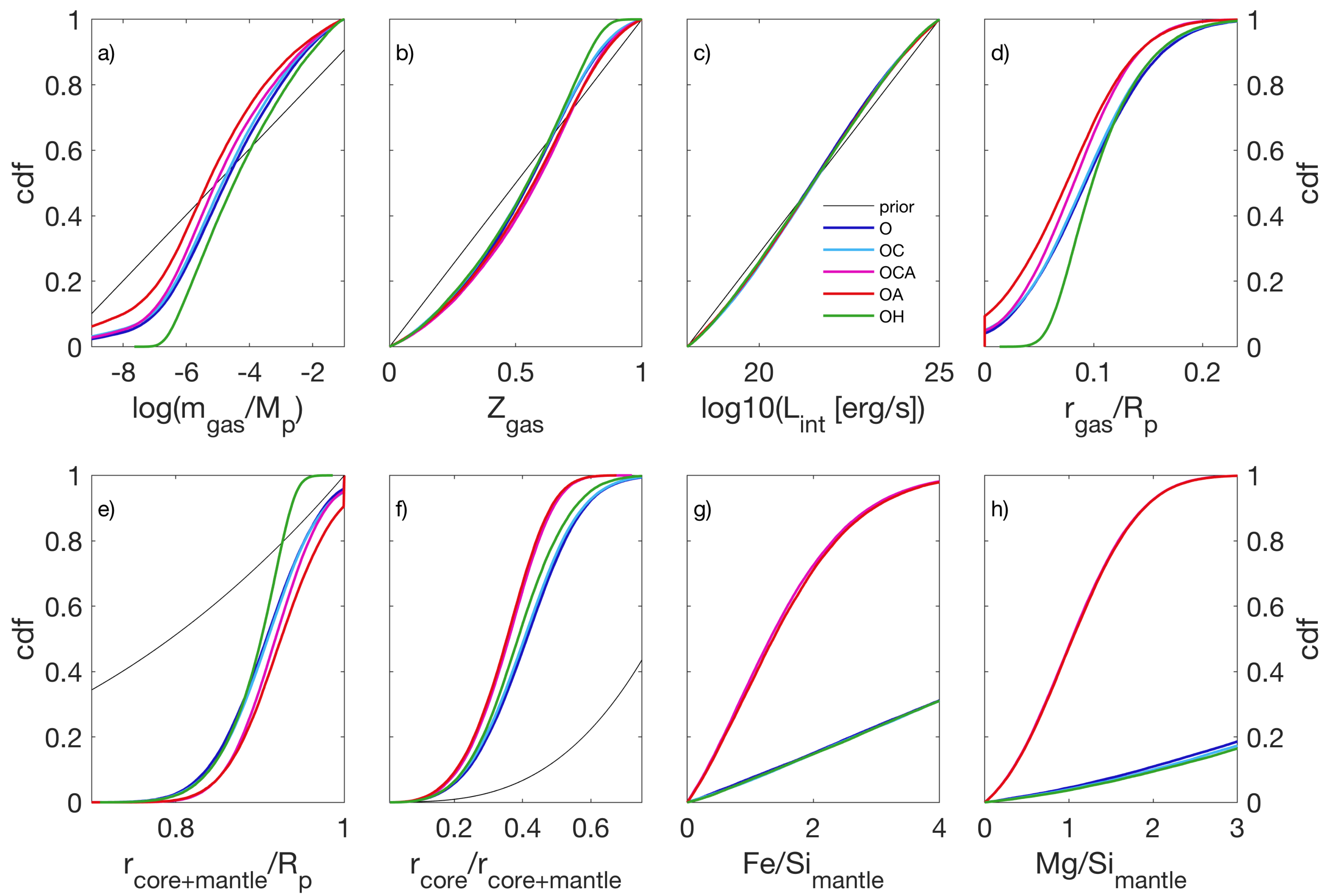

Stellar abundances and exoplanet interiors

OCA case: our best constrains on all the parameters.

Atmosphere thickness
= **3% of R_p**

➔ not a good target for transmission spectroscopy

➔ chemistry of the interior non necessarily carbon-rich

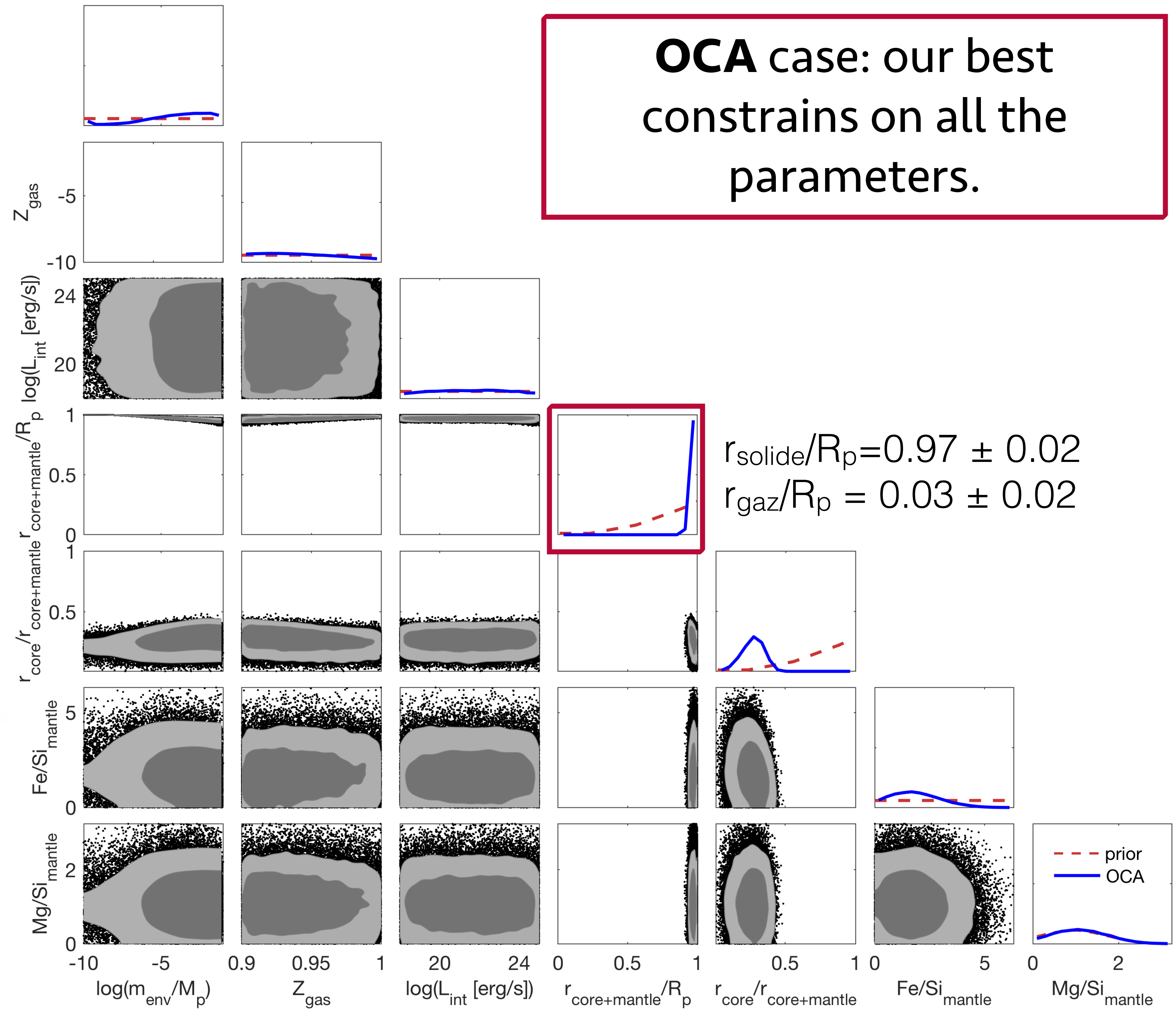

Stellar abundances and exoplanet interiors

Gaia also provides stellar abundances in a homogeneous way for millions of stars. Stellar abundances are introduced into planetary models to derive exoplanet internal structure.

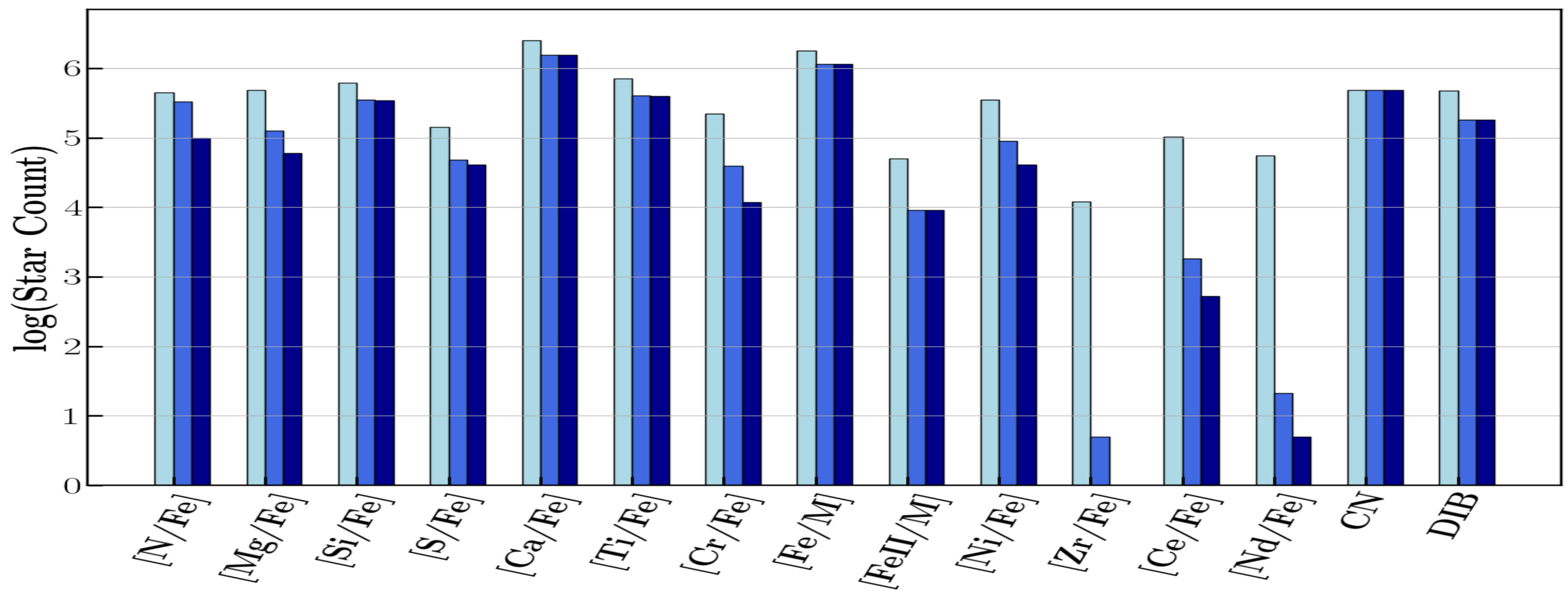

Recio-Blanco+ 2022

Parameter	Prior range	Distribution
Core radius r_{core}	(0.01–1) $r_{\mathrm{core+mantle}}$	Uniform in r^3_{core}
$\mathrm{Fe/Si_{mantle}}$	0 – $\mathrm{Fe/Si_{star}}$	Uniform
$\mathrm{Mg/Si_{mantle}}$	$\mathrm{Mg/Si_{star}}$	Gaussian
f_{mantle}	0.–0.2	Uniform
Size of rocky interior $r_{\mathrm{core+mantle}}$	(0.01–1) R_{p}	Uniform in $r^3_{\mathrm{core+mantle}}$
Pressure imposed by gas envelope P_{env}	20 mbar–100 bar	Uniform in log-scale
Temperature of gas envelope α	0.5–1	Uniform
Mean molecular weight of gas envelope μ	16–50 g mol^{-1}	Uniform

Ligi+ 2019

Stellar density and mass

HD219134

Smaller planets than previous estimates

→ These new radii put the planets on the left side of the evaporation valley, while they were thought to be in the gap.

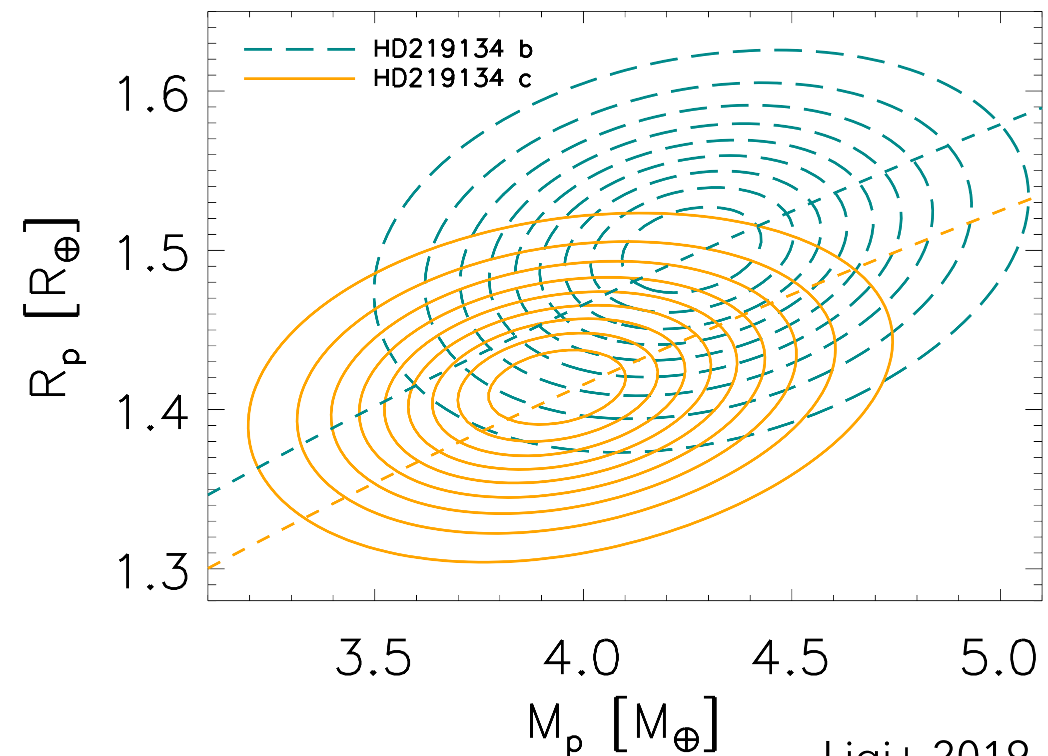

Ligi+ 2019

	PLANET B	PLANET C
Radius [$R_\oplus$]	1.50 ± 0.06	1.41 ± 0.05
Mass [$M_\oplus$]	4.27 ± 0.34	3.96 ± 0.34
Density [$\rho_\oplus$]	1.27 ± 0.16	1.41 ± 0.17
Corr. (M_p -	0.22	0.23

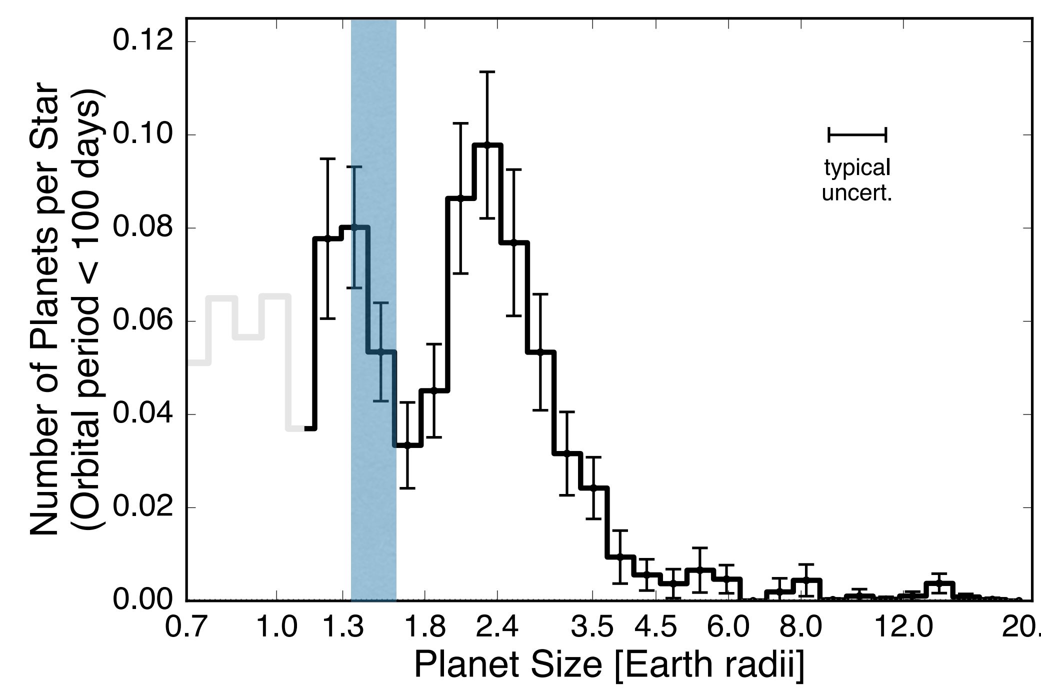

Fulton+ 2017

Stellar density and mass

HD219134

Smaller planets than previous estimates

→ These new radii put the planets on the left side of the evaporation valley, while they were thought to be in the gap.

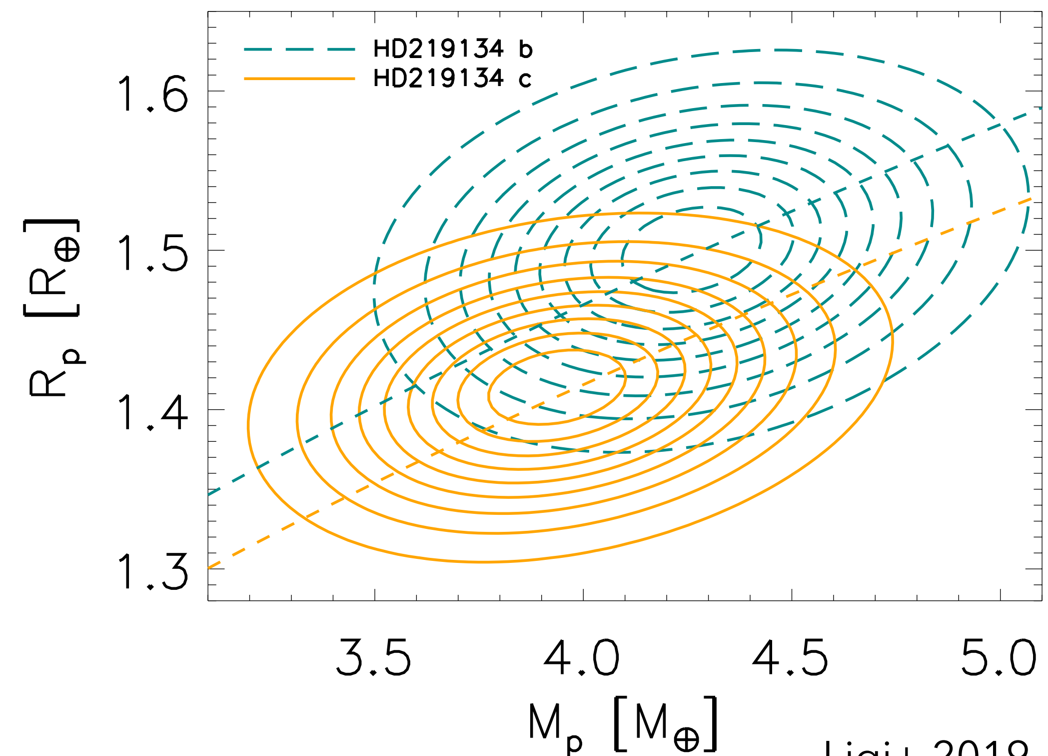

Ligi+ 2019

	PLANET B	PLANET C
Radius [$R_\oplus$]	1.50 ± 0.06	1.41 ± 0.05
Mass [$M_\oplus$]	4.27 ± 0.34	3.96 ± 0.34
Density [$\rho_\oplus$]	1.27 ± 0.16	1.41 ± 0.17
Corr. (M_p -	0.22	0.23

ρ_b/ρ_c = 0.905 ± 0.131 (0.95 for Venus/Earth)
→ 50 % chance that their densities differ more than 2× more than those of Venus and Earth…

The more massive one (b) is the less dense.
→ Different core/mantle ratio ? Thick gas envelope ? Enrichment in refractory elements ?

Stellar density and mass

HD219134

Smaller planets than previous estimates

→ These new radii put the planets on the left side of the evaporation valley, while they were thought to be in the gap.

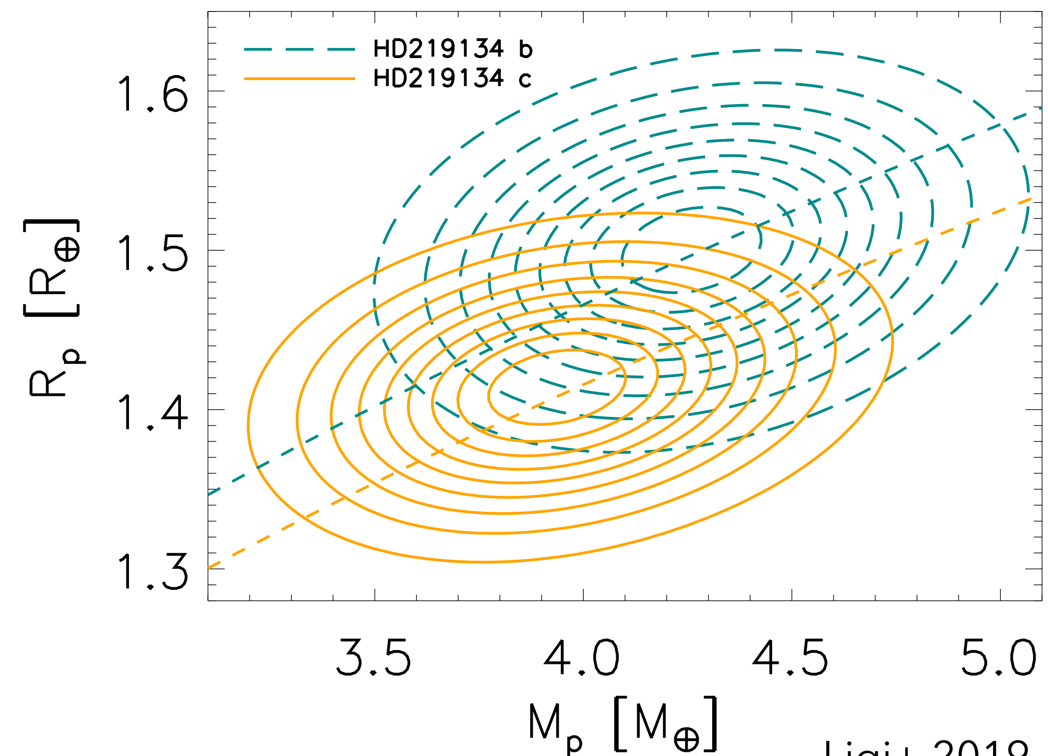

Ligi+ 2019

	PLANET B	PLANET C
Radius [$R_\oplus$]	1.50 ± 0.06	1.41 ± 0.05
Mass [$M_\oplus$]	4.27 ± 0.34	3.96 ± 0.34
Density [$\rho_\oplus$]	1.27 ± 0.16	1.41 ± 0.17
Corr. (M_p -	0.22	0.23

ρ_b/ρ_c = 0.905 ± 0.131 (0.95 for Venus/Earth)
→ 50 % chance that their densities differ more than 2× more than those of Venus and Earth...

The more massive one (b) is the less dense.
→ Different core/mantle ratio ? Thick gas envelope ? Enrichment in refractory elements ?

Bower+ 2019: a molten mantle is 25% less dense than a solid one. Could HD219134 b be partially molten?

Stellar density and mass

Tidal heating from the host star dissipates energy and circularizes the orbit.

→ Sustainable energy source if and only if the eccentricity is pumped by other planets (ex: Io).

N-body simulations of the system:
e_b oscillates between 0.005 and 0.037.

→ tidal heating up to 100 times more than Io!
HD219134 c: less tidal heating than Io (because further from the star).

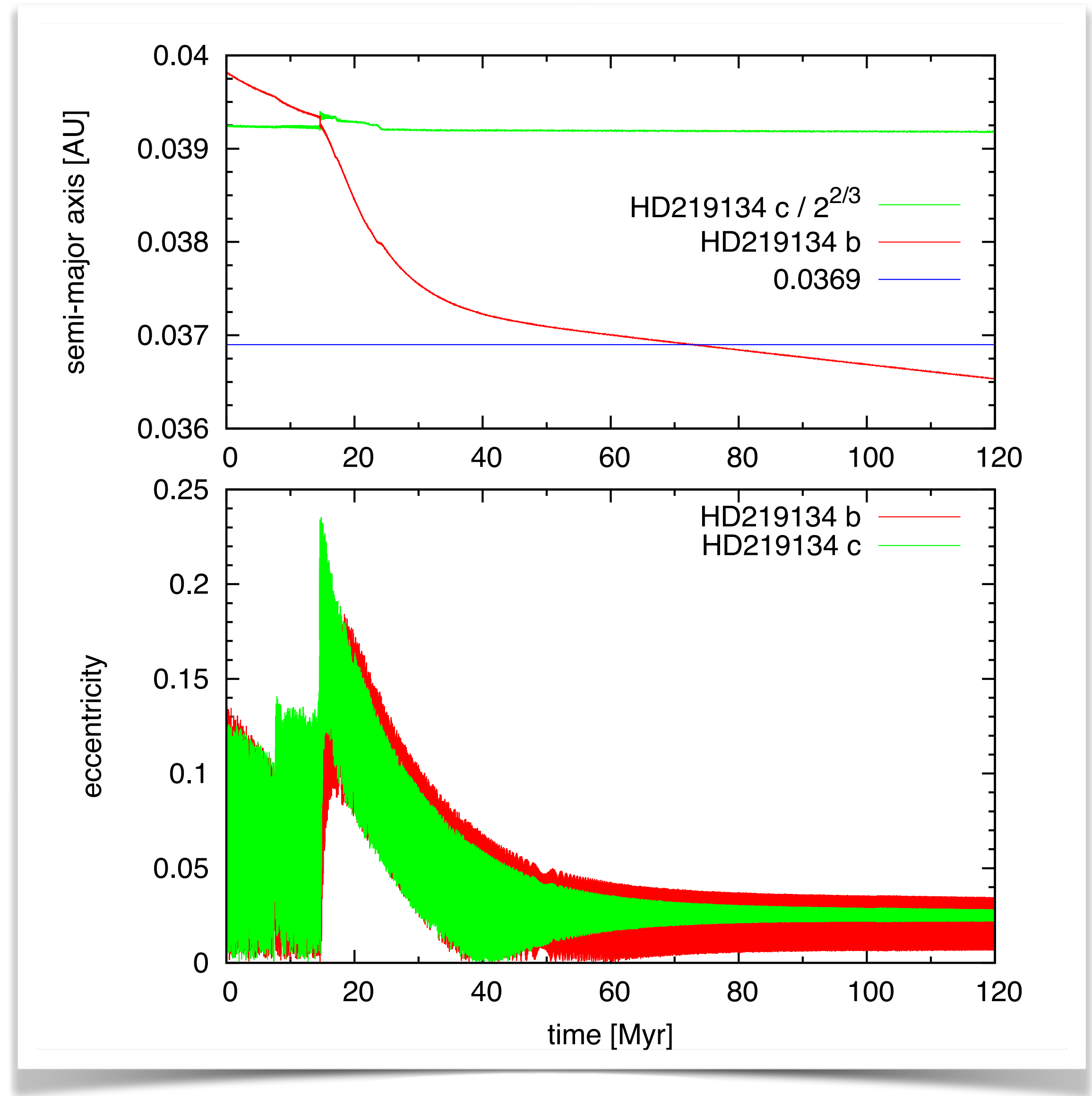

Stellar density and mass

Tidal heating from the host star dissipates energy and circularizes the orbit.

→ Sustainable energy source if and only if the eccentricity is pumped by other planets (ex: Io).

N-body simulations of the system:
e_b oscillates between 0.005 and 0.037.

→ tidal heating up to 100 times more than Io!
HD219134 c: less tidal heating than Io (because further from the star).

Result
→ N-body simulations: planet b's eccentricity is excited despite not measurable.

→ Assuming a dissipation inside this planet equivalent to that of Earth, this strongly suggests that this planet could be at least partially molten, explaining its lower density than its neighbor HD219134 c, even if they have identical composition.

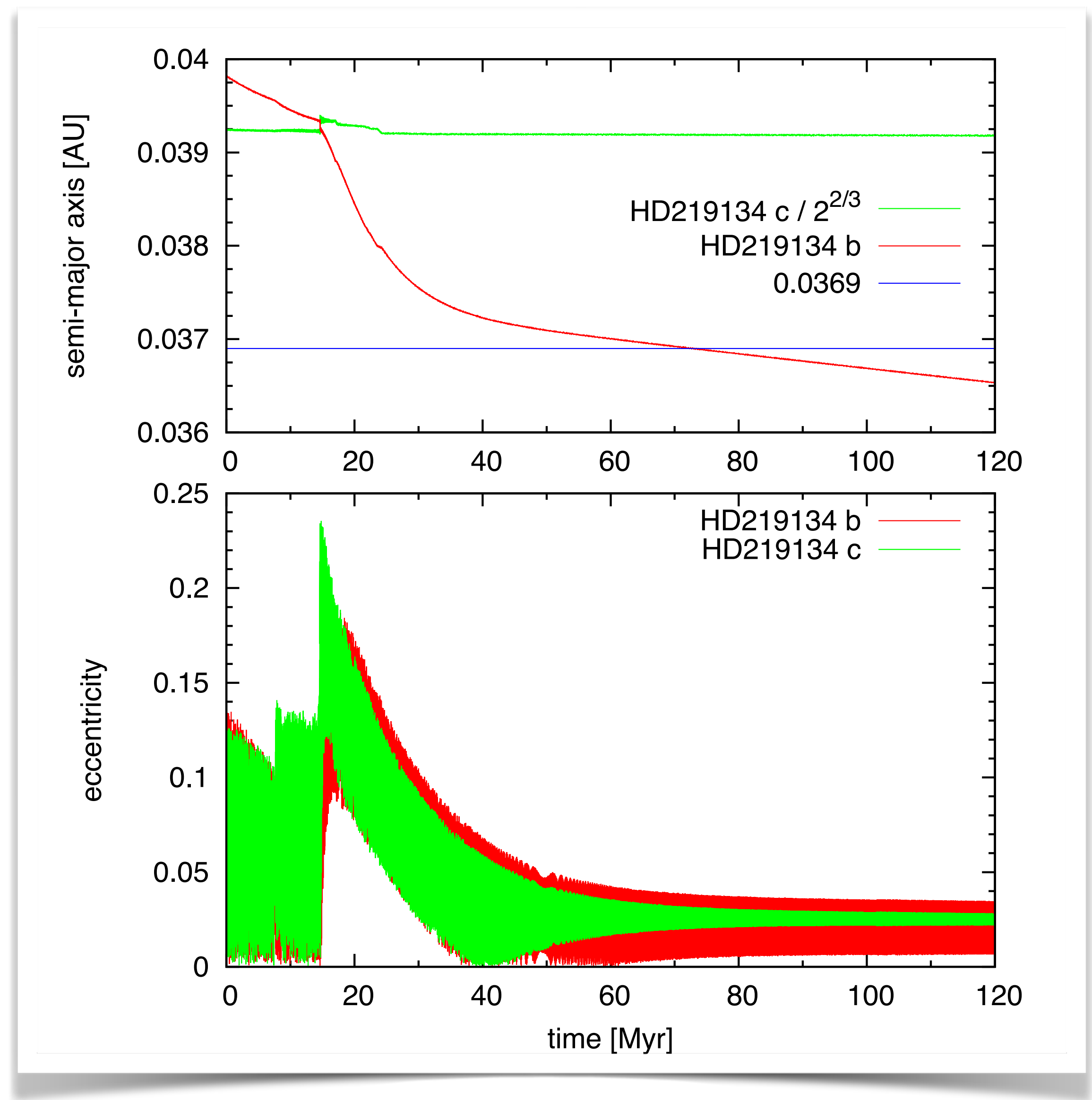

Error budget

Error budget for ρ_p of HD219134 and 55 Cnc

relative error

absolute error

$$\tilde{\sigma}_{\rho_p}{}^2 = 4/9\,\tilde{\sigma}_{\rho_\star}{}^2 + \tilde{\sigma}_{R_\star}{}^2 + 9/4\,\tilde{\sigma}_{\Delta F/F2}{}^2 + \tilde{\sigma}_K{}^2$$

	$\tilde{\sigma}_{\rho_p}{}^2$		$4/9\,\tilde{\sigma}_{\rho_\star}{}^2$		$\tilde{\sigma}_{R_\star}{}^2$		$9/4\,\tilde{\sigma}_{\Delta F/F2}{}^2$		$\tilde{\sigma}_K{}^2$
55 Cnc e	5.3%	=	0.5%	+	1.6%	+	1.6%	+	4.0%
	$24 \cdot 10^{-4}$	=	$0.1 \cdot 10^{-4}$	+	$2.6 \cdot 10^{-4}$	+	$5.4 \cdot 10^{-4}$	+	$16 \cdot 10^{-4}$
HD219134 b / HD219134 c	~22%	=	10.4%	+	1.9%	+	6.7% / 6.0%	+	3.1% / 4.4%
	$\sim 106 \cdot 10^{-4}$	=	$48 \cdot 10^{-4}$	+	$3.6 \cdot 10^{-4}$	+	$45 \cdot 10^{-4}$ / $36 \cdot 10^{-4}$	+	$9.9 \cdot 10^{-4}$ / $19 \cdot 10^{-4}$

Error budget

Error budget for ρ_p of HD219134 and 55 Cnc

relative error

absolute error

$$\tilde{\sigma}_{\rho_p}^{2} = 4/9\ \tilde{\sigma}_{\rho_\star}^{2} + \tilde{\sigma}_{R_\star}^{2} + 9/4\ \tilde{\sigma}_{\Delta F/F2}^{2} + \tilde{\sigma}_{K}^{2}$$

	$\tilde{\sigma}_{\rho_p}^{2}$		$4/9\ \tilde{\sigma}_{\rho_\star}^{2}$		$\tilde{\sigma}_{R_\star}^{2}$		$9/4\ \tilde{\sigma}_{\Delta F/F2}^{2}$		$\tilde{\sigma}_{K}^{2}$
55 Cnc e	5.3%	=	0.5%	+	1.6%	+	1.6%	+	4.0%
	$24 \cdot 10^{-4}$	=	$0.1 \cdot 10^{-4}$	+	$2.6 \cdot 10^{-4}$	+	$5.4 \cdot 10^{-4}$	+	$16 \cdot 10^{-4}$
HD219134 b HD219134 c	~22%	=	10.4%	+	1.9%	+	6.7% 6.0%	+	3.1% 4.4%
	$\sim 106 \cdot 10^{-4}$	=	$48 \cdot 10^{-4}$	+	$3.6 \cdot 10^{-4}$	+	$45 \cdot 10^{-4}$ $36 \cdot 10^{-4}$	+	$9.9 \cdot 10^{-4}$ $19 \cdot 10^{-4}$

Can be resolved with new missions for transits (TESS, PLATO)

Error budget

Error budget for ρ_p of HD219134 and 55 Cnc

relative error

absolute error

$$\tilde{\sigma}_{\rho_p}^2 = 4/9\,\tilde{\sigma}_{\rho_\star}^2 + \tilde{\sigma}_{R_\star}^2 + 9/4\,\tilde{\sigma}_{\Delta F/F}^2 + \tilde{\sigma}_K^2$$

	$\tilde{\sigma}_{\rho_p}^2$	$4/9\,\tilde{\sigma}_{\rho_\star}^2$	$\tilde{\sigma}_{R_\star}^2$	$9/4\,\tilde{\sigma}_{\Delta F/F}^2$	$\tilde{\sigma}_K^2$
55 Cnc e	5.3%	0.5%	1.6%	1.6%	4.0%
	$24 \cdot 10^{-4}$	$0.1 \cdot 10^{-4}$	$2.6 \cdot 10^{-4}$	$5.4 \cdot 10^{-4}$	$16 \cdot 10^{-4}$
HD219134 b / HD219134 c	~22%	10.4%	1.9%	6.7% / 6.0%	3.1% / 4.4%
	$\sim 106 \cdot 10^{-4}$	$48 \cdot 10^{-4}$	$3.6 \cdot 10^{-4}$	$45 \cdot 10^{-4}$ / $36 \cdot 10^{-4}$	$9.9 \cdot 10^{-4}$ / $19 \cdot 10^{-4}$

Can be resolved with new missions for transits (TESS, PLATO)

Can be resolved with new generation spectrographs (ESPRESSO…)

Error budget

Error budget for ρ_p of HD219134 and 55 Cnc

relative error

absolute error

$$\tilde{\sigma}_{\rho_p}^2 = 4/9\,\tilde{\sigma}_{\rho_\star}^2 + \tilde{\sigma}_{R_\star}^2 + 9/4\,\tilde{\sigma}_{\Delta F/F}^2 + \tilde{\sigma}_K^2$$

	$\tilde{\sigma}_{\rho_p}^2$	$4/9\,\tilde{\sigma}_{\rho_\star}^2$	$\tilde{\sigma}_{R_\star}^2$	$9/4\,\tilde{\sigma}_{\Delta F/F}^2$	$\tilde{\sigma}_K^2$
55 Cnc e	5.3%	0.5%	1.6%	1.6%	4.0%
	$24 \cdot 10^{-4}$	$0.1 \cdot 10^{-4}$	$2.6 \cdot 10^{-4}$	$5.4 \cdot 10^{-4}$	$16 \cdot 10^{-4}$
HD219134 b HD219134 c	~22%	10.4%	1.9%	6.7% 6.0%	3.1% 4.4%
	$\sim 106 \cdot 10^{-4}$	$48 \cdot 10^{-4}$	$3.6 \cdot 10^{-4}$	$45 \cdot 10^{-4}$ $36 \cdot 10^{-4}$	$9.9 \cdot 10^{-4}$ $19 \cdot 10^{-4}$

Can be resolved with interferometry+Gaia

mas → µas

Can be resolved with new missions for transits (TESS, PLATO)

Can be resolved with new generation spectrographs (ESPRESSO…)

Stellar models

Integration of the stellar radius from interferometry

HD97658 (Ellis+ 2020)

Planetary Properties		
Transit Depth [ppm]	712±38	§4 Exofast
Period [days]	$9.48971157 \pm 0.00000077$	§4 Exofast
T_0 [BJD]	2458904.9366 ± 0.0008	§4 Exofast
$R_p/R_\star$	0.02668 ± 0.0007	§4 Exofast
Inclination [deg]	$89.05^{+0.41}_{-0.24}$	§4 Exofast
Impact Parameter	$0.39^{+0.11}_{-.018}$	§4 Exofast
Eccentricity	$0.054^{+0.039}_{-0.034}$	§4 Exofast
Mass [$M_\oplus$]	7.52 ± 0.86	§4 Exofast
$a/R_\star$	24.16 ± 0.69	§4 Exofast
R_p [$R_\oplus$]	2.12 ± 0.061	§4
ρ_p [g cm^{-3}]	3.681 ± 0.51	§4
T_{Eq}[K]	749 ± 12	§4
Stellar and Planetary Properties from Transit Observables		
$\rho_\star$ [g cm^{-3}]	3.11 ± 0.27	§4
$M_\star$ [$M_\odot$]	0.85 ± 0.08	§4
$\log(g)$ [cgs]	4.64 ± 0.04	§4
Corr($R_\star$,$M_\star$)	0.41	§4
ρ_p [g cm^{-3}]	4.835 ± 0.70	§4
R_p [$R_\oplus$]	2.11 ± 0.059	§4
Mass [$M_\oplus$]	8.25 ± 1.01	§4
Corr(R_p, M_p)	0.09	§4

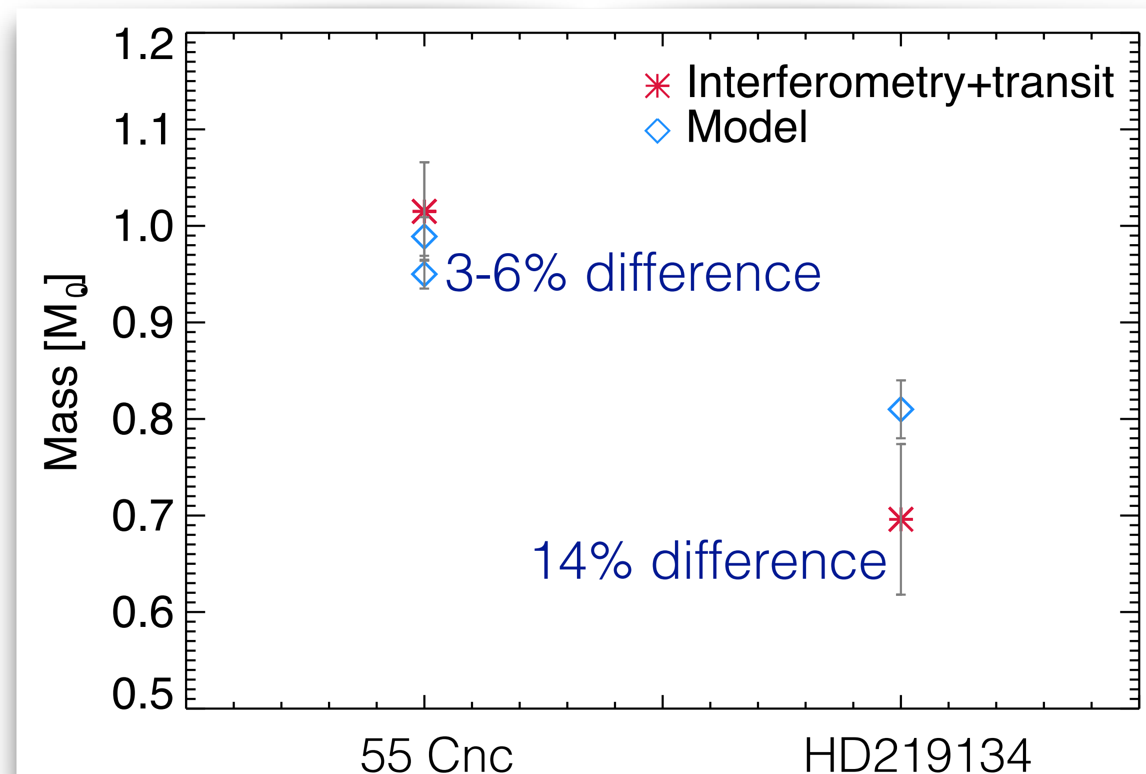

- Discrepancies between models, methods, measures
- Need measures to calibrate models
- → Interferometry + planetary transits can bring very important information on usually non-measurable properties

Stellar models

Integration of the stellar radius from interferometry

HD97658 (Ellis+ 2020)

Planetary Properties			
Transit Depth [ppm]	712±38	§4	Exofast
Period [days]	$9.48971157 \pm 0.00000077$	§4	Exofast
T_0 [BJD]	2458904.9366 ± 0.0008	§4	Exofast
$R_p/R_\star$	0.02668±0.0007	§4	Exofast
Inclination [deg]	$89.05^{+0.41}_{-0.24}$	§4	Exofast
Impact Parameter	$0.39^{+0.11}_{-.018}$	§4	Exofast
Eccentricity	$0.054^{+0.039}_{-0.034}$	§4	Exofast
Mass [$M_\oplus$]	7.52±0.86	§4	Exofast
$a/R_\star$	24.16 ± 0.69	§4	Exofast
R_p [$R_\oplus$]	2.12±0.061	§4	
ρ_p [g cm^{-3}]	3.681 ± 0.51	§4	
T_{Eq}[K]	749 ± 12	§4	
Stellar and Planetary Properties from Transit Observables			
$\rho_\star$ [g cm^{-3}]	3.11 ± 0.27	§4	
$M_\star$ [$M_\odot$]	0.85 ± 0.08	§4	
$\log(g)$ [cgs]	4.64±0.04	§4	
Corr($R_\star$,$M_\star$)	0.41	§4	
ρ_p [g cm^{-3}]	4.835 ± 0.70	§4	
R_p [$R_\oplus$]	2.11±0.059	§4	
Mass [$M_\oplus$]	8.25±1.01	§4	
Corr(R_p, M_p)	0.09	§4	

Lebreton & Goupil 2014

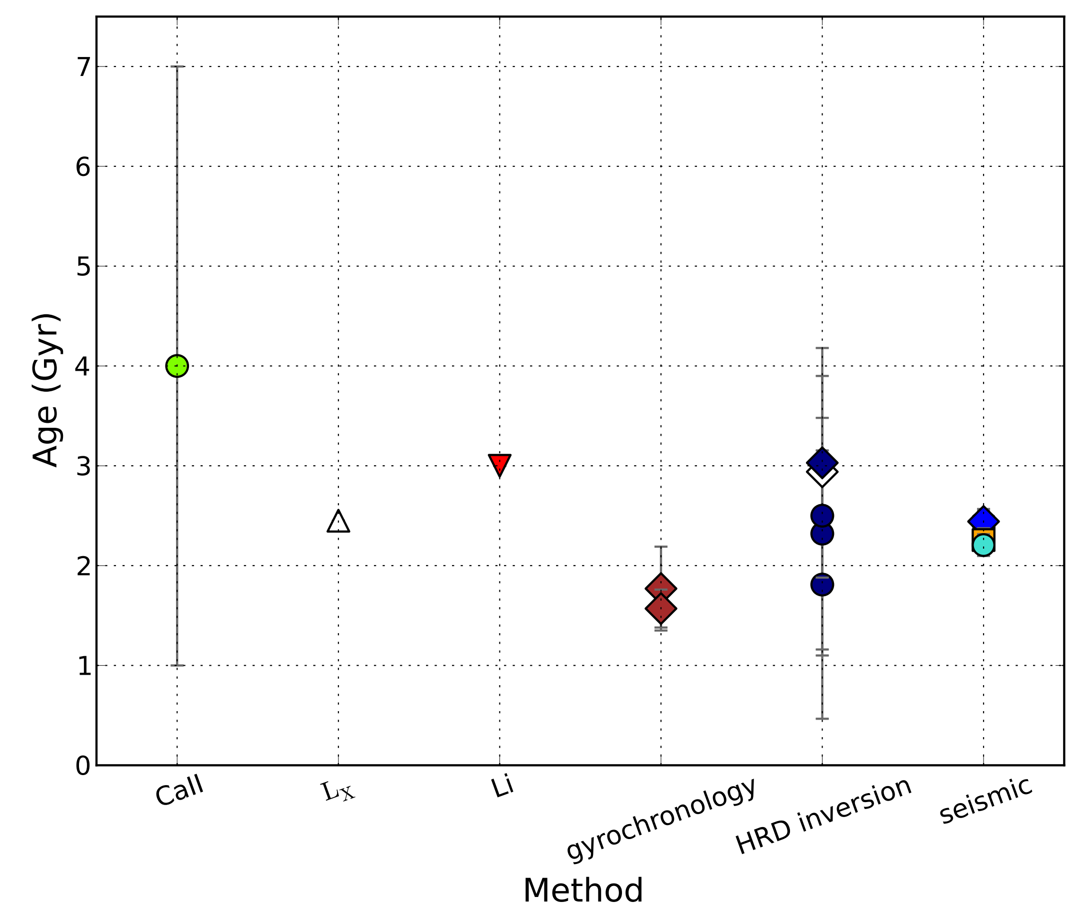

- Discrepancies between models, methods, measures
- Need measures to calibrate models
- → Interferometry + planetary transits can bring very important information on usually non-measurable properties

Stellar models

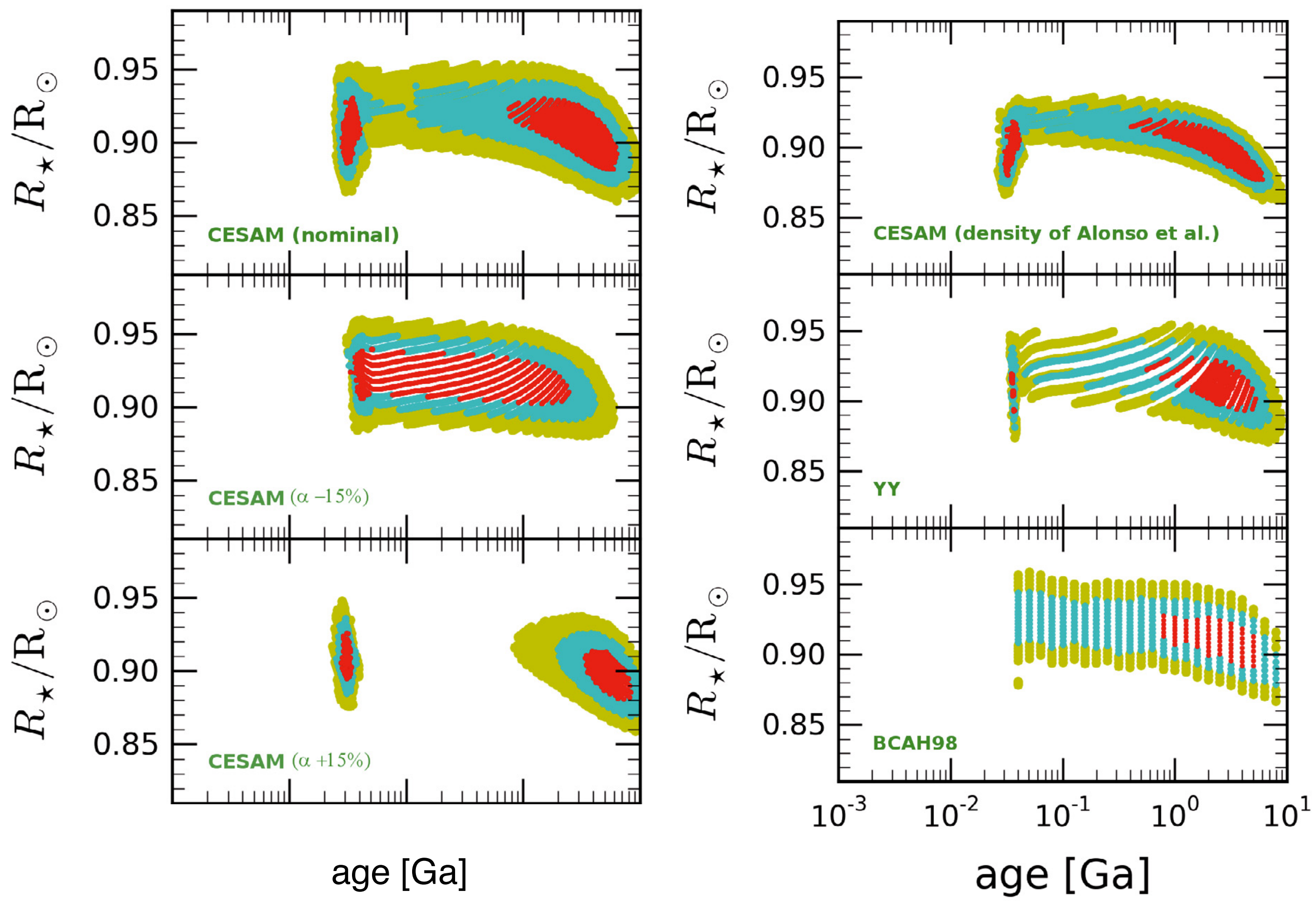

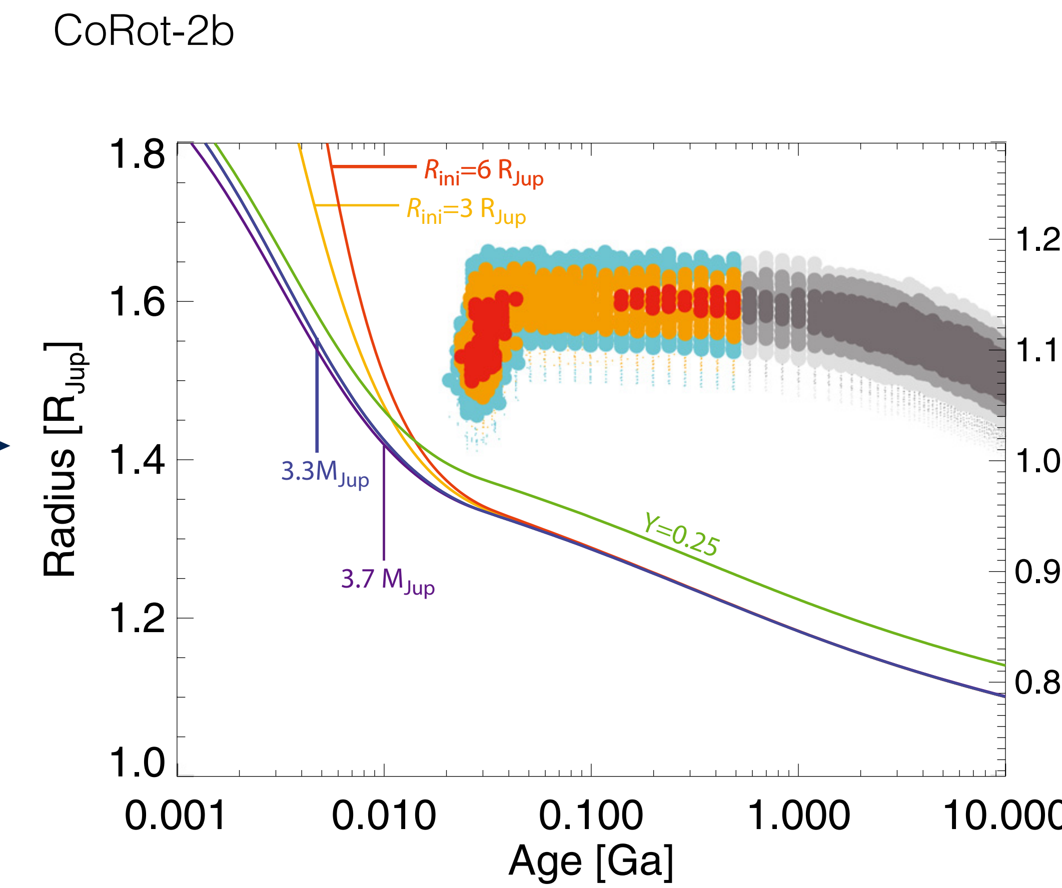

Guillot & Havel 2011

→ Inconsistency in stellar parameters perturbs the exoplanet composition

→ Composition of planets that we do not find in our solar system?

Surface-brightness color relationship

- We can't measure the angular diameter of all stars
- SBCR are here for that!

Surface-brightness color relationship

- We can't measure the angular diameter of all stars
- SBCR are here for that!

Before

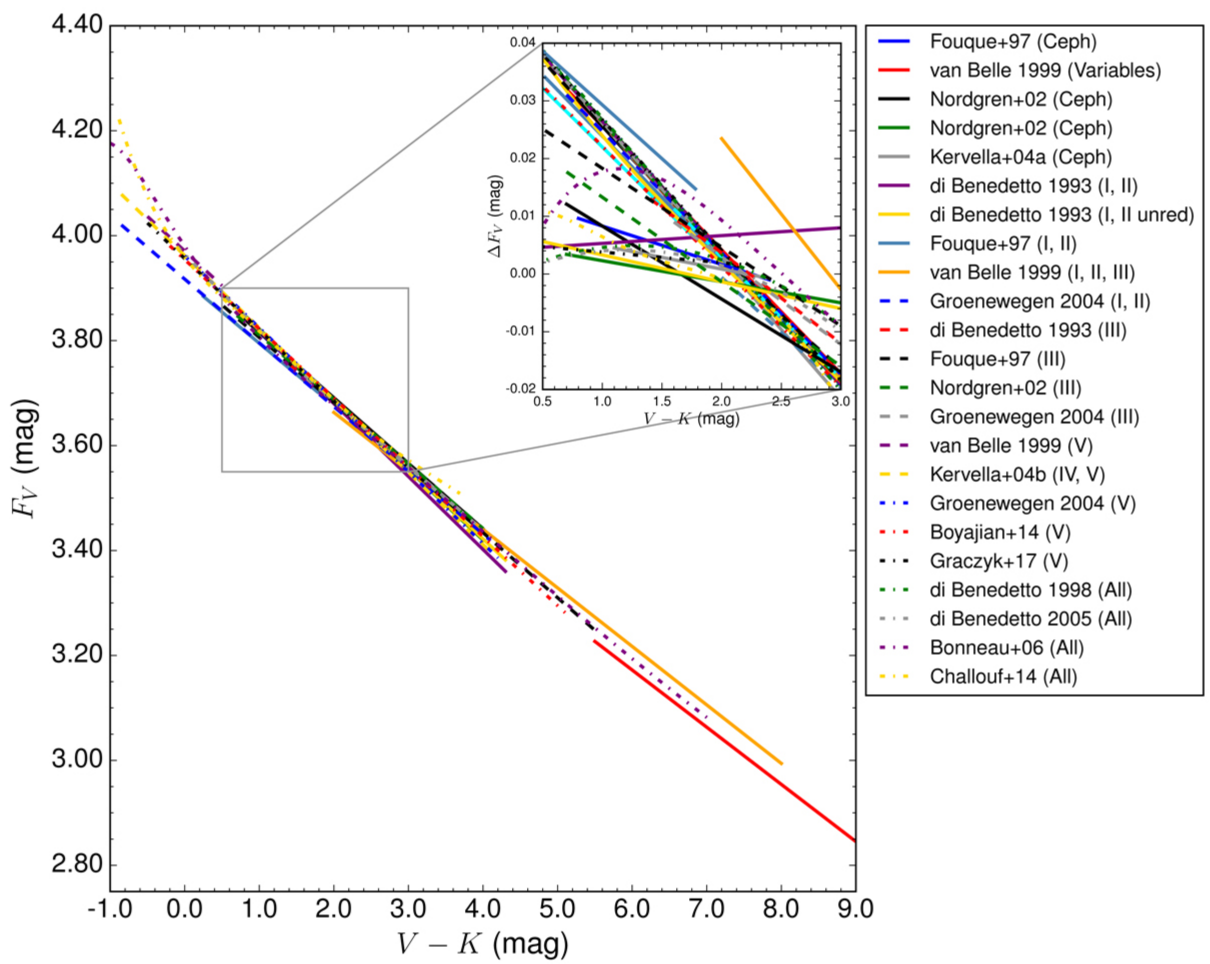

Discrepancy up to 18%

Surface-brightness color relationship

- We can't measure the angular diameter of all stars
- SBCR are here for that!

Before

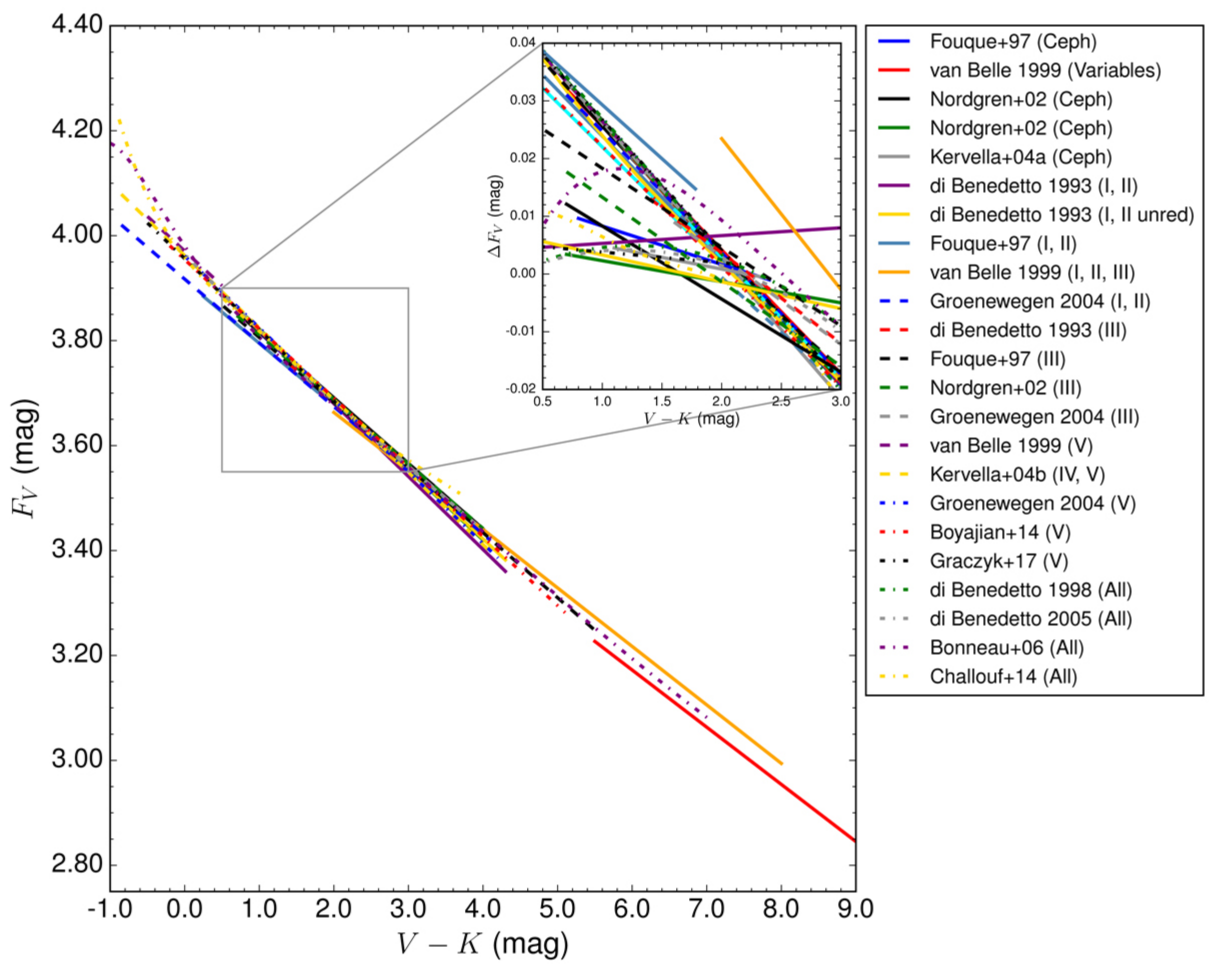

Discrepancy up to 18%

After

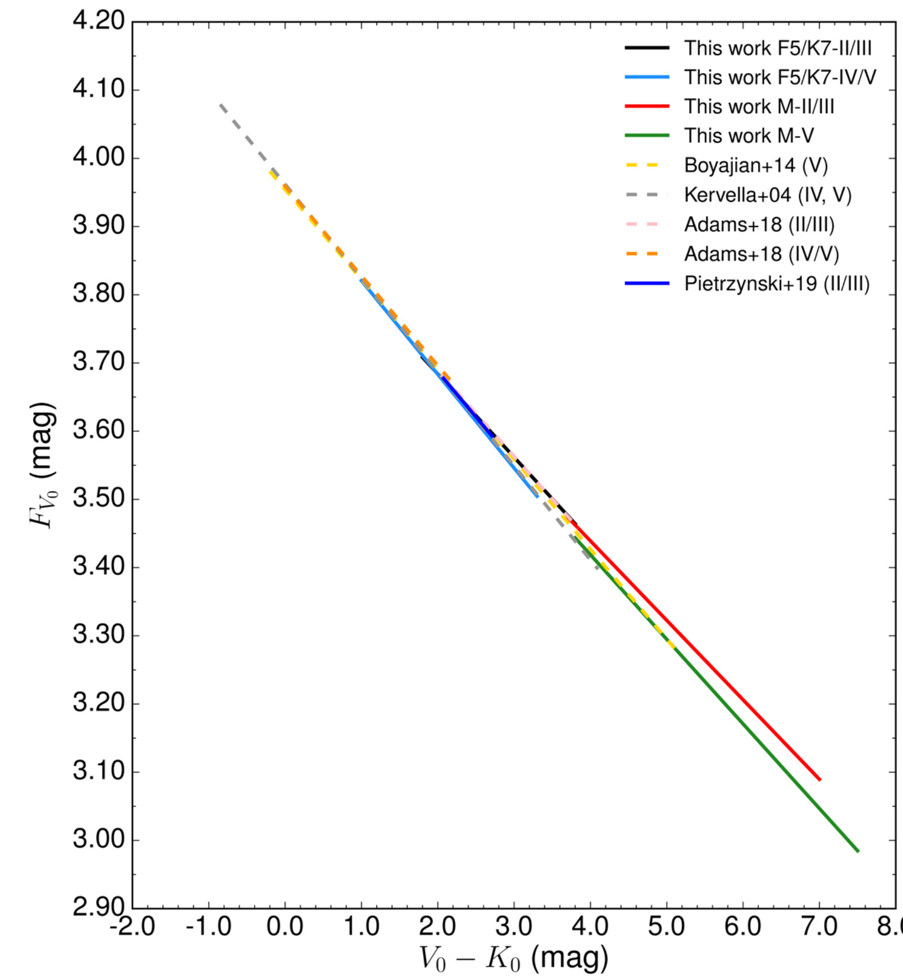

Precision between 1 and 2% with photometric precision better than 0.04 mag

$$\theta_{\rm LD} = 10^{8.4392-0.2V_0-2F_{V_0}}.$$

Salsi+ 2020, 2021

CONCLUSION

Conclusion

- Stellar parameters are very important for exoplanetary characterization
- Interferometry can help in many direct and indirect ways

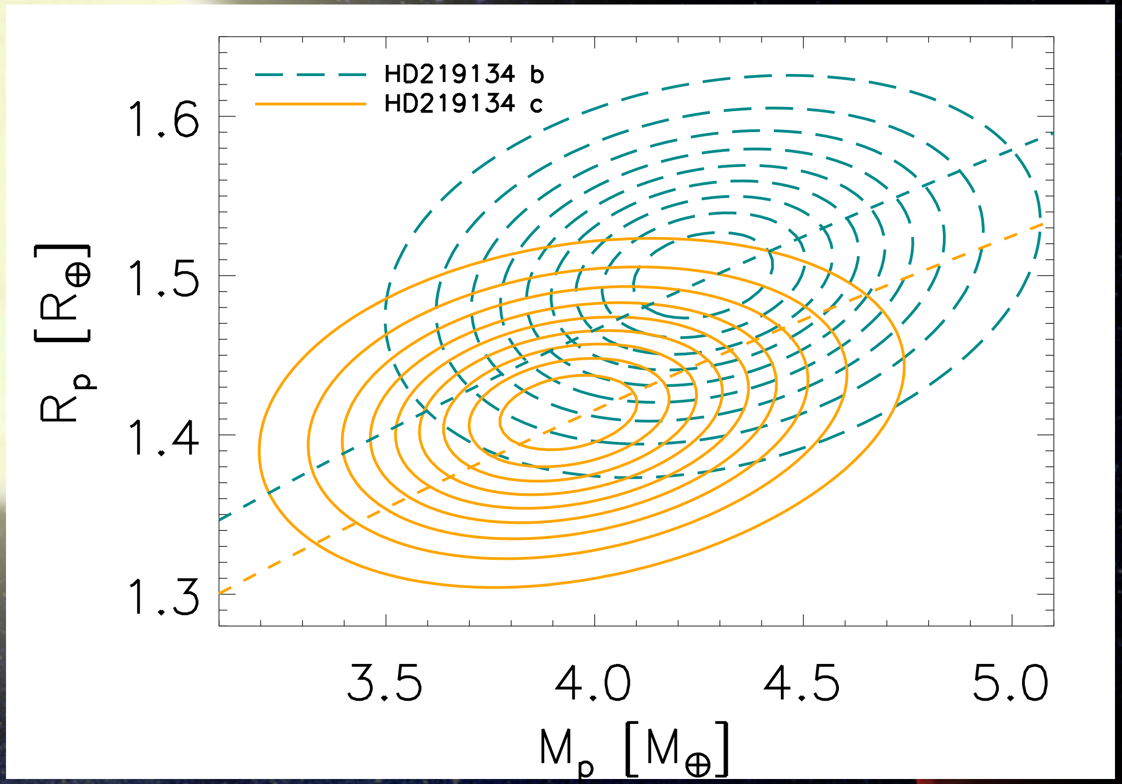

- The most important parameter derived from interferometry plus distances (Gaia) is the stellar radius:
  - Mandatory for determining exoplanet radius
  - Incorporated in stellar models that is used for exoplanets characterization
  - Incorporated in exoplanet interior models

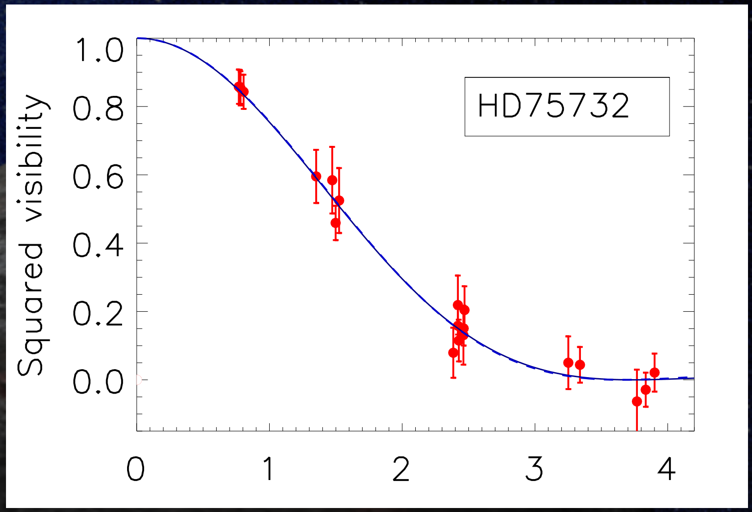

Conclusion

- Gaia brings unprecedented precisions on distances, which brings very precise radii
- New interferometric developments like SPICA/CHARA will allow the study of a bench of exoplanet host stars.

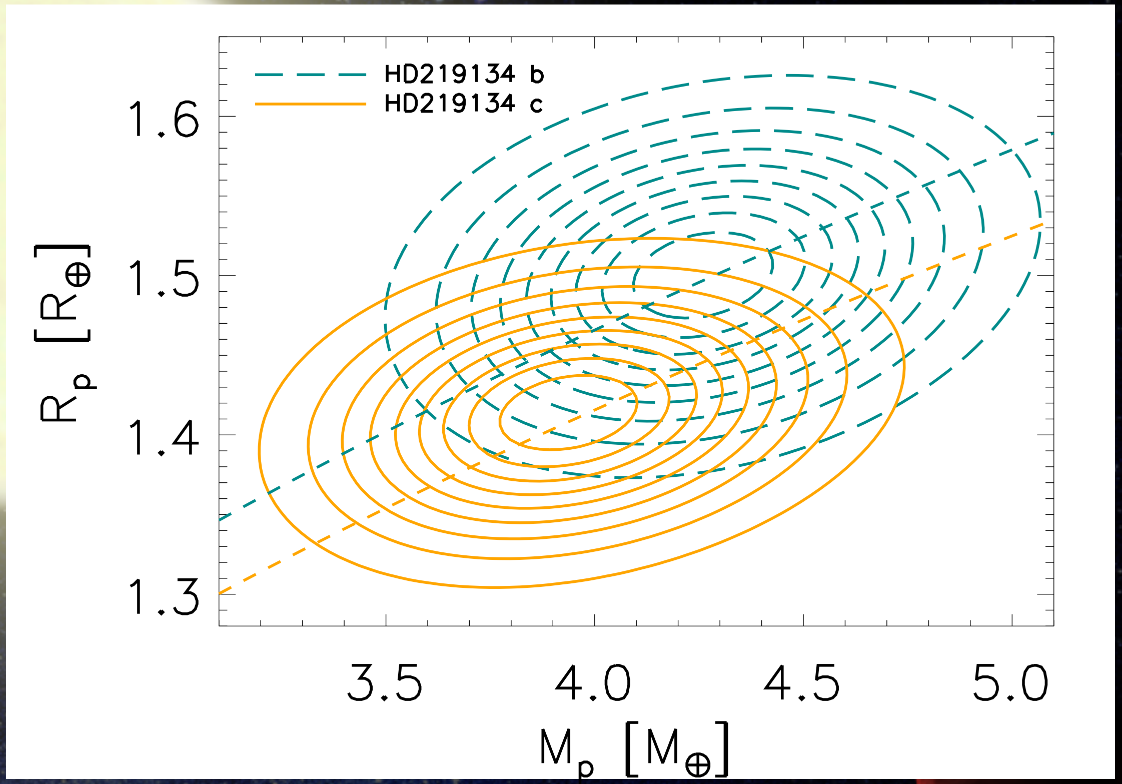

- Gaia is not only useful for interferometry, but also for detection through astrometry and transits.
- Gaia also provides stellar abundances that are used to determine exoplanet interiors.

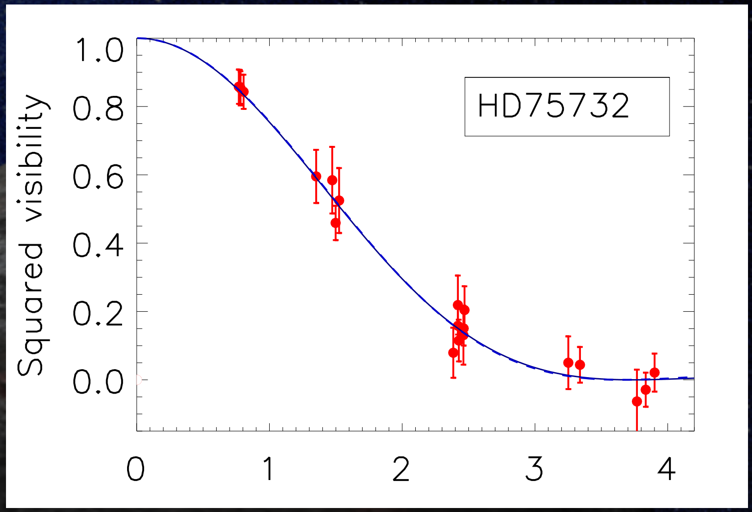


THANK YOU!
Credits: ESA